MONTHLY NOTICES

OF THE

ROYAL ASTRONOMICAL SOCIETY

Vol. 110 No. 5 1950

Published and Sold by the
ROYAL ASTRONOMICAL SOCIETY
BURLINGTON HOUSE
LONDON, W. 1

Price Nine Shillings

NOTICE TO AUTHORS

1. *Communications.*—Papers must be communicated to the Society by a Fellow. They should be accompanied by a summary at the *beginning* of the paper conveying briefly the content of the paper, and drawing attention to important new information and to the main conclusions. The summary should be intelligible in itself, without reference to the paper, to a reader with some knowledge of the subject; it should not normally exceed 200 words in length. **Authors are requested to submit MSS. in duplicate. These should be typed using double spacing and leaving a margin of not less than one inch on the left-hand side. Corrections to the MSS. should be made in the text and not in the margin.** Unless a paper reaches the Secretaries more than seven days before a Council meeting it will not normally be considered at that meeting. By Council decision, MSS. of accepted papers are retained by the Society for one year after publication; unless their return is then requested by the author, they are destroyed.

2. *Presentation.*—Authors are allowed considerable latitude, but they are requested to follow the general style and arrangement of *Monthly Notices*. References to literature should be given in the standard form, including a date, for printing either as footnotes or in a numbered list at the end of the paper. Each reference should give the **name and initials** of the author cited, irrespectively of the occurrence of the name in the text (some latitude being permissible, however, in the case of an author referring to his own work). The following examples indicate the style of reference appropriate for a paper and a book, respectively :—

A. Corlin, *Zeits. f. Astrophys.*, **15**, 239, 1938.
A. S. Eddington, *Internal Constitution of the Stars*, Cambridge, p. 182, Table 24, 1926.

3. *Notation.*—Authors should conform closely to the recommendations of Commission 3 of the International Astronomical Union (*Trans. I.A.U.*, Vol. VI, p. 345, 1938). Council has decided to adopt the I.A.U. 4-letter abbreviations for constellations where contraction is desirable (Vol. IV, p. 221, 1932).

4. *Diagrams.*—**These should be drawn about twice the size required in print and prepared for direct photographic reproduction except for the lettering, which should be inserted in pencil. Legends should be given in the manuscript indicating where in the text the figure should appear.** Blocks are retained by the Society for 10 years; unless the author requires them before the end of this period they are then destroyed.

5. *Tables.*—**These should be arranged so that they can be printed upright on the page.**

6. *Proofs.*—Costs of alterations exceeding 5 per cent of composition must be borne by the author. Fellows are warned that such costs have risen sharply in recent years, and it is in their own and the Society's interests to seek the maximum conciseness and simplification of symbols and equations consistent with clarity.

7. *Revised Manuscripts.*—When papers are submitted in revised form it is especially requested that they be accompanied by the original MS.

Reading of Papers at Meetings

8. When submitting papers authors are requested to indicate whether they will be willing and able to read the paper at the next or some subsequent meeting, and approximately how long they would like to be allotted for speaking.

9. Postcards giving the programme of each meeting are issued some days before the meeting concerned. Fellows wishing to receive such cards whether for Ordinary Meetings or for the Geophysical Discussions or both should notify the Assistant Secretary.

MONTHLY NOTICES

OF THE

ROYAL ASTRONOMICAL SOCIETY

Vol. 110 No. 5

MEETING OF 1950 OCTOBER 13

Professor W. M. Smart, President, in the Chair

The President referred to the death on 1950 September 21 of Professor E. A. Milne, and read the following tribute paid to him by the Council at its meeting that afternoon (the Fellows standing) :—

" In the sudden death at the early age of fifty-four of Professor Edward Arthur Milne, the Royal Astronomical Society has suffered a grievous loss, one shared not only with astronomers the world over but with the whole world of science. Milne's early work on radiation problems connected with the outer atmospheres of the Sun and stars won in 1935 the award of our Gold Medal, the highest honour that the Society can bestow. In his later years Milne devoted his keen intellectual faculties to a persistent and courageous attack on the problem of the ultimate nature of the physical universe. His book " Kinematic Relativity " will provide food for keen discussions for many years to come.

" As President, as Member of Council over many years, Professor Milne served the Society faithfully and loyally, never sparing himself, despite failing health, when asked to undertake any duty for the Society. His loss will be severely felt by our Fellows and the Council knows that they will wish to associate themselves with an expression of deep sympathy with his family in their tragic bereavement."

The election by the Council of the following Fellows was duly confirmed :—

Norman Robert Blackmore, 12 Victoria Street, Middle Brighton, Melbourne, Australia (proposed by E. B. Walton);

Dennis Jack Fulcher, 19 Gloucester Road, Ipswich, Suffolk (proposed by E. H. Collinson);

John Barrows Irwin, Goethe Link Observatory, Indiana University, Bloomington, Indiana, U.S.A. (proposed by W. A. Hiltner); and

Eric Smith, 6 Fiennes Road, Herstmonceux, Sussex (proposed by W. A. Scott).

Seventy-seven presents were announced as having been received since the last meeting, including :—

British Astronomical Association, *Index to the Association's Journal for Volumes* 1–50 (presented by the Council of the Association); and

Yusuke Hagihara, *Foundations of Celestial Mechanics* (presented by the author).

THE ELECTRICAL PHOTOMETRY OF STARS AND NEBULAE

George Darwin Lecture, delivered by Professor Joel Stebbins on 1950 *October* 13

My feeling of pleasure on being with you today is mixed with a sense of responsibility, not to mention humility. Dr George E. Hale once said that the meetings of the Royal Astronomical Society are the most stimulating astronomical meetings in the world ; and I heard Professor Willem de Sitter say in this room that the Royal Astronomical Society acts as astronomical conscience, astronomers come from everywhere to confess what they have been doing. In the present case my task is lightened by the fact that some months ago our President told you all about my work ; he did such a thorough job that I suggested that I sign my name to his paper and call it the George Darwin Lecture. My one criticism of his address is that he was forced to limit it to the successes ; he could not give you a true picture of the troubles and failures of the work in photometry.

I never had the privilege of meeting Sir George Darwin, but I knew very well his disciple, Ernest W. Brown. Brown once told me that the training he received from Darwin consisted simply in going to his study and talking with him about Brown's problems. Likewise it was an education to talk with, or rather listen to, Ernest Brown. I met Sir James Jeans several times, the last when he was presiding here over a meeting of this Society. My first collaborator in photometry, F. C. Brown, had been a student of Jeans at Princeton ; and so in a way I might claim to be a descendant of both Darwin and Jeans, though not in direct line.

The electrical photometry of stars involves the technique of experimental physics at the end of a telescope, and since all my work in this field has been in collaboration with others, it is only fair at the outset to acknowledge my debt to those without whose aid I should not be here. There was F. C. Brown, as mentioned, who started me off for a few years with the selenium photometer ; the late Jacob Kunz, who for twenty-five years produced photoelectric cells of the best quality with his own hands, and cooperated in other ways until his death a dozen years ago ; C. M. Huffer, who has divided the observing time at the telescope for many years ; A. E. Whitford, who first applied the thermionic amplifier, and continued with notable improvements and applications ; and Gerald E. Kron, a former student with whom I am working, the relation of teacher and student being at least partially reversed. For the institutions involved I should mention twenty years at the University of Illinois, twenty-five years at the Washburn Observatory of the University of Wisconsin, fifteen summers at the Mount Wilson Observatory, and the past two years at the Lick Observatory of the University of California, under the auspices of the United States Office of Naval Research.

Instruments.—The present is a fine opportunity to open the floodgates of reminiscence, but I shall go back only to the last time I spoke in this room, during the meeting of the International Astronomical Union in 1925. After that meeting had dispersed I had the pleasure of going to Oxford and calling on Lord Cherwell, then Professor Lindemann, and I discussed with him the troubles we were having with a Lindemann electrometer which we had obtained for experiment a short time before. After a few minutes' conversation he told me that the drift or instability we had found must be caused by a defect in the instrument. I returned to

Wisconsin, obtained another electrometer from the Cambridge Scientific Instrument Company and from the first night that this second electrometer was used on the telescope the previous installation was discarded, and Lindemann electrometers were used in all photoelectric work at Madison and Mount Wilson for the next six or eight years. It would have paid my institution to send me across the Atlantic simply to learn that we had a defective sample of a very useful instrument!

This and other forms of electrometer were finally supplanted, in our case, by the thermionic amplifier which Whitford successfully applied to the measurement of the minute current produced by the light of a star falling on a photosensitive surface, down to 5×10^{-18} amperes. The series of photometers developed during the past twenty years represent the struggle to obtain greater effective sensitivity, either by finding a better photocell to increase the light signal or by reducing the irregularities or " noise " in the electrical circuit. Actually, more progress has been made in reducing the noise than in increasing the signal; the advances can be illustrated by specific cases as we proceed.

The final items in the improvement of a single-stage amplifier include mounting both photocell and amplifying tube in an evacuated chamber to improve surface insulation and to eliminate the effects of stray ions caused by cosmic rays, and refrigerating the cell down to the temperature of dry ice, −80 deg. C., to reduce the thermionic dark current. All this is standard procedure in a laboratory but is somewhat out of ordinary at the end of a telescope. Also, whereas formerly it was our practice to make visual readings of a spot of light on a galvanometer scale, for several years past most of the American workers in this field have been using a recording potentiometer, which lightens the work at the telescope, enables one observer to operate alone, and gives a permanent record; but like the chronograph for time observations, the recording instrument simply piles up more work for the daytime.

Colour Systems.—If a photographic or visual observer publishes a set of stellar magnitudes or the light-curve of a variable star, his work may be taken as it is, but if the same task is accomplished with a photocell, then it seems that a determination of the colour curve or effective wave-length of the receiver is expected. This requirement is not onerous because experience has shown that there is little value in measuring the brightness of a star in fewer than two colours, so that comparison with any other system like that of the International can be made. Likewise, light-curves of a variable star in two colours always give more information than a single curve. After one has once tried colour photography for snapshots with a hand camera the old-fashioned black-and-whites have little appeal. So for ten years or more we have followed multicolour photometry of stars and nebulae, always working in at least two colours, but more often using combinations of a cell and filters which isolate six spectral regions ranging from 3530 A. to 10,300 A. (1). With filters the limits of such regions are not sharp; there may even be some overlapping of adjacent regions, but for faint diffuse objects like the nebulae the saving of light makes up for this drawback. To isolate the spectral regions of an extragalactic nebula with a slit spectrograph would reduce the intensities below practicable measurement with a photocell.

Another shortcoming of the method of filters is that the effective wave-length of the whole combination: star, atmosphere, telescope, filter, and receiver, depends upon the temperature or colour of the source. As we go along the spectral sequence from hot to cool stars the effective wave-length for any filter increases progressively, but, fortunately, for any two filters this change may be a nearly

parallel shift, the base line for colour index remaining of about the same length. Any method which integrates the intensities over all wave-lengths of a given interval also takes in the absorption lines and bands, and this condition holds for any system of colour index.

The foregoing remarks apply with even greater force to the International photographic magnitudes and colours. As Seares (**2**) has shown, the photovisual system includes a range of about 1000 A. from 4900 to 5900 A., but the photographic range is about twice as great, from 3000 to 5000 A. Thus, while the computed effective wave-lengths of Pv for black-body sources vary from 5420 A. at 30,000 deg. to 5480 A. at 3000 deg., the corresponding change in Pg is from 4160 A. to 4560 A., a change of 400 A. as against 60 A. for Pv. Similar changes in effective wave-length are present in all our six-colour work, but because of the parallel displacements for different filters, unless absolute measurements are involved, the relative colours for ordinary giant and dwarf stars are as useful as the results in any two-colour system. The reason that such crude methods are used with the photocell and filters, or with the photographic plate, is of course to reach faint objects. The spectrophotometry of the Greenwich gradients, where definite regions of continuous spectrum can be selected for each star, ends at about the 5th magnitude with a 36-inch reflector. To go ten magnitudes fainter with any telescope requires a change of procedure.

η Aquilae.—As a sample of recent work in six colours we give the light-curves of the well-known variable star, η Aquilae, determined with the 36-inch Crossley reflector of the Lick Observatory. While in the similar curves for δ Cephei (**3**), obtained with the 60-inch at Mount Wilson, we were able to smooth out most of the suspected secondary fluctuations—actually this smoothing had already been done by Dr Smart (**4**) with a photoelectric photometer at Cambridge—in η Aquilae the secondary "hump" still remains, and there are evidences of minor waves on the main curve, but not strong enough to be convincing. As in δ Cephei, these new curves show decreasing amplitudes with increasing wave-length; the range of variation is about four times as great at 3530 A. as at 10,300 A. The overall colour class of η Aquilae varies through the cycle from about cf 7 to cg 4; in δ Cephei the range is from cf 4 to cg 2. As might have been expected, the same retardation of phase with increasing wave-length is found; the maxima and minima come about $\frac{1}{20}$ period later in the infra-red than in the ultra-violet.

As pointed out by others, this effect is readily explained in a pulsating star by the combination of varying diameter and surface brightness of the apparent disk. At maximum light, when the radial-velocity measures indicate that the star is expanding, the increasing size of the disk is more than counterbalanced by the decreasing intensity in the short wave-lengths, and the star begins to fade; but in the long wave-lengths the same increase of area outweighs the much smaller decrease of intensity and the star still brightens. The reverse conditions obtain at minimum. As far as I am aware, no satisfactory complete theory of η Aquilae, accounting for the hump in the light-curve, has been worked out. Since δ Cephei and η Aquilae are prototypes of their respective subdivisions of classical Cepheids, it is no great generalization to predict that the same phase effect is probably present in most other variables of these types, and also in the ζ Geminorum stars. In an incomplete study we find this same effect in the cluster-type variable, RR Lyrae.

Algol.—Another star studied in six colours, this time an eclipsing system, is our old friend Algol, but because of other problems the observational data were

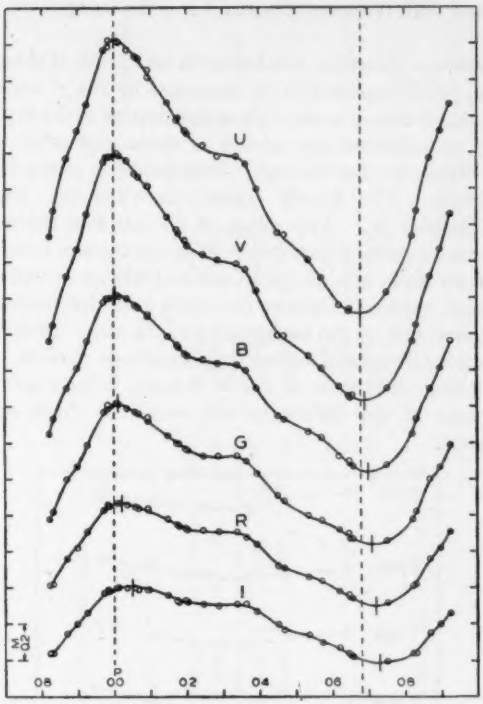

FIG. 1.—*Light-curves of η Aquilae.*

not quite completed in the season 1949–1950. Suffice it to say that the ranges of variation at 3530 A. and 10,300 A. are roughly 1·28 and 0·86 mag., respectively, for primary minimum; 0·03 and 0·13 mag. for secondary minimum; and 0·05 and 0·08 mag. between minima; with proportional values for the intermediate wave-lengths. The data at hand would probably be sufficient for a solution for all the elements of the system, including the spectral type and relative size of the companion—the brighter component has a B8 spectrum—but it seems inadvisable to undertake such calculations before the data are definite, especially at the critical times of beginning and ending of the eclipses.

M8 and Trifid Nebulae.—The six-colour measures of stars can often be compared with conventional two-colour results for the same objects, and we revert to some previous studies of reddened B stars near the centre of the galaxy. In the grouping of heavily obscured, strongly reddened B stars within 2° or 3° of the galactic equator, there is a gap at $l = 335°$, $b = -2°$ (Lund pole), where a few stars at distances greater than 400 parsecs are of normal or near normal colour, the only such gap in 40° of longitude (**5**). It cannot be a mere coincidence that just in this gap are found the two conspicuous objects, M8 and the Trifid nebula. More likely is it that we see these two nebulae simply because there is a large hole in the intervening absorbing clouds, and no doubt many other such nebulae are present along and near the galactic equator, illuminated by the high-temperature B stars but obscured by the interstellar dust. Both M8 and the

Trifid are involved with reddened stars and it is the foreground that seems to be relatively clear.

Globular Clusters.—However, not far north and south of these nebulae are the globular clusters, NGC 6440 and 6553, separated by the 7° zone of no globular clusters and reddened almost as strongly as any objects in the sky. In Table I are some previously unpublished six colours of these and other globular clusters taken at Mount Wilson in 1940 to 1945. The headings of the first three columns are self-explanatory. The fourth column contains the total photographic magnitudes by Christie (**6**). The values of C_2, our first colours with the short base line, are from a previous paper (**7**). The six colours from U to I, referred in magnitude to the mean of blue, green and red, are on our standard system for stars. In the faint reddened clusters the violet and ultra-violet intensities were too weak to be measured on the background of the sky. Probably most of these clusters have varying integrated colour from centre to outside. We have found as much as 0·17 mag. difference in the V–I scale, inner redder than the outer region, but a study of this difference will involve a check upon the possible instrumental effects.

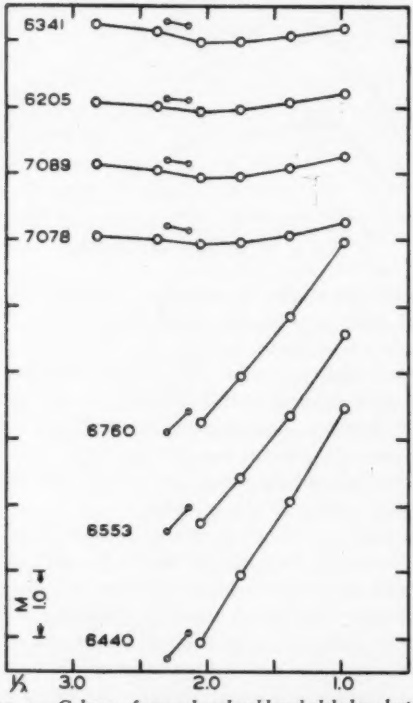

FIG. 2.—*Colours of normal and reddened globular clusters.*

The data of Table I are shown graphically in Fig. 2. The normal clusters have the curves to be expected from mixtures of stars, brighter in the U and I. A straight, horizontal line represents the mean colour of stars of spectrum dG6. Values for C_2, drawn properly to scale, show that even with such a short base

TABLE I

Colours of Globular Clusters

NGC	Messier	Year	m	C_s	U	V	B	G	R	I	Obs.	Remarks
					$1/\lambda = 2{\cdot}83$	2·37	2·05	1·75	1·39	0·97		
6205	13	40, 41	6·8	−0·03	−0·07	−0·02	+0·05	+0·02	−0·07	−0·20	2	Normal
6205	13	44	6·8	−0·03	−0·07	0·00	+0·08	+0·01	−0·09	−0·20	3	
6341	92	41, 44	7·3	−0·09	−0·22	−0·12	+0·04	+0·02	−0·06	−0·17	2	
7078	15	45	7·3	−0·08	−0·05	−0·01	+0·06	+0·02	−0·08	−0·28	2	
7089	2	45	7·3	−0·06	−0·12	−0·04	+0·06	+0·04	−0·10	−0·26	2	
6440	...	45	12·0	+0·37	...	...	+1·06	+0·04	−1·09	−2·48	3	Reddened
6553	...	45	10·2	+0·36	...	...	+0·78	+0·07	−0·86	−2·08	2	
6760	...	45	11·2	+0·30	...	...	+0·76	+0·09	−0·86	−1·97	3	

All measures with 60-inch; diaphragm 5′·7.

line a good indication of the amount of reddening was possible. The globular clusters are good qualitative indicators of space reddening, but because of the dispersion in their intrinsic colours they are not as good as B stars for standards. As has been pointed out by Becker (**8**), the integrated spectral types of non-reddened globular clusters, determined by Mayall (**9**) at the Lick Observatory, show a strong correlation with the photoelectric colours, the difference between equivalent types A5 and G5 being about 0·10 mag. on the C_2 scale. Moreover, there is small chance of estimating the spectral types of the strongly reddened clusters. The difference between average O and B2 stars is only about 0·02 mag. on the same scale; and the dispersion within any subclass of the O's and early B's is very small indeed.

Andromeda Nebula.—We have published elsewhere (**10**) the six-colour results on a number of bright extragalactic nebulae, but there are some differential measures in the Andromeda nebula which I reported at the meeting of the I.A.U. in Copenhagen in 1946. The observations were taken with the 60-inch reflector at Mount Wilson. With the same photocell as for six colours, the special system C_5 has two light filters giving effective wave-lengths at about 4250 A., near photographic, and at 7500 A., a base line about double that of the International system. The infra-red was shortened to eliminate the strong emission at 10,400 A. in the night sky. The photograph in Fig. 3 (Plate 7) has been retouched to bring out the fainter regions. The colour index for each area is referred to the mean of five such areas along the major axis; as usual the + sign means redder than the mean. The greatest difference, between +0·30 in the dark lane and −0·10 in the opposite region, is 0·40 mag. in C_5 or 0·20 mag., International.

If we assume that the light of the nebula is symmetrical in these inner regions, except for intranebular absorption, then with the blue filter giving photographic magnitudes we have at once the ratio of total to selective absorption. To get more light, this determination was made with diaphragms twice the diameter of those in the figure. The relation between the scales of C_5 and C_{int} was found from the North Polar Sequence. If ΔA_{pg} is the change in total photographic absorption from one region to another, and ΔC_5 the corresponding change in colour, then we have:

$$\left\{\begin{aligned} \Delta A_{pg}/\Delta C_5 &= 1{\cdot}82 \pm 0{\cdot}06 \text{ (p.e.)},\\ \Delta C_5/\Delta C_{\text{int}} &= 2{\cdot}13 \pm 0{\cdot}05,\\ \Delta A_{pg}/\Delta C_{\text{int}} &= 3{\cdot}87 \pm 0{\cdot}16. \end{aligned}\right.$$

$$\text{Another result} = 4{\cdot}17 \pm 0{\cdot}53.$$

$$\left.\begin{aligned} &\text{Mean } \Delta A_{pg}/\Delta C_{\text{int}}\\ &\text{or } A_{pg}/E_{\text{int}} \end{aligned}\right\} = 4{\cdot}0 \pm 0{\cdot}2.$$

The second result is from an independent but poorer determination made previously with other filters giving two-thirds the scale of C_5. This ratio of about 4·0 is all right for M31 if we place the dark lane on the near side of the nebula and permit the assumption of symmetry. We may note also that Holmberg (**11**) has found $A_{pg}/E_{\text{int}} = 4{\cdot}3$ from a similar study of NGC 5195, the companion nebula to M51. Either value is not too different from various results found for the interstellar absorption in our galaxy, though I prefer a figure nearer 5 as determined from B stars.

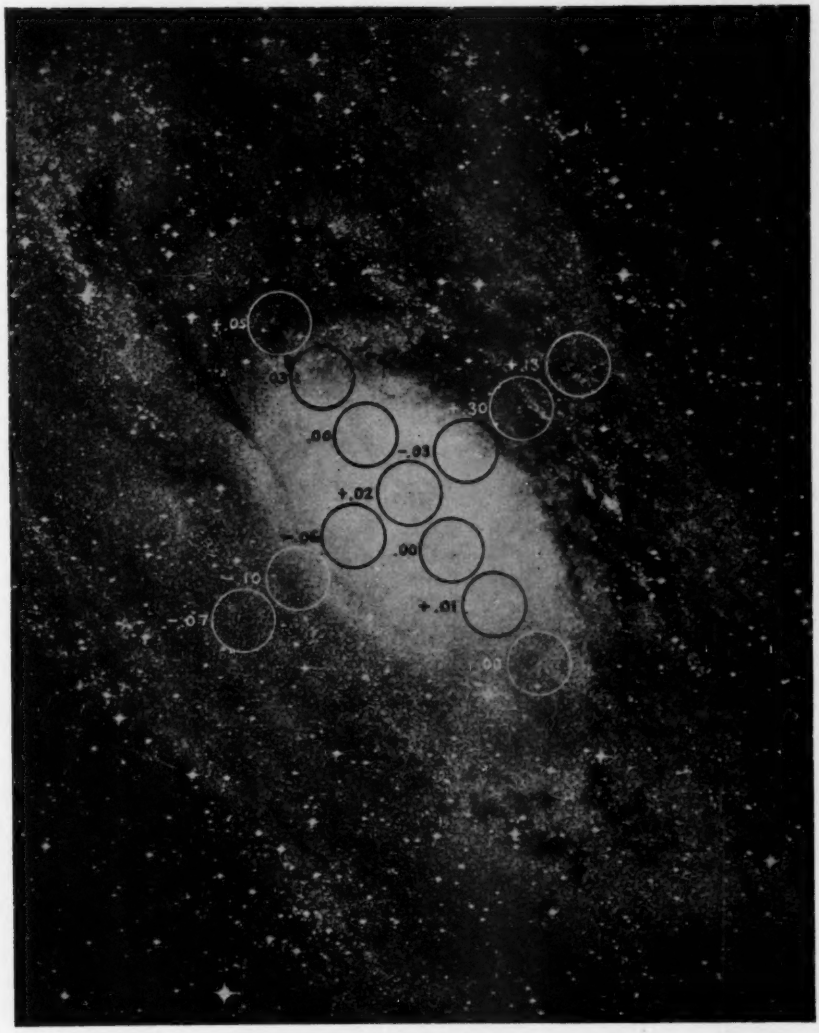

Colours in M31.
Retouched photograph by Mayall and Chappell, Lick Observatory.
Diameter of circles : 2'·04.

Standard Lamp.—To calibrate the six-colour results on an absolute scale, Dr Kron and I have recently undertaken some comparisons of the stars with a standard lamp of known temperature and spectral distribution. The procedure was to measure with the Crossley reflector an artificial star at different distances on the peaks of Mount Hamilton. The star was produced by a hole $\frac{1}{70}$ inch (0·3 mm.) in front of the enclosed lamp with tungsten ribbon filament, operated by storage batteries at a colour temperature near 2500 deg. K. as calibrated by the U.S. Bureau of Standards. At a distance of 1100 feet the hole subtended an angle of $0''{\cdot}2$, and visually the star appeared red and between zero and 1st magnitude; brighter than Antares but fainter than Arcturus. With a wire screen absorbing five magnitudes, the light was reduced for convenient comparison with real stars of the 4th or 5th magnitude.

For determination and elimination of the horizontal atmospheric extinction, the lamp, equipment and batteries were carried by jeep to Kepler Peak, 3200 feet from the Crossley; at the greater distance a 2·5-mag. screen again equalized the artificial and real stars. Contrary to expectation the elimination of the extinction gave little difficulty. The most we could find for the lamp was a difference of 0·02 mag. for 4220 A. between the longer and shorter distances, or 0·01 mag. for 1100 feet. The extinction for longer wave-lengths was negligible; because of the red colour of the lamp we did not attempt to measure the weak ultra-violet at 3530 A.

Similarly, the regular atmospheric extinction was determined on the same nights by measuring stars at high and low altitudes. With an air mass, sec z, varying from 1·2 to 3 or 4, the reduction to no atmosphere for each colour could be made with little uncertainty. All told, the accidental errors of the comparison between lamp and stars on different nights were satisfactorily small, though such measures would be difficult if not impossible with a sky less favourable than that of Mount Hamilton.

The difficulty of the comparison turns out to be the uncertainty of the effective wave-lengths of the combinations of the photocell and filters, which are still in process of determination in the laboratory. We have found differences in colour sensitivity from spot to spot over the surface of the photocell. As used on the stars a positive lens in the focal plane forms an image of the main mirror about 1 cm. in diameter on the cathode of the cell, and the problem in the laboratory is to form such an image and measure its energy with a thermocouple. Until this calibration is accomplished, the observations cannot be reduced to an absolute standard.

Magnitude of Sirius.—We turn for the moment from colours to stellar magnitudes, where again the photocell has the great advantage of a linear relation between the response and the intensity of the incident light. Actually the brightest star we have observed is the Sun, which at the 1937 eclipse in Peru was used as comparison for the corona, and to determine the extinction at the low altitude of 5° at totality. An optical "sun reducer", essentially a compound microscope, gave an out-of-focus image on the photocell of the same order of intensity as the corona or the full Moon.

Of the regular stars we begin with Sirius, the brightest of all. Naturally it does not require a 36-inch telescope to measure Sirius, but we were interested in the colours, and incidentally we determined the visual magnitude, which is not too easy to get with the eye. The light of Sirius was reduced with a 5-mag. wire screen, and the visual magnitude was interpolated between our blue and green magnitudes.

In TableII are the results from four polar stars and five southern stars in the vicinity of Sirius. The magnitudes in the second column are Harvard visual. The spectra are for information only; the photoelectric colours were used in the reductions. Each visual magnitude in the fourth column is based upon that of the corresponding star. On any night a number of later type G or K stars were used to get the proper interval for interpolating between our blue and green, just as polar stars are used for collimation or azimuth in time determinations. The average deviations of the photoelectric measures on different nights indicate that the discordances in the column for Sirius must be in the magnitudes of the comparison stars. I see no way out of the conclusion that the generally used visual magnitude of $-1\cdot58$ is too bright, and that $-1\cdot42$ is nearer right when referred either to the stars near the pole or to the other white stars in the vicinity of Sirius. Incidentally the effective wave-length of the Harvard visual system is found to be 5380 A. for the stars in the table.

TABLE II

Visual Magnitude of Sirius

Star	*m*	Spec.	Sirius *m*	A.D.	No.
NPS 1	4·44	A2	−1·32	±0·025	2
4	5·86	A3	−1·34	±0·010	2
2s	6·28	F2	−1·44	±0·005	2
3s	6·33	F4	−1·47	±0·005	2
BS 2294	1·99	B1	−1·36	±0·000	2
2596	4·39	B5	−1·42	±0·027	3
2504	5·19	B8	−1·52	±0·005	2
2498	5·30	A2	−1·45	...	1
2448	5·93	A0	−1·48	...	1
	Four polar stars		−1·39	±0·06	
	Five southern stars		−1·45	±0·05	
	All		−1·42	±0·03	
	Harvard		−1·58	...	

Faint Magnitudes.—From the bright end of the magnitude scale we now go to the faint limit of our observations. The advent of the RCA 1P21 photomultiplier has introduced a new epoch into photoelectric photometry of the stars. With only a few precautions such a multiplier on a telescope will give satisfactory results over a wide range of magnitudes. With the refinement of refrigeration of the multiplier, and the use of a recording instrument, the effective sensitivity, or ratio of signal to noise, may be something like 10 to 50 times better than what was previously attainable with an ordinary photocell.

A record has been taken by Whitford and H. L. Johnson of a star of photographic magnitude 19·3 with the 100-inch telescope in 1949. Through a diaphragm of diameter 11 seconds of arc the light of the sky background was more than ten times that of the star; the zero for the dark reading had to be depressed off the scale. Also, the noise or irregularities at the tops of the deflections are caused mostly by the sky light. A smaller diaphragm might be used, but under ordinary conditions of seeing and guiding we prefer to take no chances of losing some of the light. In the present case the star was kept centred as in photography, with an auxiliary eyepiece and guiding star. The measures required about 30 minutes plus the time for finding the field, setting on the star, selecting a good guiding star, etc.; so the rate of observing for these faint objects is rather slow. Since the average

absorption of the yellow and blue filters is about 0·9 mag., the intensities in those colours were slightly less than for a clear magnitude of 20·0, but both magnitude and colour must be measured to compare with any other system.

Someone said (I believe it was Paul Merrill) that the best way to take an infra-red photograph is simply to wait. After another year or so the manufacturers will bring out a new red-sensitive plate which will reduce the exposures to half or less, and the work will be made that much easier. In 1907 with a selenium cell on a 12-inch telescope I managed to get a barely detectable response from the first-magnitude star, Aldebaran. By waiting 40 years I have seen useful measures go to magnitude 19 with the 100-inch, and mere detection, say, to magnitude 21. I can mention this fact with due modesty because my own direct contribution toward the improvement of some 20 magnitudes has been nil. The Radio Corporation of America developed the photomultiplier, and Whitford and Johnson perfected, installed and operated the photometer. In the very first trials with selenium, F. C. Brown and I got nothing at all from Jupiter, so we turned to the Moon and measured it without a telescope. In a way, the improvement has been perhaps 23 magnitudes, which is a measure more of the crudeness of the first attempts than of the perfection of the latest achievement. The use of the 100-inch telescope under the California sky, accounting for 4 or 5 magnitudes, has been an important if not a major factor in the advance.

Selected Areas.—In a paper soon to be published (**12**) we are giving a series of photoelectric magnitudes, reduced to the International system, of stars in Selected Areas 57, 61 and 68, with a comparison with the North Polar Sequence. The agreement with the polar stars, taken with the 60-inch, is very good from magnitude 7 to 15, but with the NPS as standard the discordances from the *Mount Wilson Catalogue* (**13**) in all three areas are surprisingly large both in accidental errors and in scale. The details are given in the paper, and we seem to have exhausted the possibilities of finding systematic errors in our work; the internal accidental errors of the photoelectric magnitudes are negligible in the comparison. In a word, on the basis of our results the zero points of the catalogue magnitudes in the three areas agree with NPS somewhere between magnitudes 9 and 14, different for each area, but the catalogue magnitudes at 18·5 are about 0·5 mag. too bright. From these increasing discordances toward the faint end of the magnitude scale we believe that any further conclusions based upon magnitudes in these Selected Areas should be postponed until the disagreement is straightened out.

Hubble's (**14**) surveys of nebulae with limits of Pg magnitude 18·5 to 21·0, based in part upon Selected Areas, are mostly fainter than our limit with the photocell, and we can say nothing about the scale from 19 to 21; but from comparisons with SA68, Baade (**15**) has given corrections to Hubble's magnitudes of stars in the region of M31, ranging from +0·35 at 18·3 to +0·63 at 20·0. The exact relations between our magnitudes and those of Baade in SA68 are not yet available. I have heard that some philosophers say that the only time you can be sure you are talking sense is when you are counting. In cosmology you can make sense only if you know exactly when and where you have stopped counting.

Nebulae.—We come to the observations of faint nebulae. In 1947, in cooperation with Messrs. Hubble and Baade, Whitford and I started, in addition to the work on Selected Areas, the measurement of more than one hundred nebulae for magnitude and colour with the reflectors at Mount Wilson. Most of these objects of various types were on a routine programme, but we also concentrated on a few clusters of nebulae where the red shifts had been determined by Humason.

The clusters were in Virgo, Coma Berenices, Corona Borealis and Bootes, the last a single nebula with a red shift giving a velocity of 38,900 km./sec. The results were published two years ago (**16**). By limiting the discussion to the E types, the dispersions in the intrinsic colours were minimized, and we came to the unexpected result that these faint nebulae were reddened more than would be expected from their red shifts. Some of the conclusions were:—

1. The energy-curves of the nebulae are those to be expected from mixtures of stars; they show excess in both the infra-red and ultra-violet over that of a black body or of a single star. The ultra-violet excess must be taken into account in evaluating the effect of the red shift.

2. The E nebulae show a reddening proportional to the red shift. This fact may be taken as corroborative evidence for a linear velocity-distance relation. About 60 per cent of the reddening is a colour excess not explained as a consequence of the red shift. The figures of the Bootes nebulae are: colour excess, 0·52 mag.; amount attributable to red shift 0·22 mag., amount unaccounted for, 0·30 mag.

3. If the excess reddening is a distance effect caused by selective absorption by internebular material similar to the interstellar material in our galaxy, then, with a ratio of four to one for total to selective absorption, the photographic absorption for the Bootes nebula becomes $A_{pg}=4\times0{\cdot}30=1{\cdot}2$ mag. for an uncorrected distance of 70,000,000 parsecs, corrected to 40,000,000 parsecs because of absorption. Any such absorption would mean a virtual impenetrability of space within only a few times the distance to the Bootes cluster. Also, with the run of the nebular counts, which Hubble has found to indicate nearly uniform distribution in transparent space, this reddening would mean a strong outward increase in density of distribution.

4. An alternative to the absorption effect is a time effect, namely, that the E nebulae were formerly redder than now, and what we see is their progressive change in colour in the interval of 2×10^8 years from the Bootes nebula inward. The effect could be produced if the E nebulae formerly contained large numbers of high-luminosity red giant stars which have faded since the light left the distant ones. The corrections to the photometric distances on the time-effect hypothesis would be less than for the space-reddening hypothesis and of the opposite sign.

The foregoing alternatives of absorption effect and time effect summarize the situation as Whitford and I saw it three years ago after one season of observations. We were aware that a further test would be to measure the colours of spirals in the clusters of Corona and Bootes, if they could be found. The difficulties are that because of greater dispersion in their intrinsic colours the spirals are poorer standards than the elliptical ones, and with less concentration of light toward their centres their red shifts are more difficult if not impossible to determine.

In 1949 Whitford measured the colours of seven nebulae of types Sb and Sc in the vicinity of the Corona cluster. The results have been referred to privately as indicating that the Sb's exhibit the same excess as the E's, but that the Sc's have colours agreeing with the red shift of 22,000 km./sec. One of the complications is whether some of the objects should be classified as Sb or Sbc. Also, since the red shifts have not been measured for these spirals, any inferences from their colours should wait until they are shown really to have the velocity of the Corona cluster.

The case for the Bootes cluster is different. Within the past month, in 1950 September, Whitford has sent me the latest measures by himself and

Johnson of three additional E nebulae in Bootes, taken with the 100-inch telescope. All of magnitude 19·0 or fainter, they form a little group not far from the previously measured No. 1 nebula ; and while their red shifts are lacking, there can be little doubt that they belong to the cluster. The preliminary data are in Table III.

TABLE III

Magnitudes and Colours of Nebulae in Bootes

Nebula	Pg_p	C_p	A.D. of C_p	Obs.	Remarks
No. 1	18·23	+1·36	±0·07	3	
2	19·33	+1·39	±0·10	3	1 poor
3	19·17	+1·31	±0·05	2	
4	18·97	+1·17	...	1	Good
	Mean C_p		+1·31	±0·07	
	Standard, E nebula		+0·84		
	ΔC, obs.		+0·47		
	ΔC, comp.		+0·22		
	Excess		+0·25		

The unexplained excess is reduced to 0·25 mag. from the 0·30 mag. given by the single No. 1 nebula. The agreement of the first three nebulae is too good to be true; and a discordance like that of No. 4 is to be expected from the dispersion in colour of the E's in Virgo and elsewhere. The evidence for the reddening of the nebulae is much strengthened by having four objects instead of one at the farthest limit; and whether the excess is 0·25 or 0·30 mag. makes little difference; we are back to where we were in the discussion.

Now that the observed reddening of the Bootes nebula has been confirmed, the only way to reduce the infra-red colour excess would seem to be to revise our calculated effect of the red shifts. The procedure, depending upon the energy curves of the Sun and the elliptical nebula, M32, can be found in our original paper. To the criticism that far-reaching conclusions should not be based upon observational results on a single cluster of nebulae, the answer is that up to recently only one other velocity near 40,000 km./sec. has been measured, that of a nebula in Ursa Major No. 2. The assumption that the linear relation between red shift and distance holds to magnitude 21, involves an extrapolation of 3 magnitudes from the last measured red shift at magnitude 18; that is, an extrapolation by a factor of 4 in the distance and by a factor of more than 60 in the volume of space considered. These uncertainties, combined with the uncertainties in the zero point and scale of the magnitudes indicate that the whole picture of the observable region of space can be subject to serious modification by further work on faint nebulae.

In his studies of the distribution of the nebulae, Hubble (**17**) considered both the possibilities of space absorption and of the change of luminosity of the nebulae with time, but he decided that the effect of the red shifts was more important in modifying the calculated departures from uniform distribution. Whether this view is to be maintained or not, the assumption that the nebulae radiate like black bodies at 6000 deg. must be changed, and, as mentioned, the zero point and scale of magnitudes down to the limit of discussion will have to be checked beyond question. Lest there be any misunderstanding about Hubble's attitude on these matters, I repeat that it was on his initiative and with his cooperation that we undertook the photoelectric observations of the nebulae herein described.

We should like to apply the photocell to something constructive in the problems of cosmology. One possibility could be the testing of faint field nebulae for cases

of large colour excess. No matter what the interpretation of the reddening may be, if the linear relation between colour index and red shifts holds, the search for non-cluster nebulae with large red shifts could presumably be made more rapidly with the photometer than with the spectrograph; say something like one hour per object as against several hours or even all night for the same limit, with the probability of a negative result most of the time. Here again, however, we can refer such problems to photography where hundreds of objects are recorded simultaneously and where there should be little difficulty in searching on yellow or red photographs down to photographic magnitude 21, because the reddened nebulae will be more than a magnitude brighter on the photovisual scale. If such a search for very red nebulae were made photographically, the suspicious objects could be checked with a photocell.

Conclusion.—In closing this account of some of the problems we have attempted to attack with the photoelectric cell, I am somewhat appalled, even embarrassed, by the range of the problems, as well as by the range of the brightnesses of the objects we have observed. From the Sun to the Moon to Sirius to a star of magnitude 19, is about 45 magnitudes, or a change of intensity of 10^{18} to 1; and throughout this whole interval the constant effort has been to get a large value for the ratio, signal to noise, also expressible as the ratio of data to errors; or, if you like, the ratio of what you want to what you do not want. During the improvement in the sensitivity of the apparatus by a factor of some hundreds of millions, the increase in relative precision has been something like a factor of only ten, from errors of a few hundredths to errors of a few thousandths of a magnitude; but the achievement of another decimal place is always welcome in any division of physical science. From my own considerable experience in the past, perhaps I should have ideas about some of the next steps in astronomical photometry; but I cannot predict what will happen in this field even in the near future. In any event it now seems truer than ever that in astronomy as elsewhere the applications of the photoelectric cell are limited only by the imagination of the experimenter.

The recent and current investigations at the Lick Observatory, University of California, have been carried on as a project under the United States Office of Naval Research, and have also been supported by grants from the American Philosophical Society.

References

(1) Stebbins and Whitford, *Mt. W. Contr.* No. 712; *Ap. J.*, **102**, 318, 1945.
(2) F. H. Seares, *Mt. W. Contr.* No. 685, p. 9; *Ap. J.*, **98**, 310, 1943.
(3) J. Stebbins, *Mt. W. Contr.* No. 704; *Ap. J.*, **101**, 47, 1945.
(4) W. M. Smart, *M.N.*, **95**, 644, 1935.
(5) Stebbins, Huffer and Whitford, *Mt. W. Contr.* No. 617, p. 13; *Ap. J.*, **90**, 221, 1939.
(6) W. H. Christie, *Mt. W. Contr.* No. 620; *Ap. J.*, **91**, 8, 1940.
(7) Stebbins and Whitford, *Mt. W. Contr.* No. 547; *Ap. J.*, **84**, 132, 1936.
(8) W. Becker, *Die Himmelswelt*, **55**, 177, 1948.
(9) N. U. Mayall, *Lick Contr.*, Ser. II, No. 15, p. 198; *Ap. J.*, **104**, 305, 1946.
(10) Stebbins and Whitford, *Mt. W. Contr.* No. 753; *Ap. J.*, **108**, 413, 1948.
(11) E. Holmberg, *Lund Medd.*, Ser. I, No. 170, 1950.
(12) Stebbins, Whitford and Johnson, *Ap. J.*, **112**, 1950.
(13) Seares, Kapteyn and van Rhijn, Carnegie Institution of Washington, 1930.
(14) E. Hubble, *Mt. W. Contr.* No. 557; *Ap. J.*, **84**, 517, 1935.
(15) W. Baade, *Mt. W. Contr.* No. 696, p. 6; *Ap. J.*, **100**, 142, 1944.
(16) Stebbins and Whitford, *Mt. W. Contr.* No. 753; *Ap. J.*, **108**, 413, 1948.
(17) E. Hubble, *op. cit.*

A PHOTOGRAPHIC SURVEY OF BRIGHT SOUTHERN PLANETARY NEBULAE

David S. Evans and A. D. Thackeray

(Received 1950 June 5)

Summary

Twenty-six objects believed to be planetary nebulae with diameters greater than 8 seconds of arc, south of declination $-40°$, have been investigated. Descriptions, and photographs of those which definitely are planetary nebulae, are presented. Some comments on the classification of planetary nebulae are offered, and the proportions exhibiting various types of symmetrical form are tabulated.

The present project originated in a suggestion by Professor J. H. Oort, made during a visit to the Radcliffe Observatory in 1948. It was felt that, although the proper motions of planetary nebulae would probably be very small, it was nevertheless desirable that plates which might provide first-epoch positions should be obtained as soon as possible. The project was later extended, and much longer exposure plates were taken, in order to provide, in addition, a descriptive catalogue of bright southern planetaries. A list of objects believed to be planetary nebulae, having diameters of more than 8 seconds of arc, south of declination $-40°$, contained 26 objects. In the course of 1948–50, a total of 123 plates of these objects was obtained. This included 16 plates of IC 4406 (already described elsewhere by one of us, DSE)* and of the remainder, 89 plates are by DSE and 18 by ADT.

Table I lists the objects observed, with references to the literature, the numbers of the plates in the Radcliffe files which are recommended for possible proper motion studies, and the numbers of the accompanying illustrative photographs.

At first sight it appears that there is a large literature on the planetary nebulae described here, but, in actual fact, a great many of the works cited are compilations from earlier publications. In the NGC (1), based to a considerable extent on the work of the Herschels, the classification of southern planetaries as such is by appearance, and rests on Sir John Herschel's "Results of Astronomical Observations made in 1834–8 at the Cape of Good Hope" (London, 1847). Campbell and Moore's work (2), done with the spectroscope, represents the most reliable source. A number of identifications by Mrs Fleming, quoted in the Index Catalogue, also have a spectroscopic basis. For the southern nebulae the source of the magnitudes and diameters given by Vorontsov-Velyaminov and Parenago (3) is the examination of the Franklin-Adams plates. The results obtained are repeated by Vorontsov-Velyaminov in his compilation (4). In this work it is stated that all the images were stellar, and that the appearance of the stellar images was used to assign integrated magnitudes. In addition the image diameters were used to assign diameters to the nebulae. This seems to be a double use of the same material, and does not seem very reliable. Indeed,

* *M.N.*, **110**, 37, 1950.

Vorontsov-Velyaminov himself does not regard the results of any of these southern nebulae as meriting more than assignation to his class of third quality results. In addition all "stellar" nebular images were arbitrarily assigned a diameter of ?2″. Most of the other references are to particular individual nebulae. It follows, therefore, that in fact the observational basis for previous

TABLE I

No.	Designation	Position (1950)		Galactic coords.		Literature	PM plates	Figure No.	Remarks
1	...	$5^h\,43^m.4$	$-67°\,53'$	$244°$	$-32°$	(7), (9), (11)	...	1	PNP
2	IC 2448	$9^h\,06^m.6$	$-69°\,44'$	$253°$	$-15°$	(1), (2), (3), (4)	A648 A684	2	P
3	NGC 2792	$9^h\,10^m.6$	$-42°\,14'$	$234°$	$+5°$	(1), (2), (3), (4), (8), (14)	A649 A665	3	P
4	NGC 2867	$9^h\,20^m.0$	$-58°\,06'$	$246°$	$-6°$	(1), (2), (3), (4), (18)	A685	4	P
5	NGC 3132	$10^h\,04^m.9$	$-40°\,11'$	$240°$	$+13°$	(1), (2), (3), (4), (12), (13)	A252 A253	5	P
6	NGC 3195	$10^h\,10^m.1$	$-80°\,37'$	$264°$	$-20°$	(1)	A265	6	P
7	NGC 3211	$10^h\,16^m.2$	$-62°\,26'$	$254°$	$-5°$	(1), (2), (3), (4)	A701	7	P
8	...	$11^h\,26^m.2$	$-52°\,39'$	$258°$	$+9°$	(2), (4)	A297 A298	8	P
9	NGC 3918	$11^h\,47^m.8$	$-56°\,54'$	$263°$	$+5°$	(1), (2), (3), (4)	A704	9	P
10	NGC 5189	$13^h\,29^m.9$	$-65°\,43'$	$275°$	$-4°$	(1), (2), (4), (12)	...	10	PNP
11	NGC 5307	$13^h\,47^m.9$	$-50°\,58'$	$280°$	$+10°$	(1), (2), (3), (4)	A706	11	P
12	IC 4406	$14^h\,19^m.3$	$-43°\,55'$	$288°$	$+15°$			...	P
13	...	$15^h\,30^m.2$	$-58°\,59'$	$290°$	$-2°$	(3), (4), (5)	A305 A337	13	P
14	...	$15^h\,47^m.4$	$-51°\,21'$	$297°$	$+1°$	(6)	A335 A342	12	P
15	...	$16^h\,10^m.5$	$-54°\,50'$	$297°$	$-4°$	(4), (5)	A336 A343 A349	14a 14b	P
16	...	$16^h\,13^m.5$	$-51°\,52'$	$300°$	$-1°$	(4), (5)	A403 A430	15	P
17	NGC 6153	$16^h\,28^m.0$	$-40°\,08'$	$310°$	$+4°$	(1), (2), (3), (4), (10), (11)	A344 A404	16	P
18	IC 4642	$17^h\,07^m.6$	$-55°\,20'$	$302°$	$-10°$	(1), (2), (3), (4), (6)	A345 A353	17	P
19	NGC 6326	$17^h\,16^m.8$	$-51°\,42'$	$306°$	$-10°$	(1), (2), (3), (4)	A433	18	P
20	...	$18^h\,02^m.8$	$-50°\,37'$	$310°$	$-15°$	(6)	...	...	NP
21	NGC 6630	$18^h\,27^m.7$	$-63°\,19'$	$299°$	$-23°$	(1), (6)	A434	19	?P
22	IC 4723	$18^h\,31^m.1$	$-63°\,26'$	$299°$	$-23°$	(1), (6)	...	20	?P
23	NGC 6707	$18^h\,51^m.3$	$-53°\,53'$	$310°$	$-23°$	(1), (17), (19)	...	...	NP
	NGC 6708	Nf 6707 by 6′							
24	NGC 6902	$20^h\,21^m.2$	$-43°\,50'$	$325°$	$-36°$	(1), (15), (16), (17)	...	...	NP
25	...	$22^h\,35^m.5$	$-57°\,29'$	$298°$	$-53°$	(3), (4), (5)	...	...	NP
26	NGC 7408	$22^h\,52^m.7$	$-63°\,58'$	$289°$	$-49°$	(1), (3), (4), (5)	...	...	NP

In the Remarks column: P denotes an accepted planetary.
NP denotes " not a planetary ".
PNP denotes " probably not a planetary ".

discussions of southern planetary nebulae has been very slight, and is by no means as extensive as might be inferred from our reference list.

We now proceed to a short discussion of each object in turn:—

No. 1:

Innes (**9**), studying three plates taken with the 10-inch Franklin-Adams cameras, gives the three descriptions:—

"Large but faint spiral with stars: a small cluster forms the nucleus."

"Fine circular spiral with stars."

"Very fine circular spiral with stellar nucleus."

In 1927 the same author (**11**) says: "The stars in this spiral nebula are shown as a letter S but the nebulosity is virtually invisible". Jenka Mohr (**7**) discusses plates taken with the 24-inch Bruce, the 10-inch Metcalf and the 3-inch Ross Fecker instruments at Bloemfontein. The diameter is given as 420 seconds of arc, and it is stated that the nucleus "appears to be a central star of magnitude 12·6, but it is possible that this star is merely superposed". It is pointed out that the nebula is almost certainly superposed on the Magellanic Cloud, since, at the distance of the cloud, it would have the very large diameter of 50 parsecs. Estimates based on statistical discussions of planetaries, assuming the selected star to be the central star, give distances of 1200 parsecs and 2000 parsecs.

Our plates show very faint nebulosity (invisible to the eye in the telescope) with a diameter of 420 seconds of arc. The nebulosity is much brighter on the preceding side. There is a wispy structure with some suggestion of a spiral or helical form. The nebula does not seem to be a typical planetary, and it is quite impossible to designate any particular star as the nucleus. Our photographs show the central area to be occupied by two distinct and compact groups of stars, some of which appear to be directly mingled with nebulous wisps. The galactic latitude is greater than that of any accepted planetary in our list, and in view of the great variety of nebulosities with complex forms appearing throughout the Magellanic Cloud, the explanation in terms of a galactic planetary superposed on the Cloud is not clearly demanded. Evidence in favour of its belonging to the Cloud is strengthened by the presence of the double cluster in the central region, which is unlikely to be galactic. If it belongs to the Cloud it must be rejected as a true planetary, and the problem arises of how such regularity can be exhibited by nebulosity 50 parsecs in diameter. Purely on appearance the nebula might be thought to resemble the final stage of a supernova outburst. The photograph, Plate 8, Fig. 1, has been intensified to bring up the faint nebulosity.

No. 2: IC 2448.

This planetary (**1**) was found on the basis of its spectrum by Mrs Fleming, who designated it as "Planetary, stellar". Campbell and Moore (**2**) give a diameter of 8″, magnitude 9, spectrum N_1, N_2, $H\beta$ (10:4:1), velocity $= -24$ km./sec. Vorontsov-Velyaminov (**3**), (**4**) gives diameter 8″, integrated magnitude 11·5. Our plates, Fig. 2, show a bright central star, with a small oval patch of luminosity placed slightly eccentrically; dimensions $9'' \times 7''$.

No. 3: NGC 2792.

Dreyer (**1**) says: "Remarkable planetary, pretty bright, equivalent to 9th magnitude star, very small, round, among stars". Campbell and Moore (**2**) give a diameter of 10″, 10th magnitude, spectrum N_1, N_2, velocity $= +14$.

Innes (**8**) says: "An 11th magnitude planetary about 20″ in diameter. Is Np a pair of 10·5 mag. stars. No stars within 3′". Gregory (**14**) has: "Planetary, pretty bright, small, very little extended in P.A. 165° ±. Appears as a nearly uniform disc without a central star". Vorontsov-Velyaminov (**3**), (**4**) assigns diameter 10″, magnitude 13·5. We find a typical, almost symmetrical, ring nebula, with central star. The ring is slightly brighter to the south. Diameter 13″. (Plate 8, Fig. 3.)

No. 4: NGC 2867.

Dreyer (**1**) says: "Very remarkable planetary, equals 8th mag. star, very small, round. 15th mag. star at P.A. 59°, distant 13″". Delisle Stewart (**18**) gives a diameter of 18″. Campbell and Moore (**2**) have: "Diameter 8″, round, edges sharply defined. Centre appears fainter. May be very small ring nebula. Mag. 8·5. Velocity = +18 km./sec.". Vorontsov-Velyaminov (**3**), (**4**) has diameter 8″, magnitude 9·7. The object is a bean-shaped ring nebula, the ring being broken up into spots of brightness, brightest in the Sp sector. The central star is faint. About 13″ × 11″. (Plate 8, Fig. 4.)

No. 5: NGC 3132.

Dreyer (**1**) says: "Very remarkable planetary; very bright, very large; little extended; star of 9th magnitude in the middle, 4^s diameter". Campbell and Moore say: "Ring nebula with 8·8 magnitude star in centre. Diameter of ring about 30″. Spectrum: N_1, N_2, $H\beta$, N_3 (10 : 4 : 1 : 1); $V = -8$ km./sec.". There is a drawing by Wilson. Vorontsov-Velyaminov (**3**), (**4**) gives diameter 30″, integrated magnitude 8·2, central star, magnitude 10·6. Knox Shaw (**13**) has: "Very bright, pretty small, little elongated in P.A. 150° ± : annular ring, fainter on preceding side. B star not quite central and thus probably unconnected". A note says that the spectrum of the bright central star is continuous. Shapley and Paraskevopoulos (**12**) say: "A series of photographs of varying exposures would be necessary to bring out the intricate details . . . . It could well be named the "8-burst" planetary from the number of distinct arcs on the boundary of the main disc or shell. The class A star, HD 87892, mag. 9·5 is centrally superposed". A photograph is given.

The object has a complex structure, including a bean-shaped ring, very bright, with fainter, helical, extensions. Dimensions about 84″ × 53″. The object is illustrated in Plate 8, Fig. 5. Photographic manipulation has been employed to bring up the centre on the print, but the structure has not been falsified. There is a nucleus or foreground star on the ring in the Sp sector.

LEGENDS TO PLATE 8.

FIG. 1.
Object: $5^h\,43^m{\cdot}4$, −67° 53′
× 2·7.
Kodak 103–*a O*, 30 *mins.*

FIG. 2.
IC 2448, × 7·0.
Ilford Astronomical Zenith, 90 *secs.*

FIG. 3.
NGC 2792, × 7·0.
Ilford Astronomical Zenith, 5 *mins.*

FIG. 4.
NGC 2867, × 7·0.
Ilford Astronomical Zenith, 60 *secs.*

FIG. 5.
NGC 3132, × 5·8.
Kodak 103–*a O*, 16 *mins.*

FIG. 6.
NGC 3195, × 6·3.
Kodak 103–*a O*, 15 *mins.*

FIG. 7.
NGC 3211, × 6·3.
Ilford Astronomical Zenith, 10 *mins.*

Note.—The magnifications are relative to the original plate scale of 22″·5/mm.

FIG. 1.

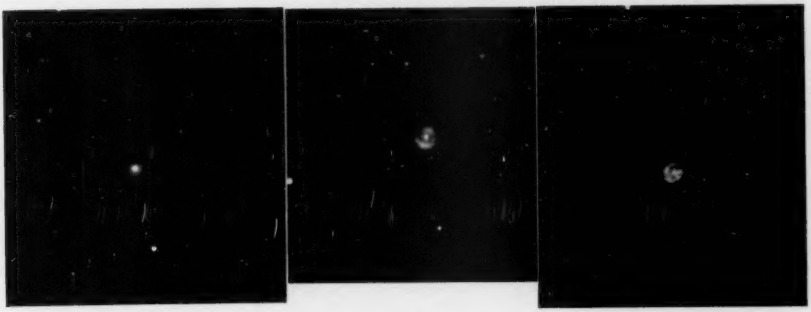

FIG. 2. FIG. 3. FIG. 4.

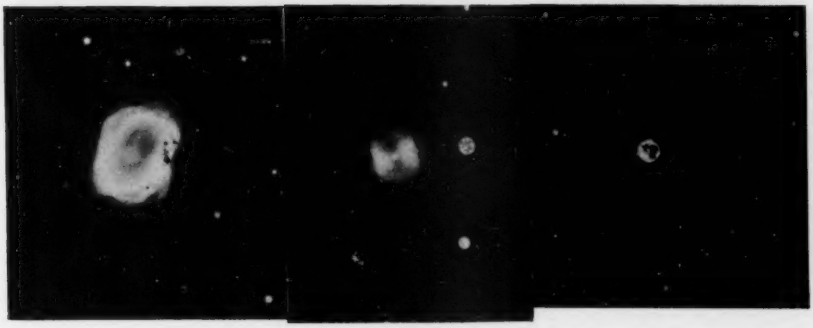

FIG. 5. FIG. 6. FIG. .7

David S. Evans and A. D. Thackeray, A Photographic Survey of Bright Southern Planetary Nebulae.

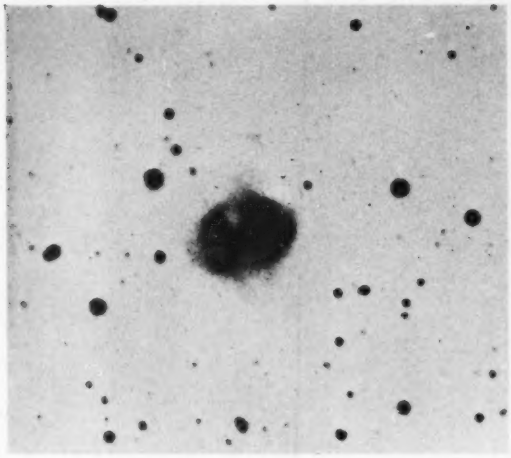

FIG. 8.
Object: $11^h\ 26^m{\cdot}2$, $-52^\circ\ 39'$
×9·0.
Kodak 103–*a O*, 30 *mins.*

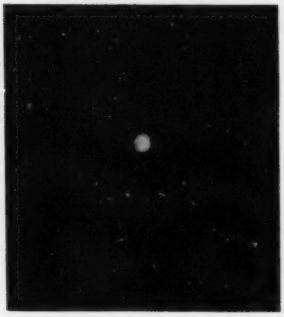

FIG. 9.
NGC 3918, ×5.
Ilford Astronomical
Zenith, 20 *secs.*

FIG. 10.
NGC 5189, ×7·0.
Kodak 103–*a O*, 30 *mins.*

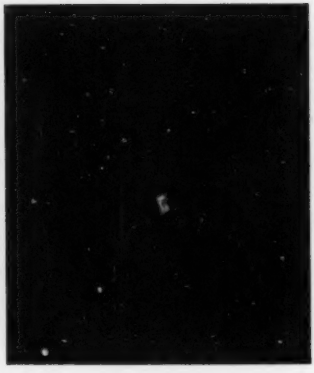

FIG. 11.
NGC 5307, ×7·0.
Ilford Astronomical
Zenith, 5 *mins.*

David S. Evans and A. D. Thackeray, A Photographic Survey of Bright Southern Planetary Nebulae.

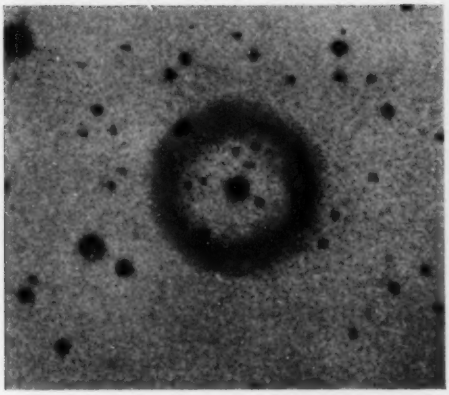

FIG. 12.
Object: $15^h\ 47^m{\cdot}4$, $-51°\ 21'$
$\times 8{\cdot}8$.
Kodak 103–*a E*, 20 *mins.*

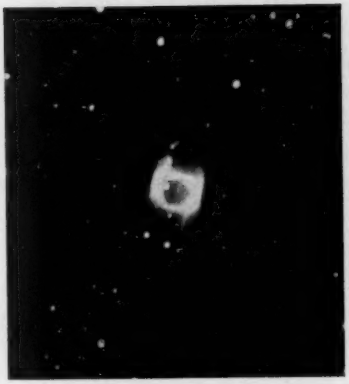

FIG. 13.
Object: $15^h\ 30^m{\cdot}2$, $-58°\ 59'$
$\times 6{\cdot}3$.
Kodak 103–*a E*, 20 *mins.*

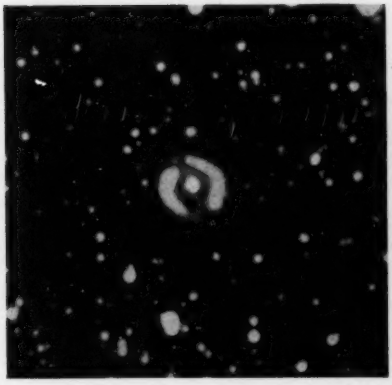

FIG. 14 *a*.
Object: $16^h\ 10^m{\cdot}5$, $-54°\ 50'$
$\times 10$.
Kodak 103–*a O*, 40 *mins.*

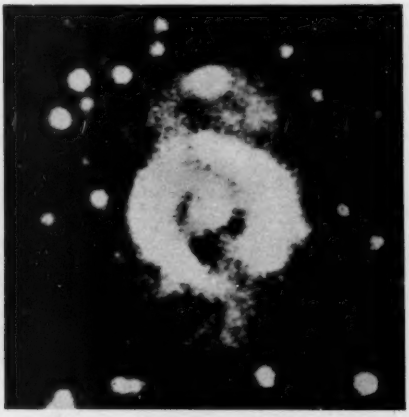

FIG. 14 *b*.
Object: $16^h\ 10^m{\cdot}5$, $-54°\ 50'$
$\times 23$.
Kodak 103–*a O*, 40 *mins.*

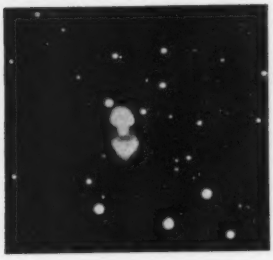

FIG. 15.

FIG. 16.

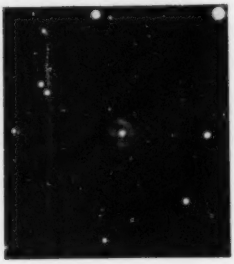

FIG. 17.

FIG. 18.

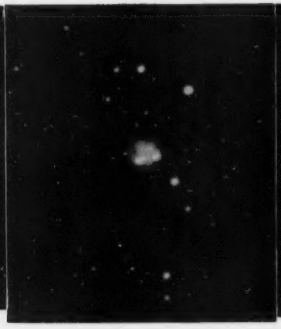

FIG. 19.

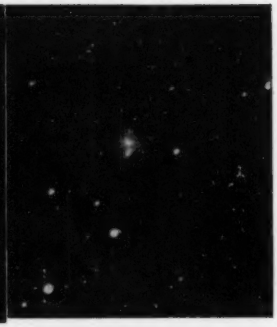

FIG. 20.

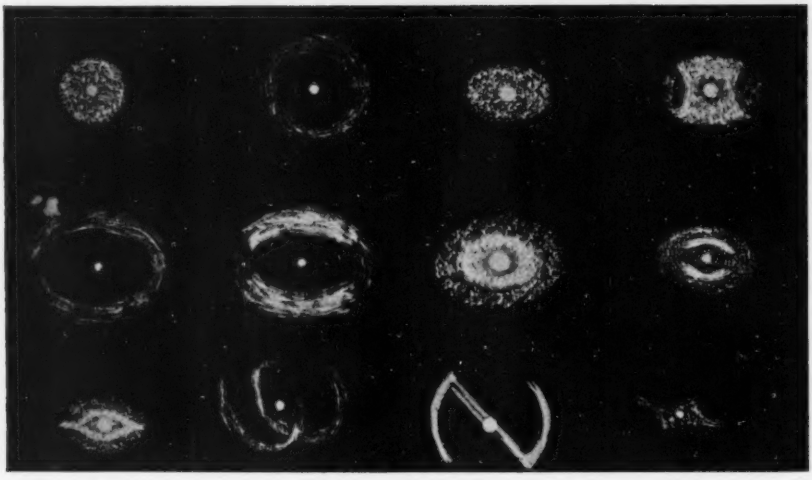

FIG. 21.

David S. Evans and A. D. Thackeray, A Photographic Survey of Bright Southern Planetary Nebulae.

No. 6: NGC 3195.

Dreyer (**1**) says: "Remarkable planetary, pretty bright, small, little extended; 13^s diameter; three small stars near". We find (Plate 8, Fig. 6) an oval nebula with central star. There are two sectors of great brightness on the oval to east and west, and faint extensions in the form of a ring to north and south. Dimensions about $44'' \times 33''$.

No. 7: NGC 3211.

Dreyer (**1**) says: "Planetary, equals 10th magnitude star, round, among 150 stars". Campbell and Moore (**2**) give: "Planetary, round, diameter $8''$, 10th magnitude. Spectrum N_1, N_2, $H\beta$, N_3 (10:4:1:2). $V = -16$ km./sec.". Vorontsov-Velyaminov (**3**), (**4**) has diameter $8''$, integrated magnitude 11·8. The object (Plate 8, Fig. 7) is a bright disk $14''$ in diameter, with a slight bump on the northern edge. The central star is barely visible.

No. 8:

Campbell and Moore (**2**) give the description: "Faint patch of nebulosity slightly elongated: trace of nucleus: diameter about $15''$, but limits are quite indefinite. Spectrum; N_1; $V = +2{\cdot}8$ km./sec. All the plates are much underexposed". Vorontsov-Velyaminov (**4**) merely repeats these details.

Positive prints show an image precisely like the face of a circus clown, but a negative is more revealing. The central star is surrounded by an oval extended roughly east and west, and having dimensions about $45'' \times 30''$. There is a faint dark lane concentric with the main oval, so that in fact we have an oval outer ring. On the following side is a dark indentation (the clown's mouth), while the "eyes" are dark areas extending almost north and south from the central star. The ring is brighter on the north preceding side, while on the preceding end is a bright nucleus (? star). There is a very faint equatorial hoop extending north and south (the clown's "ears"), having a total extent of about $60''$. The contrast of the negative print (Plate 9, Fig. 8) has been increased.

No. 9: NGC 3918.

Dreyer (**1**) says: "Planetary, remarkable, small, round, blue, equals 7th magnitude star. Diameter $1^s{\cdot}5$". Campbell and Moore (**2**) say: "Very bright planetary, magnitude 8·5, diameter $10''$, spectrum:—N_1, N_2, $H\beta$, N_3, $\lambda 4363$, $H\gamma$, $H\delta$, $\lambda 3768$; $V = -16{\cdot}4$ km./sec. Intensities, N_1, N_2, $H\beta$, N_3 (10:3:1:1)". Vorontsov-Velyaminov (**3**), (**4**) gives a diameter of $10''$ and integrated magnitude 8·4. We find a simple disk with very slight equatorial structure. No central star is visible.

LEGENDS TO PLATE 11.

FIG. 15.
Object: $16^h\ 13^m{\cdot}5$, $-51°\ 52'$ $\times 6{\cdot}5$.
Kodak O–E, 20 mins.

FIG. 16.
NGC 6153, $\times 9{\cdot}0$.
Ilford Astronomical Zenith, 10 mins.

FIG. 17.
IC 4642, $\times 6{\cdot}5$.
Ilford Astronomical Zenith, 10 mins.

FIG. 18.
NGC 6326, $\times 6{\cdot}6$.
Kodak O–O, 3 mins.

FIG. 19.
NGC 6630, $\times 6{\cdot}6$.
Kodak 103–a E, 15 mins.

FIG. 20.
IC 4723, $\times 6{\cdot}6$.
Kodak 103–a E, 15 mins.

FIG. 21.
Types of symmetrical planetary nebulae.

a	*b*	*c*	*d*
e	*f*	*g*	*h*
j	*k*	*l*	*m*

Note.—The magnifications are relative to the original plate scale of $22''{\cdot}5$/mm.

Efforts by one of us (ADT) to reveal it, using green filters and F-type plates to cut out the nebulium lines, have met with no success. Diameter 13″. (Plate 9, Fig. 9.)

No. 10: NGC 5189.

The NGC says: "Remarkable, blue, pretty large: considerably extended: brighter towards the middle: curved axis: 4 stars involved". There is a drawing by Sir John Herschel (*loc. cit.*). Campbell and Moore (**2**) say: "Nebulous field about 1′·3 in length. Composed of three nebulae. NGC 5189, the following one of the three is about 20″ in diameter, and slightly fainter than the spindle shaped nebula in the centre. Spectrum, N_1, N_2 (10:3). $V = -6$ km./sec.". There is a drawing by Wilson. It is evident from this that Campbell and Moore regard NGC 5189 as being one of a group of nebulae, whereas in fact the whole mass is a single complex nebula which is not a typical planetary. Vorontsov-Velyaminov (**4**) simply quotes Campbell and Moore (**2**). Shapley and Paraskevopoulos (**12**) give a drawing and say: "NGC 5189, near the galactic equator is a gaseous nebula of such remarkable knotted structure that it is here best represented by a drawing. No bright star is involved in the nebulosity, but 6′ to the south is the 7th magnitude star HD 117694, B9. In the HD catalogue there is no star with a spectrum earlier than B5 within a degree of the nebulosity. Overall dimensions 3′·0 × 2′·0". Our photograph, Plate 9, Fig. 10, shows no central star; the object is clearly not an ordinary planetary. Dimension, east–west 185″; north–south 130″. The structure is helical or S-shaped*.

No. 11: NGC 5307.

Dreyer (**1**) says: "Planetary, or very faint extended small double nebula". Campbell and Moore (**2**) say: "Planetary, elongated in north and south direction, 8″ × 10″. Magnitude 11. Spectrum: N_1, N_2, $H\beta$ (10:3:?). $V = +42$ km./sec.". Vorontsov-Velyaminov (**3**), (**4**) gives the same dimensions, but integrated magnitude 12·1. We find (Plate 9, Fig. 11) a small gaseous parallelogram elongated roughly north and south with a central star. Dimensions about 15″ × 10″.

No. 12: IC 4406.

This nebula has been discussed at length by one of us (DSE).†

No. 13:

Found by Menzel (**5**) on a Bruce plate taken at Arequipa and classified as planetary on the basis of its appearance. Menzel states that it is bi-nuclear and gives an angular diameter of 24″. Vorontsov-Velyaminov (**3**), (**4**) gives a diameter of 24″, integrated magnitude 12·5. Our photograph, Plate 10, Fig. 13, shows a very complex structure. A bright ring 34″ in diameter and of oval shape, shows two stars within it. The appearance is as if this bright ring formed the base of a cylinder with generators extending roughly northward, with the exception of one line, which also extends slightly south. The nebula terminates in the north with a second, fainter and slightly smaller ring, seeming to form the top of the cylinder. This ring has three bright spots on it, and also has a bright nucleus (? faint star). Total length about 55″.

* NGC 5189 is referred to by Radlova, Katz and Dokychaeva, *Russian Astronomical Journal*, **26**, 160, 1949 (in Russian). The data are however merely derived from Franklin-Adams and Wolf Palisa charts.

† *M.N.*, **110**, 37, 1950.

No. 14:

Shapley (**6**), who found this fine ring nebula on plates of Milky Way field 233, gives a magnitude of 3·16 and a diameter of 72″. He says: "The width of the ring, which is circular, and nearly uniform all the way round, is 15 seconds of arc". Plate 10, Fig. 12, in which the contrast of the faint ring has been increased, shows these data to be correct. The ring is brighter on the preceding side.

No. 15:

Found by Menzel (**5**) and classified on appearance. Diameter 30″, quoted by Vorontsov-Velyaminov (**4**). Menzel says that it appears to be annular. The object consists of a ring of diameter 28″, breached to north and south, so that in effect, it is composed of two comma-shaped masses of gas. From the tails of the commas extend curved wisps of faintly illuminated gas with small radii of curvature. The northern one has a bright knot on it, almost in line with the breach in the main ring. Total extent, north to south, about 45″. Plate 10, Fig. 14*a* is a normal print: the contrast of Plate 10, Fig. 14*b* has been increased, the better to show the fainter parts of the nebula.

No. 16:

Found by Menzel (**5**), who gives a diameter of 12″ and says that it appears to be annular. Vorontsov-Velyaminov (**4**) quotes this diameter. This peculiar object consists of a central star with luminous masses to north and south (Plate 11, Fig. 15). That to the north is almost globular and appears slightly to overlap the central star. The mass to the south is concave towards the star, and shows some trace of an absorption shell. Extending southward from this second mass is a faintly luminous pointed "beard". Dimensions: north–south, 35″; east–west about 16″.

No. 17: NGC 6153.

Dreyer (**1**) describes this planetary, discovered by Copeland, as "planetary, stellar". Campbell and Moore (**2**) observed the N_1 line, and assigned $V = +39$. Van den Bos (**11**), observing with the 26-inch refractor of the Union Observatory, described it as a planetary, with major axis 28″ in P.A. 7°–187°, minor axis 22″. Finsen (**10**) describes it as a ring nebula. Vorontsov-Velyaminov (**3**), (**4**) assigns his conventional diameter ?2″, and magnitude 11·5.

We find (Plate 11, Fig. 16) an object with a central star surrounded by a circular area of luminosity of diameter 20″. On this is superposed a curious arched structure resembling a geometrical diagram. It is a line of gas in the form of part of an elongated ellipse terminated by an asymmetrical chord. The curved part, which extends beyond the circular area, is faint. The sharper (preceding side) join of the chord and the ellipse is slightly extended in the form of a faint point projecting a little beyond the circular patch of luminosity. Dimensions: east–west, 21″; north–south, 28″.

No. 18: IC 4642.

Dreyer (**1**) takes this from the list of planetaries discovered by Mrs Fleming from their spectra. It is "planetary, stellar". Campbell and Moore (**2**) say: "This nebula is remarkable for the strength of the N_3 radiations. The exposures are too short. $V = +44$ km./sec.".

Vorontsov-Velyaminov (**3**), (**4**) assigns the conventional diameter ?2″, and integrated magnitude 12·4. Shapley (**6**) gives magnitude 14·4 and diameter 30″.

We find (Plate 11, Fig .17) an oval ring nebula with central star. The principal axis is in the direction Nf–Sp. The illumination of the ring is not uniform, and dark areas form a cross on the major and minor axes of the oval. Dimensions $18'' \times 15''$.

No. 19: NGC 6326.

Dreyer (**1**) says: "Very, very remarkable: pretty bright: very small, round". Herschel (*loc. cit.*) has a drawing. Campbell and Moore found the lines N_1, N_2, $H\beta$ (10:3:1±) ($H\beta$ very very faint), and give $V = +11$ km./sec. Vorontsov-Velyaminov (**3**), (**4**) assigns a magnitude 12·2 but no diameter. The object (Plate 11, Fig. 18) consists of a roughly rectangular area of luminosity about $12'' \times 10''$ with a central star. This forms the main "ring" of the nebula and in the south following corner it has a bright spot. There is a smaller, fainter, rectangular extension from the southern half of the preceding side. Dimensions about $16'' \times 11''$.

No. 20:

Shapley (**6**) reports a nebula, magnitude 11·9, diameter 36″ at position (1900) $17^h 58^m 53^s$, $-50° 37'·1$. We find nothing at the corresponding 1950 position.

No. 21: NGC 6630.

Dreyer (**1**) says: "Planetary, faint, small, round, gradually brighter in the middle". Shapley (**6**) gives magnitude 15·3, diameter 30″. The classification is by appearance. We find an object with a quadrilateral of four stars or nuclei surrounded by a nebulous envelope. The object is difficult, and it seems open to doubt whether the object is correctly classified as a planetary nebula. Dimensions about $19'' \times 15''$. (Plate 11, Fig. 19.)

No. 22: IC 4723.

The object enters the Index Catalogue (**1**) as one classified as a planetary on appearance by Dudley Stewart. His description is: "very faint, very small, round". Shapley (**6**) gives magnitude 15·4, diameter 27″.

We find (Plate 11, Fig. 20) a curious round object of diameter about 19″ with three distinct nuclei running along a north–south line across it. The designation as a planetary again seems doubtful.

No. 23: NGC 6707, 6708.

For the former, Dreyer (**1**) has: "Faint, small, very little elongated, gradually brighter in the middle". For the second: "Pretty faint, small, round, gradually pretty much brighter in the middle, last of group". Reynolds (**17**) has NGC 6707 as "Faint spiral, $3' \times 1'$". The classification as planetaries is by Frost (**19**): "very faint planetary elongated about 2′", and "Round planetary, magnitude 14". The objects prove to be definitely extragalactic.

No. 24: NGC 6902.

Dreyer (**1**) says: "Faint, considerably small, round, brighter in middle". Shapley and Ames (**16**) make it extragalactic: they give no description. Reynolds (**17**) also calls it a spiral, without description. The classification as a planetary nebula is by Madwar (**15**), who says: "Faint, round, 30″ diameter; planetary with a bright, almost stellar, nucleus".

Short exposures do show a structure closely resembling a planetary nebula, but longer ones reveal spiral arms. These are very faint, but the object is extragalactic, presumably a late-type spiral.

No. 25:

Discovered by Menzel (5), who gives a diameter of 30″. Vorontsov-Velyaminov (3), (4) makes it a planetary fainter than the 15th magnitude with diameter 30″. Our plates show a faint ring structure broken up into bright spots surrounding a blurred nucleus. The field is full of extragalactic nebulae, and we regard the classification as a planetary as incorrect.

No. 26: NGC 7408.

The NGC says: "Pretty bright, pretty small, round, very gradually a little brighter in middle". Vorontsov-Velyaminov gives a diameter of 72″ and a magnitude of 12·8. Menzel (5) assigns it to the planetary nebulae on the basis of appearance and assigns a diameter of 72″. The object is a barred spiral with a line of condensations or giant stars crossing it.

It is not the purpose of the present paper to offer a theoretical analysis of the forms of these planetaries, but we are undoubtedly in a somewhat favoured position in having the original material to hand, and there would seem to be no harm in mentioning some of the theoretical points—avowedly speculative—which we have discussed between ourselves. It is possible that these may suggest sound lines of investigation to theoretical workers.

A first problem is the question of the stability of ring structures: the classical form of the planetary nebula is a star surrounded by a uniform shell such as No. 14. Is this form stable, or if not, will the ring later be breached at roughly opposite points as in No. 15?

A second problem is provided by the frequency of axially symmetrical forms such as Nos. 6, 8, 16 and 18. This type of form would seem to link up with the fairly common helical form such as Nos. 5 and 13, where the impression is, for all the world, as if matter had been squirted out from two opposite poles of a rotating star and left behind as it went along. This crude picture is palpably ridiculous: the ejected matter must have the momentum of the parent star. Can it then be that this type of form results from the interaction of two bodies or of the star with an interstellar medium? No. 13 is designated in the literature by "? two nuclei", while No. 5 has a second star or nucleus superposed on the nebula or involved in it. We can say nothing more here on this point.

Finally, the form of No. 15 is especially intriguing. One is almost compelled to see the structure as one in which matter is being driven away through the two breaches by radiation pressure. Then when it gets clear of the inner ring it becomes less luminous, since it is now partly screened by the central ring. Possibly the bright knot to the north represents a region crossing back across the full stream of stellar radiation escaping through the northern breach. But why, we may ask ourselves, does this wispy material show so marked a curvature? The track is impossible for matter moving under a purely gravitational force, and radiation pressure would reduce the curvature, not increase it. Is it merely fanciful to see a resemblance to solar prominences in these arched structures? Qualitatively one might see the central star, plus the inner ring, as a region from which energetic electrons might readily escape to form a space charge around the structure, while the wisps of gas themselves must be regions in which, outside the main radiation blast of the central star, recombination is the dominant process: that is to say, the wisp must be rich in ions. Have we here a situation somewhat

similar to that proposed by one of us (DSE)* in connection with prominences, where, it was suggested, ions move in electric or magnetic fields? If this were so it might account for the opposite senses of the curvatures of the northern and southern wisps.

Now that we have good photographs of planetary nebulae available all round the Milky Way, it may be useful to offer some comments on the subject of the classification of planetary nebulae. Curtis† proposed a classification on the basis of form, but, as has been pointed out by Stoy‡, this classification is not very satisfactory. It does not satisfy the essential conditions that the system must be so devised that each planetary goes into one and only one class, and that independent workers, classifying the same material, must arrive at substantially the same results. A classification on the basis of the observed spectrum is also possible, and has been proposed by Wright.§ However, it seems desirable that both types of classification should be attempted, since the relations between the two may throw light eventually on the origin and evolution of planetary nebulae.

One of the most striking things about planetary nebulae is that a high proportion of them possess symmetry of various types. Any system which has symmetry properties immediately becomes much more amenable to the mathematics of theoretical discussion, and it therefore seems desirable in order to assist theoretical development to concentrate on the symmetrical forms which occur. This may be only a temporary expedient, but, as the result of trial and error, the authors have found that the use of symmetry properties as a basis for classification is one (and indeed the only one) which enables a substantial measure of agreement to be secured between independent workers attempting to classify the same material.

In Plate 11, Fig. 21 we illustrate some of the symmetrical forms which are of common occurrence. Plate 11, Fig. 21 *a* and *b* illustrate what we call the spherically symmetrical forms, the simple disk and the simple ring respectively. Fig. 21 *c*, *d*, *e*, *f*, *g*, *h* and *j* are forms having biaxial symmetry about two axes at right angles. The first two we call the simple disk and the doubly indented disk. The next two are the simple ring and the doubly indented ring. The last three represent three examples of what we call complex biaxial forms. Plate 11, Fig. 21*k* is the helical form. Finally *l* and *m* represent centrally symmetric forms in which the structure is unchanged by reflection of each point of itself in the central star. We have proceeded on the system that no nebula which does not strictly fall into one of these classes should be classified as regular. The results of this classification for the 81 nebulae in our list and in Curtis's list having dimensions over 8 seconds of arc are as follows:—

Spherical symmetry	: 10 per cent,
Biaxial symmetry	: 45 per cent,
Helical	: 5 per cent,
Central symmetry	: 10 per cent,
Irregular	: 30 per cent.

That is to say, 70 per cent of planetary nebulae exhibit a high degree of symmetry. Further, we find that classification on this basis is unambiguous. If desired, it

* *M.N.*, **106**, 300, 1946. See also Eddington, *Internal Constitution of the Stars*, Cambridge, 1930, p. 389, footnote.

† H. D. Curtis, *Lick Obs. Publ.*, **13**, 57, 1918.

‡ R. H. Stoy, *The Observatory*, **56**, 269, 1933.

§ W. H. Wright, *Lick Obs. Publ.*, **13**, 193, 1918.

is possible to split the first two classes into the sub-classes already enumerated, e. g. simple disk, simple ring and so forth, but then the classification by independent workers becomes more ambiguous.

One final point of interest is provided by the question of projection. The maximum axis ratio exhibited by symmetrical nebulae is about 2 : 1. If this is the true form of planetaries of this type, i. e. if they are prolate spheroids with axes in the ratios 2 : 1 : 1, what proportion will appear circular as the result of projection? It can readily be shown that the proportion of nebulae with observed axis ratios in the range R to $R+dR$ is

$$\frac{RdR}{\sqrt{\{3(4-R^2)\}}},$$

where R runs from 1 to 2. The integral of this, giving the proportion with axis ratios between 1 and $1+x$, is

$$1-\sqrt{(1-2x/3-x^2/3)}.$$

This gives 3·5 per cent of cases with axes differing by less than 10 per cent and 7·6 per cent of cases with axes differing by less than 20 per cent. That is to say that the observed percentage of spherically symmetric cases is much too high to be accounted for by projection alone.

We hope that the material and comments presented here will be found to be in a form particularly adapted to the needs of theoretical workers.

Radcliffe Observatory,
Pretoria:
1950 *May* 11.

References

(1) J. L. Dreyer, NGC and IC, *Memoirs R.A.S.*, **49**, 1888; **51**, 1895; **59**, 1908.
(2) W. W. Campbell and J. H. Moore, "Velocities of Bright Line Nebulae", *Publ. Lick Obs.*, **13**, 77, 1918.
(3) B. Vorontsov-Velyaminov and P. P. Parenago, *Russian Astronomical J.*, **8**, 206, 1931.
(4) B. Vorontsov-Velyaminov, "General Catalogue of Planetary Nebulae", *Astronomical Journal of the Soviet Union*, **11**, 40, 1934.
(5) D. H. Menzel, "Five New Planetary Nebulae", *Harvard Bull.*, No. 777, 1922.
(6) H. Shapley, "Five Planetary Nebulae and a Globular Cluster", *Harvard Bull.*, No. 902, 26, 1936.
(7) Jenka Mohr, "A Planetary Nebula superposed on the Large Magellanic Cloud", *Harvard Bull.*, No. 907, 13, 1938.
(8) R. Innes, *Union Observatory Circular*, No. 41, 345, 1918.
(9) R. Innes, *Union Observatory Circular*, No. 61, 233, 1924.
(10) W. S. Finsen, *Union Observatory Circular*, No. 69, 374, 1926.
(11) R. Innes, *Union Observatory Circular*, No. 73, 419, 1927; W. van den Bos, *ibid.*, p. 424.
(12) H. Shapley and J. S. Paraskevopoulos, "Photographs of Thirty Southern Nebulae and Clusters", *Harvard Reprint*, No. 184, 1940; and *Proc. Nat. Acad. Sci.*, **26**, 31, 1940.
(13) H. Knox Shaw, "Observations of Nebulae, 1912–14", *Helwân Obs. Bull.*, No. 15, 129, 1915.
(14) C. C. L. Gregory, "Fourth List of Nebulae Photographed with Reynolds Reflector", *Helwân Obs. Bull.*, No. 22, 219, 1921.
(15) M. R. Madwar, "Sixth List of Nebulae Photographed with the Reynolds Reflector", *Helwân Obs. Bull.*, No. 38, 1935.
(16) H. Shapley and A. Ames, "Survey of External Galaxies Brighter than 13th Magnitude", *Harvard Annals*, **88**, No. 2, 1932.
(17) J. H. Reynolds, "Spiral Nebulae in the Zone −40° to −90° (from the Franklin-Adams plates)", *M.N.*, **81**, 598, 1921.
(18) Delisle Stewart, *Harvard Annals*, **60**, 174, 1908.
(19) R. H. Frost, *Harvard Annals*, **60**, 190, 1908.

ON THE LUMINOSITY-VELOCITY RELATION OF CEPHEIDS

Svein Rosseland

(Received 1950 April 17)

Summary

The purpose of the paper is to clarify the ideas with respect to the phase relationship between luminosity and velocity of pulsating stars, which was recently discussed by Milne. Using a generalization of Milne's procedure and known results of non-adiabatic pulsation theory, it is shown that for small deviations from adiabatic equilibrium and a constant ratio of specific heats, the luminosity is closely in phase with the negative displacement, irrespective of the stellar model employed.

---

1. *Introduction.*—Since the inception of the pulsation theory of Cepheids various authors have attempted to explain quantitatively the observed approximate coincidence of maximum luminosity with maximum velocity of approach, which contrasts sharply with the common-sense expectation of maximum luminosity occurring at the time of highest compression. It was obvious that a *small* lag of the kind might be expected because of dissipation of wave energy by viscosity, conduction and similar causes. A *large* lag like the observed amount of about 70° was unexpected and inexplicable without postulating special conditions not envisaged in a standard star model, for example.

In several papers Eddington (**1**) showed that the hydrogen ionization zone provides physical conditions of the right character to produce large phase differences, though it seems to be stretching the matter too far to say that this idea has been proved (or disproved) by quantitative means. One might also think of other means of transforming wave energy into thermal energy like prominence activity, turbulence in a wide sense, shock waves, etc. None of these possibilities has been investigated in a quantitative manner as yet.

In a recent paper Milne (**2**) has reconsidered the phase-lag problem from a new angle. Stripped down to essentials Milne's contribution to the problem is to show that, under certain assumptions with regard to the manner in which non-adiabatic conditions influence the oscillation frequency and the displacement, it is indeed possible to have the luminosity variation in phase with the surface velocity, a quarter wave later than the negative displacement.

The mathematical technique used by Milne affords an interesting avenue of approach to the phase-lag problem. In the present paper the method has been worked out in greater generality, and it is shown that the physical assumptions underlying Milne's results are not such as we usually associate with real stars. It is shown in a completely general way that the common-sense view of the matter is correct—that is: for small deviations from adiabatic conditions and with a constant ratio of specific heats, the luminosity will be very nearly in phase with the negative displacement.

2. *The luminosity.*—The luminosity of the star L is given as the decrease in total energy E per unit time:

$$L = -\frac{dE}{dt} = -\dot{E}.$$

Let K, $-\Omega$, H and E_n denote kinetic energy, potential gravitational energy, heat energy and nuclear energy of the star. Then

$$L = -\dot{K} + \dot{\Omega} - \dot{H} - \dot{E}_n.$$

Using the equation of the virial

$$\tfrac{1}{2}\ddot{I} = 2K - \Omega + 3(\gamma - 1)H,$$

where I is the star's moment of inertia with respect to the centre and γ the ratio of specific heats, the heat content H may be eliminated, giving

$$L = -\dot{E}_n + \frac{1}{3(\gamma-1)}[(3\gamma-4)\dot{\Omega} - (3\gamma-5)\dot{K} + \tfrac{1}{2}\dddot{I}]. \qquad (1)$$

3. *Loss of nuclear energy.*—Let ϵ denote the loss of nuclear energy per unit time and mass. Then

$$-\dot{E}_n = \int_0^M \epsilon \, dm,$$

where M is the total mass of the star and dm a mass element. Owing to the pulsations ϵ will separate into a steady part, ϵ_0 say, and a variable part $\delta\epsilon$. Assuming ϵ to depend on temperature T and density ρ by the power law

$$\epsilon \propto \rho^{\mu} T^{\nu},$$

this gives to the first order

$$\frac{\delta\epsilon}{\epsilon_0} = \frac{\mu\delta\rho}{\rho} + \frac{\nu\delta T}{T},$$

where $\delta\rho$ and δT are the first-order Lagrangian variations of ρ and T. In the far interior of the star conditions are very nearly adiabatic, and we may write to a sufficient approximation for the present purpose

$$\frac{\delta T}{T} = (\gamma - 1)\frac{\delta\rho}{\rho},$$

which gives for $\delta\epsilon$

$$\delta\epsilon = [\mu + \nu(\gamma - 1)]\frac{\epsilon_0 \delta\rho}{\rho}.$$

But $\delta\rho/\rho$ depends on the displacement ζ by the equation of continuity

$$\delta\rho/\rho = -\operatorname{div}\boldsymbol{\zeta}.$$

Hence follows

$$\delta\epsilon = -[\mu + \nu(\gamma - 1)] \operatorname{div}\boldsymbol{\zeta}\,\epsilon_0,$$

and finally for the rate of loss of nuclear energy

$$-\dot{E}_n = \int_0^M \epsilon_0 \, dm - \int_0^M [\mu + \nu(\gamma - 1)] \operatorname{div}\boldsymbol{\zeta}\,\epsilon_0 \, dm$$

or

$$-\dot{E}_n = L_0 - [\mu + \nu(\gamma - 1)]\,\overline{\operatorname{div}\boldsymbol{\zeta}}\, L_0,$$

where

$$L_0 = \int_0^M \epsilon_0 \, dm$$

is the average luminosity of the star, and where a bar denotes an average taken over the stellar core where ϵ differs sensibly from zero.

This result shows that the variation in luminosity due to variations in the output of nuclear energy is essentially in phase with the displacement in the stellar core. Under nearly adiabatic conditions the displacement preserves a nearly constant phase throughout the star, making the oscillation very nearly a standing wave. In that case this term will be nearly in phase with the negative *surface* displacement and a quarter wave out of phase with the surface velocity. The only way of reversing this result is to introduce non-adiabatic processes in the part of the star outside the core and of such a nature as to convert the standing wave into a running one, as was indicated in the introduction.

4. *The dynamic terms.*—Consider next the remaining terms in the right-hand side of (1). Introducing the proper expressions for K, Ω and I we find for these terms

$$\delta L = \frac{1}{3(\gamma-1)}\frac{d}{dt}\int_0^M \left[(3\gamma-4)\frac{Gm}{r} - \tfrac{1}{2}(3\gamma-5)\dot{r}^2 + \tfrac{1}{2}\frac{d^2}{dt^2}(r^2)\right] dm. \qquad (2)$$

Here m denotes the mass inside a sphere of radius r concentric with the star, while G is the constant of gravitation. The radius r is here the distance of an individual mass element from the centre in the Lagrangian sense. Hence m and dm are constants during the motion.

Let a denote the average value of r for an individual mass element and write

$$r = ae^{\eta}. \qquad (3)$$

Performing the differentiations involved, equation (2) assumes the form

$$\delta L = -\frac{1}{3(\gamma-1)}\int_0^M \left[(3\gamma-4)\frac{Gm}{r^3}\dot{\eta} + \ddot{\eta} + (3\gamma-1)\dot{\eta}^3 + (3\gamma+1)\dot{\eta}\ddot{\eta}\right] r^2 dm. \qquad (4)$$

Restricting the consideration to harmonic oscillations of infinitely small amplitude and of frequency $\sigma/2\pi$, it follows from (3) that η becomes equal to the relative displacement ζ/r, and (4) reduces to

$$\delta L = -\frac{\dot{1}}{3(\gamma-1)}\int_0^M \left[(3\gamma-4)\frac{Gm}{r^3} - \sigma^2\right] r\dot{\zeta}\, dm. \qquad (5)$$

Under adiabatic conditions the right-hand side integral of (5) must, of course, vanish. That this is so is easy to show directly from the adiabatic wave equation. Conversely, a non-vanishing δL is conditioned by additional terms in σ^2 and $\dot{\zeta}$ which are the consequences of non-adiabatic conditions.

5. *Non-adiabatic perturbations.*—The question now arises as to how frequency and displacement are affected by non-adiabatic conditions. This problem has been discussed by various authors and the results are summarized in the book *Pulsation Theory of Variable Stars*, where, incidentally, the full formal solution of the problem is discussed (Chap. V, Section 1). It was there shown that ordinary non-adiabatic perturbations *do not change the oscillation frequency* to the first order, but may produce a damping factor, and will always produce additional terms in the displacement. These terms produce a variable *phase* of the displacement, the amplitude remaining unaltered. The damping factor may be disregarded here, as it is believed to be a characteristic of Cepheid pulsations that

they are very nearly undamped. That leaves the phase as the essential perturbation element. Writing the displacement in the form

$$\zeta = \xi \cos(\sigma t - \theta)$$

we are entitled to give both ξ and σ their adiabatic values, while θ is the perturbation element, which may be assumed to vanish in the adiabatic limit. Since θ is a small quantity we may write to the first order

$$\dot{\zeta} = -\sigma\xi \sin(\sigma t - \theta) = -\sigma\xi \sin \sigma t + \sigma\xi\theta \cos \sigma t = -\sigma\xi \sin \sigma t + \sigma\theta\zeta.$$

Introducing this expression for $\dot{\zeta}$ into (5) it follows that the integral over the term $-\sigma\xi \sin \sigma t$ will vanish, since it corresponds to adiabatic conditions, while the integral over the second term gives

$$\delta L = -\frac{\sigma}{3(\gamma - 1)} \int_0^M \left[(3\gamma - 4) \frac{Gm}{r^3} - \sigma^2 \right] r\theta\zeta \, dm. \tag{6}$$

This gives a luminosity variation *in phase with the displacement* and not with the velocity. This result is seen to be independent of the particular stellar model under consideration.

The course to follow in the further investigation of the phase-lag problem would now seem to be clear. It consists in a continued study of such conditions as will change the stationary adiabatic oscillation into a running wave. Perhaps a little more attention might be given to the possibility that the processes responsible for the energy generation in Cepheids may be of the delayed-action type. In that case all three elements of the wave—frequency, amplitude and phase, will be affected by the perturbation. However, it would seem more rational first to investigate quantitatively obvious sources of dissipation effects like the hydrogen ionization zone, shock waves in the atmospheric fringe, or similar phenomena.

Blindern, Oslo :
1950 *April* 11.

References

(1) Eddington, A. S., *M.N.*, **101**, 182, 1941; *M.N.*, **102**, 154, 1942.
(2) Milne, E. A., *M.N.*, **109**, 517, 1949.

THE PLANETS AND THE WHITE DWARFS

W. H. Ramsey

(Received 1950 June 6)

Summary

Russell's relationship between the planets and the white dwarfs is explained on the basis of the atomic theory of solids. A single mass-radius diagram can be constructed which refers to both the planets and the white dwarfs. The radius is an increasing function of the mass in the region of planetary masses, and it is a decreasing function of the mass for stellar masses. The radius is a maximum at some mass intermediate between planetary and stellar masses. The maximum radius depends on the chemical composition, and it is 85,000 km. for hydrogen.

1. *Introduction.*—At the International Astronomical Union Meeting which was held in Paris in 1935, H. N. Russell (1) pointed out that the planets and the white dwarfs form a single family, assuming that they are chemically homogeneous and that the chemical composition is the same for all. This family has only one free variable, which may conveniently be chosen as the mass. All the other bulk properties, such as the radius and the mean density, are then determined by the mass. The mean density of a planet is low because its mass is small. The mean density of a white dwarf is very high because its mass is large. It should be possible to construct a single mass-radius diagram which refers to both the planets and the white dwarfs.

Russell's reasons for grouping the planets and the white dwarfs together in this way are both simple and convincing. He points out that both the planets and the white dwarfs are cold in the sense that the density at any internal point is determined by the pressure at that point. In other words, the influence of temperature is so small that it can be neglected to a good approximation. Thus, in the accepted theory of the white dwarfs it is assumed that the electrons constitute a degenerate Fermi gas at absolute zero temperature. If the density ρ at absolute zero temperature were known at every pressure p, then the bulk properties of the planets and the white dwarfs could be deduced on the assumption of hydrostatic equilibrium. The equation to be solved is

$$dp/dr = -\rho g, \tag{1}$$

where r is the distance from the centre, and where g is the local acceleration due to gravity. The admissible solutions of this equation form a one-parameter family. A solution can be specified unambiguously by the central pressure, or, as is generally more convenient, by the total mass.* Thus the mass determines the radius and the mean density uniquely. Russell has gone one step further. Among the planets the radius increases with the mass. But the opposite trend prevails among the white dwarfs; the greater the mass of a white dwarf, the smaller is its radius. Russell therefore asserts that, somewhere between planetary and stellar masses, there must be a maximum radius for a cold body. Observations

* Under certain exceptional circumstances the mass does not determine the solution uniquely (2). But this is not important in the present connection.

on the planets and the white dwarfs are consistent with the view that this maximum radius is not much larger than the radius of Jupiter.

This ingenious argument of Russell is irrefutable. It establishes beyond doubt a simple connection between the planets and the white dwarfs. But it does not go far enough. The relationship between the planets and the white dwarfs must be understood on the basis of atomic theory. On the one hand, the planets are solid (or liquid). The properties of a solid can be reduced to those of its constituent atoms or molecules. Solids have many individual characteristics because atoms and molecules differ widely. For this reason some solids are metallic, and others are non-metallic. Also, solids can differ greatly in density; for example, at low pressures gold is more than two hundred times as dense as solid hydrogen. Again, some solids are much more compressible than others; at low pressures the compressibility of solid hydrogen is about a thousand times as great as that of gold. On the other hand, there is no such variety in the interior of a white dwarf star. This is because atoms do not exist at these pressures. The electrons form a degenerate Fermi gas, and an individual electron is not attached to any particular nucleus. All solids are metallic at these pressures. Also, the density at a given pressure is insensitive to the chemical composition; it depends only on the ratio of atomic weight to atomic number, which is about two for most elements. Again, the compressibility is a function of the pressure only, and it does not depend on the chemical composition at all. The properties of materials at the pressures in the interiors of the white dwarfs are comparatively well understood. The properties of solids at laboratory pressures are also, in principle, understood. But little attention has been paid to the intermediate pressures, such as occur in the interiors of the planets. It is this range of intermediate pressures which is of greatest interest in the present paper. It will be shown that an understanding of the behaviour of materials at these pressures automatically explains Russell's relationship between the planets and the white dwarfs.

2. *Transitions to metallic phases.*—If the pressure on any non-metal is continually increased, a critical pressure will eventually be reached at which there is a drastic change of phase and the material becomes metallic. Transitions to metallic phases have been discussed in considerable detail in other papers (**3**, **4**). The critical pressure for a phase transition of this type is usually of the order of magnitude of a million atmospheres, but in some cases it is much less. Both metallic and non-metallic allotropes of a few elements exist under laboratory conditions, notably tin, arsenic and phosphorus. In addition, detailed calculations have been made on metallic hydrogen (**5**, **6**). Hydrogen would be a metal of the alkali type at pressures above 0·8 million atmospheres. The transition to the metallic phase is distinguished from other polymorphic transitions by the large jump in density. It is not uncommon for the density to double at a transition to a metallic phase. The density of solid hydrogen increases at the critical pressure from 0·35 to 0·77 g./cm.^{3}. The density of metallic arsenic is 5·1 g./cm.^{3}, as compared with 2·0 g./cm.^{3} for yellow arsenic. In ordinary polymorphic transitions the density changes by only one or two per cent. In these transitions the atoms or molecules are merely rearranged into a different crystal pattern. But in a transition to a metallic phase the atoms or molecules themselves are partially destroyed, and electrons are set free to wander through the crystal. The author (**3**) has shown that the jump in density at the boundary

of the Earth's core is due to the material becoming metallic. The pressure at the boundary of the core is 1·4 million atmospheres, and the density increases by more than 50 per cent.

Consider a solid composed of ions with closed shells (for example, an ionic crystal) or of saturated molecules (for example, solid hydrogen). The electrons in such a solid cannot conduct electricity; a net current, even in the presence of an electric field, would violate the Pauli exclusion principle.* At high pressures these solids are difficult to compress because of the strong repulsions between the closed shells or between the saturated molecules. The solid could collapse into a dense metallic state if these units were broken, but to break them would require a large energy, often in the neighbourhood of ten electron volts per molecule. Nevertheless, if the pressure is increased, a critical pressure P will be reached at which the work done by the hydrostatic forces during the collapse to the metallic phase supplies just the energy required. This is expressed by the usual condition for the equilibrium of two phases at absolute zero temperature:

$$U_2 - U_1 = P(V_1 - V_2), \tag{2}$$

where U and V are the internal energy per mole and the volume per mole respectively, and where the subscripts 1 and 2 refer to the initial and final phases respectively.

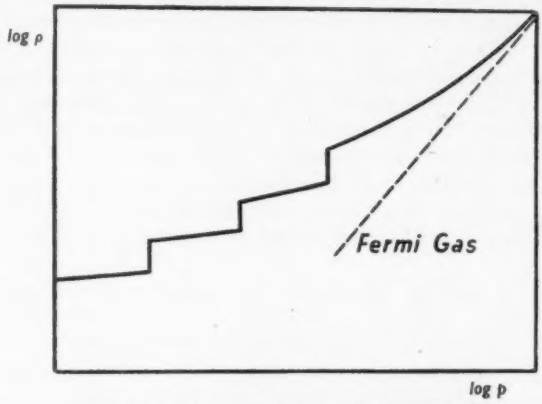

FIG. 1.—*A schematic pressure-density relationship.*

The metallic phase is stable at pressures higher than the critical pressure P, but not at pressures indefinitely higher. In general, the metallic phase also contains ions with closed shells. The transition to the metallic phase released the electrons in the outermost shell, but the inner shells remain intact. The inner shells will be broken at still higher pressures by phase transitions of the type described above. Thus, if the pressure on any material is increased indefinitely, it will undergo a series of drastic phase transitions. Each phase transition will increase the number of "free" electrons by breaking the saturated bonds of molecules or the closed shells of ions. This series of transitions will continue until every atom and molecule has been completely broken down. The electrons will then form a degenerate Fermi gas, which is imperfect only because of the electrostatic interactions.

A schematic pressure-density relationship is shown in Fig. 1. The density increases at each phase transition, and also in each phase. It has been shown in

* A survey of the atomic theory of solids has been given by Seitz (7).

another paper (**4**) that, for any particular phase, the bulk modulus k is approximately a linear * function of the pressure p:

$$k = k_0 + \alpha p. \tag{3}$$

The bulk modulus is the reciprocal of the compressibility. The constant k_0 is usually in the neighbourhood of a million atmospheres, and it is of little importance at the very high pressures which are of interest in this paper; it will therefore be neglected. On integration, equation (3) gives the following pressure-density relationship:

$$\log \rho = \alpha^{-1} \log p + \text{constant}. \tag{4}$$

Strictly speaking, the factor α is not constant but decreases slowly with pressure. But the total decrease is usually small in the range of pressure in which any one phase is stable. The segments referring to each phase in Fig. 1 are therefore approximately straight lines. The constant α is closely related to the size of the ions. It is large for large ions, and it is small for small ions. For solids composed of only very heavy atoms, such as caesium iodide, α has the value 5. The smallest possible value of α is $\frac{5}{3}$, and this is attained only in a perfect Fermi gas. Every material at high pressures has a value of α which lies between $\frac{5}{3}$ and 5. This correlation between α and the size of the ions means that materials with large atomic weight are less compressible than those with small atomic weight. Also, this difference in compressibility persists until all the atoms have been completely broken down. These conclusions are the result of a detailed investigation (**4**), but the necessity for them can be easily demonstrated. At low pressures solids with large atomic weight are up to 200 times as dense as those with small atomic weight. But at the pressures in the interiors of the white dwarf stars the density is almost independent of the atomic weight. The difference in density can be wiped out only if the denser materials are less compressible. The difference in compressibility must be maintained to very high pressures indeed. At four million atmospheres, which is the pressure at the centre of the Earth, gold is still more than thirty times as dense as metallic hydrogen (*cf.* Table I). Also, gold will undergo phase transitions at higher pressures, but hydrogen will not. The compressibility is independent of the atomic weight only at pressures more than a million times as great as that at the centre of the Earth. This result is important, as Bullen (**8**) has recently suggested that the compressibility is insensitive to the chemical composition at the pressures prevailing in the Earth. Bullen advanced this hypothesis because of the similarity of the compressibility-pressure relationships in the Earth's core and mantle, which were generally believed to be chemically distinct. It has been shown in another paper (**4**) that this similarity is due to the fact that the materials of the core and mantle are chemically identical. The general ideas behind Bullen's compressibility-pressure hypothesis can be reformulated, and the hypothesis may become a very useful guide in interpreting seismic data. A transition to a metallic phase automatically decreases the size of the ions, as it releases electrons by breaking up closed shells. For this reason the constant α always decreases at a transition to a metallic phase, but the decrease is usually small (**4**). According to equation (4), this means that the slope in Fig. 1 always increases slightly at a phase transition. The material is still not a perfect Fermi

* Deviations from the linear relation (3) occur at pressures below about $0{\cdot}5\ k_0$. But this is of no importance in the present paper.

gas when the last closed shell has been broken. The electrons interact electrostatically with the nuclei and with one another. As a result, the density is always greater than that of a Fermi gas at the same pressure, and the compressibility is always less. The magnitudes of all the electrostatic interactions are inversely proportional to the lattice spacing. But the Fermi energy, which arises from the Pauli exclusion principle, is inversely proportional to the square of the lattice spacing. Consequently, as the pressure increases, the Fermi energy becomes more and more preponderant. But, at high pressures, the Fermi energy is just the energy of a perfect Fermi gas. Hence the pressure-density relationship asymptotically approaches that of a Fermi gas, as shown in Fig. 1. The equation of state of a Fermi gas at absolute zero temperature is*

$$p = KZ^{5/3}V^{-5/3}, \tag{5}$$

where V is the molar volume and where Z is the number of electrons per molecule. The constant K is independent of the chemical composition, and its value is

$$K = 10{\cdot}04 \times 10^{12} \text{ dynes cm.}^3. \tag{6}$$

If the pressure p is expressed in atmospheres and the volume V in cm.^{3}, the numerical value of K is $9{\cdot}9 \times 10^6$. The mass of one mole is A grams where A is the molecular weight. The pressure-density relationship is therefore

$$p = K(Z/A)^{5/3}\rho^{5/3}. \tag{7}$$

The only influence of the chemical composition on this equation is through the ratio (A/Z). This ratio is about two for most materials, but it is unity for hydrogen. For an element, Z is the atomic number and A is the atomic weight.†

Hydrogen becomes metallic at a pressure of 0·8 million atmospheres, and above this pressure atoms and molecules do not exist. But very much higher pressures are required to break down the atoms of heavy elements completely. An order of magnitude estimate of the pressure required can be made as follows. Consider the last phase transition in an element of atomic number Z. The critical pressure P for the transition satisfies equation (2). Ions will not exist at pressures above this critical pressure P. As the density always increases by a large percentage at a transition to a metallic phase, the change in volume $(V_1 - V_2)$ will be comparable with the final volume V_2. Equation (2) may therefore be simplified to

$$U_2 - U_1 \simeq PV_2. \tag{8}$$

Apart from the electrostatic interactions, the final phase is a Fermi gas. The equation of state (5) for a Fermi gas may therefore be used to express the volume V_2 in terms of the critical pressure P. Equation (8) then gives the critical pressure P in terms of the energy difference $(U_2 - U_1)$:

$$U_2 - U_1 \simeq K^{3/5}ZP^{2/5}. \tag{9}$$

The last phase transition corresponds to the breaking of the K shell, which is the most tightly bound shell in the atom. The energy required to break this shell by excitation is approximately Z^2 Rydberg units‡ (**10**). The energy

* Chandrasekhar (**9**) has given a detailed account of the Fermi gas approximation and its application to the white dwarfs.

† At the highest pressures in the white dwarfs equations (5) and (7) should be replaced by the corresponding relativistic expressions ; *cf.* Chandrasekhar (**9**).

‡ One Rydberg unit is the energy necessary to ionize a hydrogen atom ; it is about 13·5 electron volts.

difference $(U_2 - U_1)$ is therefore about Z^2 Rydberg units per atom. One Rydberg unit per atom corresponds to $1{\cdot}3 \times 10^{13}$ ergs per gram-atom; hence

$$U_2 - U_1 \simeq 1{\cdot}3Z^2 \times 10^{13} \text{ ergs.} \tag{10}$$

Equations (6), (9) and (10) lead to the following expression for the critical pressure P:

$$P \simeq Z^{5/2} \times 10^{13} \text{ dynes/cm.}^2. \tag{11}$$

One atmosphere is approximately 10^6 dynes/cm.^{2}. The atomic number Z is nearly a hundred for the heaviest elements. A pressure of 10^{12} atmospheres is therefore required to break down the heaviest atoms completely. Such pressures do not exist in the planets, but pressures even thousands of times greater occur in the interiors of the white dwarf stars. The pressure at the centre of Jupiter, which is the highest in the planets, is 3×10^7 atmospheres. This pressure could break down only the lightest atoms completely, possibly only hydrogen and helium.

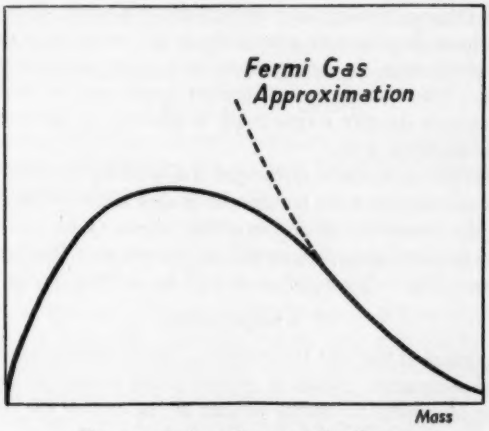

FIG. 2.—*A schematic mass-radius diagram.*

When the density is known as a function of the pressure, the bulk properties of the planets and the white dwarfs can be computed on the basis of the hydrostatic equation (1). The resultant mass-radius diagram is shown schematically in Fig. 2, and it has all the characteristics predicted by Russell (1). The internal pressures are small when the mass is small, and so atoms exist as units. For small masses, such as planetary masses, the radius increases with the mass. On the other hand, the internal pressures are enormous for masses of stellar magnitude, and atoms exist only in a thin surface layer. The equation of state (7) for a Fermi gas may be used for these masses, except in the surface layer in which atoms exist. The thickness of this surface layer decreases rapidly with the mass, and so the asymptotic behaviour of the mass-radius relationship is given by the usual theory of the white dwarfs. The mass-radius relationship corresponding to the Fermi gas approximation* is indicated by the broken curve in Fig. 2. As Russell pointed out, there is a maximum radius for a cold body. The value of the maximum radius depends on the chemical composition.

* *Cf.* S. Chandrasekhar (9).

This general treatment will now be illustrated by precise calculations on hydrogen. These calculations are more refined than is necessary for the present purposes, but they will be of value in a future paper on the internal structures and constitutions of the major planets. It turns out that Jupiter and Saturn are predominantly hydrogen; the proportion of hydrogen in these planets is about the same as that in the Sun's atmosphere.

3. *Metallic hydrogen.*—From the point of view of atomic structure, metallic hydrogen is the simplest possible solid. It is simpler than the other alkali metals in that the ion core is a proton, which rigorously has a Coulomb field. Consequently many of the properties of metallic hydrogen can be predicted accurately by not too laborious calculations in wave mechanics. Calculations on metallic hydrogen were performed first by Wigner and Huntington (**5**), and more recently by Kronig, de Boer and Korringa (**6**). The numerical predictions of the two sets of calculations are not essentially different. The calculations of Wigner and Huntington are very accurate in the region of low pressures. But the author has found the approximations developed by Kronig, de Boer and Korringa more suited to the high pressures prevailing in the interiors of the major planets. The present calculations do not contain any new mathematical methods or approximations. The calculations therefore need not be described in detail. A numerical pressure-density relationship is derived by the methods developed by the previous workers (**5**, **6**).

The calculations on metallic hydrogen will now be briefly outlined in order to clarify the connection between metallic hydrogen and a Fermi gas. To facilitate a comparison, the notations of the original papers (**5**, **6**) will be used. The energy per atom of metallic hydrogen will be written as E Rydberg units, where E is dimensionless. The volume per atom will be written in the form

$$v=(4\pi/3)r_s^3a_0^3, \tag{12}$$

where a_0 is the radius of the first Bohr orbit of the hydrogen atom, and where r_s is a dimensionless parameter which is proportional to the lattice spacing. The energy per atom of a metal is usually written as the sum of the three terms (**7**):

$$E=E_0+F+W. \tag{13}$$

The first term E_0 is the lowest energy which an electron can have in the periodic field of the lattice; it corresponds to an electron moving through the lattice with zero velocity. The second term F is the Fermi energy, which corresponds to the kinetic energy which the electrons must possess by virtue of the Pauli exclusion principle. Finally, W is an electrostatic term which arises partly from the exchange of electrons and partly from the correlation of their positions. The Fermi energy F is positive, and it prevents the lattice from collapsing. The last term W is also positive, but it is at least an order of magnitude smaller than the Fermi energy. The first term E_0 is negative, and it provides the binding of the lattice. Approximate expressions for E_0, F and W are *

$$E_0=-3/r_s, \tag{14}$$

$$F=2{\cdot}21/r_s^2, \tag{15}$$

$$W=(0{\cdot}284/r_s)-0{\cdot}58/(r_s+5{\cdot}1). \tag{16}$$

* Equations (14), (15) and (16) above should be compared with equations (13), (29) and (37) of reference (**6**).

These expressions are accurate only when r_s is small, that is, when the pressure is high. A number of corrections must be applied at low pressures; the corrections are given in convenient form in the original papers on metallic hydrogen (**5**, **6**). The importance of the corrections decreases rapidly with pressure. They are already small at a million atmospheres, and they are of little importance above ten million atmospheres. The calculations are therefore most reliable at high pressures. The region of low pressures is of little interest, as metallic hydrogen is unstable. It will be noted that, at high pressures, the electrostatic energies E_0 and W are proportional to r_s^{-1}, but the Fermi energy F is proportional to r_s^{-2}. The Fermi energy therefore becomes more and more preponderant as the pressure is increased. But the Fermi energy (15) is identical with the energy of a perfect Fermi gas. Hence, as the pressure is increased indefinitely, the energy of metallic hydrogen tends asymptotically to that of a perfect Fermi gas. In the limit of very high pressures, the equation of state of metallic hydrogen is therefore identical with that of a Fermi gas.

The best available calculations on solid molecular hydrogen are those of Kronig, de Boer and Korringa (**6**). De Boer (**11**) has shown that the interaction energy between two hydrogen molecules can be written as follows:

$$\phi(x) = (A/x^{12}) - (B/x^6), \tag{17}$$

where x is the distance between the two molecules. If the energy $\phi(x)$ is expressed in Rydberg units and the distance x in units of the Bohr radius a_0, the numerical values of the constants A and B are:

$$A = 7{\cdot}76 \times 10^5, \quad B = 27{\cdot}0. \tag{18}$$

The internal energy of the solid is obtained by summing the interaction energy (17) over the different pairs of molecules in the crystal. The present calculations differ from those of Kronig, de Boer and Korringa only by a refinement; the zero-point energy of the molecules has been taken into account by an approximate method due to Debye, *cf.* reference (**7**). The zero-point energy exerts a strong influence at low pressures. If it is neglected, the interaction (17) leads to a density of 0·144 g./cm.^{3} at zero pressure, which is more than 60 per cent greater than the empirical density of 0·089 g./cm.^{3}. The correction to the density is much less at higher pressures, and over most of the pressure range which is of interest the correction is about 7 per cent. The zero-point energy of the protons in metallic hydrogen has also been taken into account.

The critical pressure at which molecular and metallic hydrogen can co-exist in equilibrium is given by equation (2). According to the present calculations the critical pressure* is $0{\cdot}8 \times 10^{12}$ dynes/cm.^{2}. At the critical pressure the densities of the molecular and metallic phases are 0·35 and 0·77 g./cm.^{3} respectively. These results do not differ appreciably from those of Kronig, de Boer and Korringa.† These workers estimated the critical pressure to be $0{\cdot}7 \times 10^{12}$ dynes/cm.^{2}, and at the critical pressure the densities of the two phases were found to be 0·4 and 0·8 g./cm.^{3}. The results of the present calculations are given in Table I, where the density is shown as a function of the pressure. Below the critical pressure the densities refer to the molecular phase, and at higher pressures to the metallic phase. As regards the reliability of these data, the uncertainties in the

* One atmosphere is $1{\cdot}01 \times 10^6$ dynes/cm.^{2}.

† The small differences between the present results and those of Kronig *et al.* arise, of course, from the inclusion of zero-point energies.

densities of the metallic phase are too small to be of any consequence. The densities of the molecular phase are less reliable, and an error of five per cent would not be surprising. The critical pressure is the most uncertain quantity in Table I, and it may be in error by ten, or even twenty, per cent.

TABLE I

Pressure-Density Relationship for Hydrogen

Molecular Phase		Metallic Phase	
Pressure 10^{12} dynes/cm.^{2}	Density g./cm.^{3}	Pressure 10^{12} dynes/cm.^{2}	Density g./cm.^{3}
0	0·089	0·8	0·77
0·1	0·225	1·0	0·81
0·2	0·261	2·0	0·98
0·3	0·284	3·0	1·12
0·4	0·302	4·0	1·25
0·5	0·316	5·0	1·36
0·6	0·329	10·0	1·84
0·7	0·340	20·0	2·53
0·8	0·350	30·0	3·07

4. *Hydrogen planets.*—The bulk properties of planets composed of hydrogen have been computed on the basis of the pressure-density relationship given in Table I. It has been assumed that the interiors of the planets are in hydrostatic equilibrium, so that equation (1) is applicable. This equation has been solved for a number of arbitrarily chosen central pressures, using step-by-step numerical integration. The solution of equation (1) determines uniquely the mass, radius and mean density of the planet. A selection of the results of the calculations is given in Table II. The unit of mass in this table is the mass M_E of the Earth. The central pressure in a small planet is too low to support a core of metallic hydrogen. A core is possible only if the mass of the planet exceeds 88 M_E. A planet whose mass lies between 88 M_E and 95 M_E can exist either with or without a core. This is a consequence of the fact that the density of hydrogen jumps by more than 50 per cent at the critical pressure; a full explanation has been given in another paper (**2**). A planet always has a core if its mass exceeds 95 M_E, and the fraction of the total mass which is contained in the core increases very rapidly with the mass of the planet. For a planet of mass 97 M_E, the core contains 33 per cent of the total mass; but for a planet of mass 1800 M_E, the core contains over 99 per cent of the mass. The radius of a planet of mass 1800 M_E is 83,000 km., but the thickness of the mantle of molecular hydrogen is less than 3000 km. The properties of molecular hydrogen have therefore little influence on the mean density of a planet of this mass, and even less influence for more massive planets. The radius of the planet is a maximum when the mass is about 1000 M_E. The maximum radius is 85,000 km., and this is the largest possible radius for a cold body composed of hydrogen. As Russell (**1**) suspected, the maximum radius is not much larger than the radius of Jupiter, which is 69,900 km. For masses exceeding 1000 M_E, the radius decreases with the mass and the mass-radius relationship asymptotically approaches that given by the usual theory of the white dwarfs.

5. *Kothari's theory of the planets.*—As long ago as 1936, Kothari (**12**) pointed out that atoms cannot be treated as structureless particles at the pressures prevailing in the planets. An atom consists of a nucleus surrounded by a complex system of electrons, and this internal structure must be taken into account. Kothari developed a simple theory which can be regarded as a second approximation to the

Fermi gas treatment. Allowance is made for the tendency of the electrons to cluster around the nuclei. This clustering is of little importance at the pressures in the interiors of the white dwarfs, but it is more pronounced at lower pressures. Kothari's treatment leads to the formation of atoms when the lattice spacing is large; the Fermi gas treatment, of course, does not. Kothari has shown that his theory leads to a mass-radius diagram which is similar to that illustrated in Fig. 2. He therefore claims that his theory explains Russell's relationship between the planets and the white dwarfs. In Kothari's theory the maximum radius for a cold body depends on the chemical composition, and it is about 125,000 km. for hydrogen.

TABLE II

Hydrogen Planets

Mass ($M_E=1$)	Radius (km.)	Mean Density (g./cm.^{3})
10·7	46,000	0·16
60	73,000	0·22
97	75,600	0·32
208	77,100	0·65
317	79,400	0·90
623	82,600	1·57
1000	84,500	2·36
1400	83,700	3·42
1800	83,000	4·53

Kothari's theory has not been generally accepted as its predictions are incompatible with the observed properties of materials, not only at the pressures attained in the laboratory but also at the pressures in the interior of the Earth. The principal weakness in the theory is that the interactions between neighbouring atoms are ignored completely. For definiteness, let us take hydrogen as an example. The internal energy of metallic hydrogen is given by equation (13). The electrostatic energies E_0 and W are ignored in the Fermi gas approximation. Kothari's theory is an improvement on the Fermi gas treatment in that an attempt is made to include the energy E_0, which corresponds to the interactions between the electrons and the nuclei. No attempt is made to include the term W, which arises from the mutual interactions of the electrons and is the metallic equivalent of interatomic forces. If the lattice spacing of metallic hydrogen is increased indefinitely, the result will be an assembly of unexcited hydrogen atoms. Kothari's theory also leads to hydrogen atoms when the lattice spacing is large. But Kothari does not find solid molecular hydrogen, which is the stable modification at pressures below 0·8 million atmospheres. The failure of the theory is due to the fact that the interactions between atoms are ignored. If Kothari had taken the interactions between the atoms into account, he would have found the transitions to the metallic phases which are described in this paper. A transition to a metallic phase, like every other phase transition, is inherently a property of groups of atoms, and it cannot be understood if the interactions between the atoms are ignored.

In his calculations Kothari paid special attention to iron, as it is one of the most abundant elements in the Earth. His theory predicts that the density of iron will be 70 g./cm.^{3} when there is one "free" electron per atom. This is nine times the actual density of iron. A density in the neighbourhood of 70 g./cm.^{3} is not attained even at the pressures in the Earth's core, which Kothari assumed to be iron. Kothari therefore replaced the density of 70 g./cm.^{3} which appears in his

theory by the empirical density of iron. He then compared the " theoretical " mass-radius relationship with the data for the terrestrial planets.* Such a comparison is valueless when the theory was in error by an order of magnitude at planetary pressures. Kothari's theoretical densities refer to the metallic phase in which the atoms are completely broken down. According to equation (11), this phase is stable only at pressures more than ten thousand times as great as the pressure at the centre of the Earth. Kothari's calculations have therefore no bearing on the constitutions of the terrestrial planets. The density of iron at low pressures is comparatively small because of the strong repulsions between the closed shells of the ions. The compressibility of the material of the Earth, which can be derived from seismic data, shows that the repulsions between the ions predominate at all terrestrial pressures (**4**). But these repulsions are ignored completely in Kothari's theory, and so it is inapplicable. Kothari's work has been followed by a number of investigations (**13**, **14**, **15**) along the same lines, but, so far as the planets are concerned, no essential improvement has been effected.

In general, Kothari's theory is inapplicable at planetary pressures. But his numerical calculations on hydrogen have a bearing on the structures of the major planets. This is because a comparatively small pressure breaks down hydrogen molecules completely. It has been shown that the properties of molecular hydrogen are of secondary importance for planets whose mass is a few thousand times the mass of the Earth. Also, Kothari's treatment gives the density of metallic hydrogen correctly to about 25 per cent at planetary pressures. Kothari's estimate of the maximum radius for a cold body composed of hydrogen is 125,000 km., and this is in error by only 50 per cent.

Part of this investigation was carried out at the Institute of Theoretical Physics in Copenhagen, and the author would like to thank Professor N. Bohr for his hospitality. He would also like to express his appreciation to Professor L. Rosenfeld and to Professor Harold Jeffreys for the interest which they have shown in this work.

The Physical Laboratories,
The University,
Manchester, 13 :
1950 *June* 5.

References

(1) H. N. Russell, *The Observatory*, **58**, 259, 1935.
(2) W. H. Ramsey and M. J. Lighthill, *M.N.*, **110**, 325 and 339, 1950.
(3) W. H. Ramsey, *M.N., Geophys. Suppl.*, **5**, 409, 1949.
(4) W. H. Ramsey, *M.N., Geophys. Suppl.*, **6**, 42, 1950.
(5) E. Wigner and H. B. Huntington, *J. Chem. Phys.*, **3**, 764, 1935.
(6) R. Kronig, J. de Boer and J. Korringa, *Physica*, **12**, 245, 1945.
(7) F. Seitz, *The Modern Theory of Solids*, New York, 1940.
(8) K. E. Bullen, *Nature*, **157**, 405, 1946 ; *M.N., Geophys. Suppl.*, **5**, 355, 1949.
(9) S. Chandrasekhar, *An Introduction to the Study of Stellar Structure*, Chicago, 1939.
(10) L. Pauling and E. B. Wilson, *Introduction to Quantum Mechanics*, New York, 1935, p. 162.
(11) J. de Boer, *Physica*, **9**, 363, 1942.
(12) D. S. Kothari, *M.N.*, **96**, 833, 1936 ; *Proc. Roy. Soc.* A, **165**, 486, 1938.
(13) F. C. Auluck, *M.N.*, **99**, 239, 1939.
(14) A. Sommerfeld, *Nuovo Cim.*, **15**, No. 1, 1938.
(15) J. G. Scholte, *M.N.*, **107**, 237, 1947.

* Similar calculations on planets composed of silicates are open to the same objections.

DOUBLE STAR MEASURES—3rd SERIES

W. P. Hirst

(Received 1950 June 5)

The following measures were made, unless noted otherwise, with the 7-inch refractor at the Royal Observatory at the Cape by kind permission of H.M. Astronomer, Dr J. Jackson. A few were made with the 26½-inch refractor at the Union Observatory, Johannesburg, by courtesy of the Union Astronomer, Dr W. H. van den Bos. These have been noted accordingly.

The columns from left to right give: Name and ADS number (if any); right ascension and southern declination (equinox 1900.0); date (omitting century); position angle; distance; magnitude difference (estimated); number of nights; remarks.

Star	Position	Date 1900	θ	ρ	ΔM	Nights	Remarks
	h m		°	″			
I 260	0 27	45·616	294·1	0·5 est	0·6	4	
β_2 Tucn	62° 48′	48·134	271·2	0·68	...	1	ρ (est) 0″·5
Hd 182	0 37·9	45·964	3·2	0·80	0·2	1	
	39° 01′						
I 47	0 47·2	45·964	8·0	1·41	0·0	1	ρ (est) 1″·2
	44° 15′						
Slr 1	1 01·6	45·950	351·8	1·64	0·0	2	
	47° 15′						
I 27	1 11·6	45·930	42·1	1·26	0·0	2	
	69° 21′						
h 3423	1 12·0	45·913	339·2	5·53	2·1	3	
	69° 24′						
h 3494	2 15·6	45·964	299·7	1·36	...	1	ρ (est) 1″·0
	35° 54′						
Jc 8 AB	3 08·9	45·045	186·6	0·5 est	0·2	3	
	44° 48′	46·088	180·5	0·66	0·1	1	ρ (est) 0″·5
h 3556 AC	3 08·9	46·088	201·6	3·05	3·5	1	
	44° 48′						
Δ 16	3 44·9	45·036	210·5	7·92	1·0	3	
f Erid	37° 56′	46·088	210·3	7·87	0·7	1	
β 1004	3 58·2	45·044	114·8	1·44	0·6	3	
	34° 46′						
Gale 1	4 14·8	45·048	21·6	0·7 est	0·3	3	
	61° 12′						

Star	Position	Date 1900	θ	ρ	ΔM	Nights	Remarks
	h m		°	″			
β 744	4 17·4	45·043	262·9	0·6 est	0·2	2	
ADS 3159	25° 58′						
Rümker 4	4 22·3	45·029	240·9	6·11	0·3	3	
	57° 18′						
β 184	4 23·6	45·041	254·5	1·58	0·3	3	
	21° 44′						
h 3683	4 38·6	45·071	93·1	1·58	0·1	3	
	59° 08′						
h 3752	5 17·7	45·097	97·5	3·00	1·9	2	
	24° 52′	48·134	97·9	3·56	1·2	1	
I 276	5 27·5	45·077	175·6	1·31	0·2	3, 2	ρ unreliable
	68° 42′	46·088	177·7	1·38	0·3	1	ρ (est) 0″·9
		48·134	175·7	1·10	...	1	
Δ 23	6 02·0	48·134	90·0	1·69	0·3	1	
	48° 27′						
Sirius	6 40·7	47·208	194·5	3·40	...	1	U.O. 26½ inch
	16° 35′						
h 3997	7 37·6	45·033	119·6	2·0 est	...	1	Rough measure
	74° 03′						
β 101	7 47·1	47·208	301·3	0·50	...	1	U.O. 26½ inch
	13° 38′						
Hu. 115	8 08·5	47·208	104·0	0·91	...	1	U.O. 26½ inch
	13° 36′						
Σ 1216	8 16·3	47·208	246·9	0·45	...	1	U.O. 26½ inch
	1° 17′						
I 489	8 27·0	46·312	82·8	0·45 est	...	1	
	19° 14′						
β 205	8 28·8	46·312	305·9	0·55 est	0·4	1	
	24° 16′						
β 208	8 34·8	46·300	209·9	1·97	1·4	3	
	22° 19′	47·234	210·7	1·95	1·4	2	One measure U.O. 26½ inch
ψ Arg	9 26·8	46·312	116·1	1·19	0·6	1	
	40° 02′						
I 292	9 59·3	46·312	166·1	0·9 est	0·2	1	
	27° 54′						
I 13	10 07	46·386	132·9	0·73	0·3	1	
	68° 12′						

Star	Position	Date 1900	θ	ρ	ΔM	Nights	Remarks
	h m		°	″			
I 294	10 44·3	46·386	75·6	0·52	0·0	1	
	80° 12′						
I 78	11 28·7	47·435	97·2	1·29	0·2	1	
	40° 02′						
h 4478	11 47·9	47·435	4·0	1·22	0·3	1	
	33° 21′						
α Crux	12 21·2	46·386	116·1	4·50	0·1	1	
	62° 33′						
γ Cent	12 36	46·447	10·2	1·14	0·0	5	
	48° 25′	47·435	8·7	0·98	0·1	1	
		49·541	8·5	1·12	0·0	3	
R 207	12 40·2	46·386	8·0	1·43	0·2	1	
	67° 33′	47·435	10·9	1·50	0·0	1	
		49·538	11·9	1·52	0·2	3	
I 424	13 06·0	46·548	7·6	1·55	3·0	1	
	59° 33′						
Slr 18	13 16·9	46·548	235·4	0·56	0·2	1	
	47° 25′	47·435	224·6	0·63	0·2	1	
		49·537	231·6	0·66	0·2	3	
I 298	13 25·2	46·548	186·1	0·84	2·0	1	
	68° 43′						
β 343	13 46·3	46·546	81·0	1·26	1·0	3	ρ (est) 1″·0
	31° 07′						
Howe 28	13 47·7	46·534	115·5	0·7 est	0·4	4	
	35° 10′	49·537	125·5	0·70	0·3	1	
R 227	13 49·8	46·548	2·2	1·83	0·6	1	
	53° 39′						
β 1197	13 57·2	46·548	211·0	1·87	1·3	1	
	31° 12′						
Slr 19	14 01·2	46·548	287·5	1·43	0·2	1	
	49° 24′						
h 4687	14 29·5	46·548	102·0	1·57	0·2	1	
	36° 07′						
α Cent	14 32·8	46·434	13·6	9·77	1·5	5	
	60° 25′	49·533	19·4	10·70	1·1	3	
I 236	14 43·2	46·548	116·3	2·18	...	1	
	72° 47′						
β 239	14 52·7	46·546	333·8	0·81	0·2	2	
	27° 15′	49·543	334·9	1·01	0·1	2	

Star	Position	Date 1900	θ	ρ	ΔM	Nights	Remarks
	h m		°	″			
h 4728	14 58·3	46·547	75·6	1·68	0·1	3	
	46° 40′	49·548	74·6	1·76	0·1	2	
h 4753 AB	15 11·6	46·550	142·9	1·41	0·1	1	
	47° 30′	48·578	142·8	1·41	0·1	1	
h 4753 AC	,,	46·550	129·2	22·49	3·0	1	
h 4753 BC	,,	46·550	129·8	23·85	3·0	1	
h 4757	15 15·4	46·550	48·1	1·36	0·2	1	
	58° 58′	48·578	47·3	1·03	0·2	1	
λ 258 AB	15 55·4	46·547	284·4	0·58	0·3	3	
	57° 30′	48·578	277·0	0·66	0·3	1	
		49·539	268·2	0·68	0·2	3	
h 4825 AC	,,	46·550	245·3	9·98	4·0	1	
λ 268	16 08·0	46·720	176·5	1·71	0·1	1	
	38° 53′						
Cor 197	16 19·7	46·720	147·2	1·69	0·0	1	
	48° 55′						
H II 19	16 19·6	46·720	348·0	3·42	0·5	1	
	23° 13′	48·578	346·9	3·19	0·4	1	
Sh 243	17 09·2	47·630	170·0	4·60	0·1	1	
	26° 27′	49·529	167·9	4·65	0·2	3	
Brs 13	17 11·5	47·630	222·7	4·90	3·5	1	
	46° 32′						
Melb 4 AB	17 12·1	45·827	286·3	2·21	2·0	3	
	34° 53′	46·576	283·8	2·25	0·9	6	
		47·607	280·1	2·06	1·0	3	
		48·557	278·2	2·05	0·7	2	
		49·529	274·3	2·08	1·0	3	
·· 4949	17 19·5	46·679	256·6	2·16	0·3	1	
	45° 45′	47·609	257·6	2·19	0·4	3	
		49·528	257·3	2·04	0·4	3	
β 129	17 22·5	46·679	112·5	0·96	0·4	1	
	25° 26′	47·612	111·3	0·90	0·1	3	
Hd 275	17 32·3	46·679	4·2	0·75 est	0·3	1	
	72° 10′	47·615	4·9	0·81	0·0	3	
Cp 17	17 37·8	46·679	199·3	1·43	0·1	1	
	50° 44′	47·630	199·8	1·17	0·2	1	
h 5014	17 59·6	46·679	214·2	1·80	0·2	1	
	43° 26′	47·610	213·1	1·72	0·1	3	

Star	Position	Date 1900	θ	ρ	ΔM	Nights	Remarks
	h m		°	″			
Rümker 26	20 43·3 62° 48′	45·868	88·0	2·72	0·4	1	ρ unreliable
h 5246	21 03·1 54° 59′	45·868	128·6	3·94	0·1	1	ρ doubtful
h 5258	21 12·7 53° 52′	45·835	275·9	5·68	2·5	3	
β 766	21 18·0 41° 26′	43·931	279·2	1·17	0·5	1	
Σ 2909	22 23·7 0° 31′	45·818	280·7	2·67	...	2	
Jc 20	23 01·2 44° 04′	43·931	55·4	1·57	2·5	1	ρ doubtful

Cape Town:
1950 *April* 4.

DYNAMIC EFFECTS OF A LIQUID CORE (II)

Harold Jeffreys

(Received 1950 May 20)

Summary

An approximate method is applied to the Eulerian and forced nutations to take account of possible effects of differences of density within the Earth's core. It is found that all such effects are adequately taken into account by replacing the actual core by a homogeneous one with the same moments of inertia.

1. *Heterogeneity of the core.*—It was shown in an earlier paper* that the inertia of a liquid core in the Earth, with a rigid shell, would lead to too short a period for the Eulerian nutation and to a reduction of the theoretical amplitude of the 19-yearly nutation to substantially less than the observed value. Both effects were afterwards shown to be mitigated by allowance for a finite rigidity of the shell.† In both papers the core and shell were taken as homogeneous. The variation of mechanical properties within the shell could be taken into account by a numerical method, without, I think, introducing any new questions of principle. Variation of density in the core might introduce complications of a new type. The displacement of the core boundary is a rotation. Within the core there is an additional motion involving distortion. This gives rise to no gravitational energy when the density is taken as uniform, since it does not alter the density at any point. But such a motion, with the density increasing toward the centre, would be a distortion of a fluid mass from a stable steady state, and would be opposed by gravity. Hence it appears that with a heterogeneous core gravity might reduce the motion of the core relative to the shell, and that the results might again approach those for a completely rigid Earth.

As the time of travel of a longitudinal wave through the core is very short compared with a day, it is safe to treat the core as incompressible. At present we return to a rigid shell. The motion in the core will consist of three parts: the rotation of the shell; a linear distortion producing no normal motion at the boundary; and a superposed distortion varying with distance from the centre in such a way that the normal displacement due to it also vanishes at the boundary. This allows the displacement to contain cubic terms in the coordinates. With certain obvious changes from the notation of Paper II, the most general cubic forms satisfying these conditions are, to the first order,

$$\left.\begin{aligned}
\xi &= x + \left(l + \frac{a}{c}\,l_1\right)z + \frac{a}{c}\,z\left(l_2 S - l_3\frac{z^2}{c^2}\right),\\
\eta &= y + \left(m + \frac{a}{c}\,m_1\right)z + \frac{a}{c}\,z\left(m_2 S - m_3\frac{z^2}{c^2}\right),\\
\zeta &= z - x\left\{l + \frac{c}{a}\,l_1 + l_2\frac{c}{a}\,S - \frac{c}{a}\,l_3\left(1 - \frac{x^2+y^2}{a^2}\right)\right\},\\
&\quad - y\left\{m + \frac{c}{a}\,m_1 + m_2\frac{c}{a}\,S - \frac{c}{a}\,m_3\left(1 - \frac{x^2+y^2}{a^2}\right)\right\},
\end{aligned}\right\} \qquad (1)$$

* H. Jeffreys, *M.N.*, **108**, 206–209, 1948, referred to as Paper I.
† H. Jeffreys, *M.N.*, **109**, 670–687, 1949, referred to as Paper II.

where $$S = \frac{x^2+y^2}{a^2} + \frac{z^2}{c^2}. \qquad (2)$$

These do not include displacements about the axis of z because they are of the second order and would lengthen the writing greatly. The l, m displacement represents the general rotation of the shell, l_1, m_1 the linear distortion. l_2, m_2 give displacements at all points along similar ellipsoids. To represent the kinematic possibility that the motion might be along level surfaces we need an additional displacement capable of giving motion with a component normal to similar ellipsoids, and this is provided by l_3, m_3. Then the system (1) is sufficiently general to represent the main features of the actual motion. It does not satisfy the equations of motion exactly, and a full solution would be very difficult. But it is probably near enough. For small variations from the true motion, Hamilton's integral taken over a period varies by a quantity of the second order in the variations; and Rayleigh's method of deriving the principle of stationary periods from Hamilton's principle applies equally well to gyroscopic systems. Hence the error in the computed free periods will be very small. For a forced motion some of the displacements found will have errors of the first order, but as the quantities observed are only indirectly related to those that are in error it may be again expected that the form (1) is accurate enough. But then we can use Lagrange's equations as before.

We can indeed go a little further. We are interested in the effects of variation of density in the core and of the differences of the ellipticities of surfaces of equal density. The former are of the order of 20 per cent on the model that we shall use, the latter of the order of 8 per cent. Without these variations the cubic terms would not occur. It seems likely, then, that the omission of the terms in l_2, m_2, l_3, m_3 would itself be a first-order error in Hamilton's sense, and that any error due to their omission would be of the order of a few per cent. If a large correction is found it may be worth while to make a closer approximation.

In Paper II the displacements were evaluated to the second order, on account of the presence of terms $\omega\Sigma\mu(\xi\dot{\eta} - \dot{\xi}\eta)$, $\frac{1}{2}\omega^2\Sigma\mu(\xi^2+\eta^2)$ in the kinetic energy. If we restrict the adopted form of the displacements to the parts containing l, m, l_1, m_1, the second-order terms will be the same as before. For the other parts, if it should be necessary to retain them, we should have to add second-order parts to ξ, η, ζ so as to make $\partial(\xi, \eta, \zeta)/\partial(x, y, z)$ unity to the second order and leave a boundary particle on the boundary, also to the second order. This, however, is unnecessary. In $\Sigma\mu\xi\dot{\eta}$ the extra term is $\Sigma\mu x^2(\partial^2\eta/\partial x\partial t)$, which is a derivative with regard to the time and does not affect the equations of motion. $\Sigma\mu\xi^2$ will contain terms in l^2, m^2, which will be the same as for a rigid body and can be written down at once; but also terms linear in l, m and in $l_1, l_2 \ldots$, and terms in squares and products of $l_1, l_2 \ldots$. Since these terms contain no derivatives with regard to the time, it is indifferent whether we place them in the kinetic energy or the work function. Now a constant angular displacement in space of the whole body, originally in steady rotation, leaves it in steady rotation. Hence, when the equations of motion are formed for $l_1, l_2 \ldots$, the coefficient of l must vanish for disturbances of speed $-\omega$. This effectively determines the coefficients of ll_1 and analogous terms. Again, the steady rotation is a stable state and the surfaces of equal density are the surfaces of constant geopotential $U + \frac{1}{2}\omega^2(x^2+y^2)$. The part of T that depends only on the displacements can be added to the work function; but if this is done the only contribution to the work function from $l_1, l_2, \ldots$ comes

from displacements normal to the level surfaces, and can be found to the second order as for departures from a spherical gravitating mass, since the ellipticities are small.

If μ is an element of mass, we introduce the following constants:

$$\left.\begin{aligned} &A_{11}=\Sigma\mu x^2=\tfrac{1}{2}C_1; \qquad A_{33}=\Sigma\mu z^2=\tfrac{1}{2}(2A_1-C_1),\\ &A_{33}=A_{11}(1-2\epsilon_1), \qquad c=a(1-e), \qquad C_1-A_1=\epsilon_1 C_1, \qquad e-\epsilon_1=\epsilon',\\ &F_1=2\frac{c}{a}A_{11}=A_1(1-\epsilon'), \qquad F_3=2\frac{a}{c}A_{33}=A_1(1+\epsilon'). \end{aligned}\right\} \tag{3}$$

For a homogeneous core $F_1=F_3$; this is no longer true. We neglect e^2 and similar quantities. Then, if we retain only l, m, l_1, m_1,

$$\begin{aligned} 2T_{\text{core}}=&\Sigma\mu z^2\left\{\left(\dot l+\frac{a}{c}\dot l_1\right)^2+\left(\dot m+\frac{a}{c}\dot m_1\right)^2\right\}\\ &+\Sigma\mu x^2\left\{\left(\dot l+\frac{c}{a}\dot l_1\right)^2+\left(\dot m+\frac{c}{a}\dot m_1\right)^2\right\}\\ &+2\omega\Sigma\mu z^2\left\{\left(l+\frac{a}{c}l_1\right)\left(\dot m+\frac{a}{c}\dot m_1\right)-\left(\dot l+\frac{a}{c}\dot l_1\right)\left(m+\frac{a}{c}m_1\right)\right\}\\ &-\omega^2(C_1-A_1)(l^2+m^2)+2\omega^2\left(\Sigma\mu z^2\frac{a}{c}-\Sigma\mu x^2\frac{c}{a}\right)(ll_1+mm_1)\\ &+\text{term in } l_1^2+m_1^2. \end{aligned} \tag{4}$$

Adding the kinetic energy of the shell we have

$$\begin{aligned} 2T=&A(\dot l^2+\dot m^2)-\omega^2(C-A)(l^2+m^2)+\omega(2A-C)(l\dot m-\dot l m)\\ &+2A_1(\dot l\dot l_1+\dot m\dot m_1)+\omega F_3(l_1\dot m+l\dot m_1-\dot l m_1-\dot l_1 m)\\ &+C_1\omega(1+2\epsilon')(l_1\dot m_1-\dot l_1 m_1)+A_1(\dot l_1^2+\dot m_1^2)\\ &+2\omega^2\epsilon' A_1(ll_1+mm_1)+\text{term in } l_1^2+m_1^2. \end{aligned} \tag{5}$$

2. *Forms of ϵ' and of the normal displacement in the core.*—We take r_1 for the mean radius of a level surface in the core, and its ellipticity is temporarily denoted by e. Take

$$\rho=\rho_0-\rho_1\frac{r_1^2}{a^2}, \qquad e=e_0+e_1\frac{r_1^2}{a^2}, \tag{6}$$

so that e of (3) is e_0+e_1. The mean moment of inertia is

$$I=\frac{8\pi}{15}(\rho_0-\tfrac{5}{7}\rho_1)a^5, \tag{7}$$

and

$$\begin{aligned} C_1-A_1&=\frac{8\pi}{3}\int_0^a\left(\rho_0-\rho_1\frac{r^2}{a^2}\right)\frac{d}{dr}\left\{r^5\left(e_0+e_1\frac{r^2}{a^2}\right)\right\}dr\\ &=\frac{8\pi}{15}(e_0\rho_0+e_1\rho_0-\tfrac{5}{7}e_0\rho_1-\tfrac{7}{9}e_1\rho_1)a^5, \end{aligned} \tag{8}$$

$$\epsilon'=e_0+e_1-\frac{C_1-A_1}{I}=\frac{4}{63}\frac{e_1\rho_1}{\rho_0-\frac{5}{7}\rho_1}. \tag{9}$$

To the first order in the ellipticity, if a', c', e' are the semi-axes and ellipticity of a level surface in the core, the normal displacement is

$$a'\left\{\frac{x}{a'^2}\frac{a}{c}l_1z+\frac{y}{a'^2}\frac{a}{c}m_1z-\frac{z}{c'^2}\frac{c}{a}(l_1x+m_1y)\right\}=\frac{2(e_0+e_1-e')}{a'}z(l_1x+m_1y). \tag{10}$$

Since xz/r^2 and yz/r^2 are surface harmonics of degree 2, this can be written

$$2(e_0+e_1-e')rY_2=2e_1\left(1-\frac{r^2}{a^2}\right)rY_2. \tag{11}$$

3. *Gravitational work function of the core.*—In a body slightly deformed from a sphere, so that the surface of uniform density and mean radius r_1 is

$$r=r_1(1+\phi_1 Y_2), \tag{12}$$

where ϕ_1 may depend on r_1, the gravitational potential is

$$\begin{aligned}U&=4\pi f\int_0^{r_1}\rho'\frac{\partial}{\partial a'}\left(\frac{1}{3}\frac{a'^2}{r}+\frac{1}{5}\frac{a'^5\phi'}{r^3}Y_2\right)da'+4\pi f\int_{r_1}^{a}\rho'\frac{\partial}{\partial a'}\left(\tfrac{1}{2}a'^2+\tfrac{1}{5}r^2\phi'Y_2\right)da'\\&=-4\pi fY_2\int_0^{r_1}\rho'\left\{\frac{a'^2}{r_1}-\frac{1}{5r_1^3}\frac{d}{da'}(a'^5\phi')\right\}da'+\tfrac{4}{5}\pi fY_2\int_{r_1}^{a}\rho' r_1^2\frac{d\phi}{da'}da'\\&\quad+\text{function of } r_1.\end{aligned} \tag{13}$$

Here we take

$$\phi(r_1)=2e_1\left(1-\frac{r_1^2}{a^2}\right) \tag{14}$$

in the core, $\phi=0$ in the shell, so that the upper limit in the second integral is the mean radius of the core. Then the part depending on Y_2 is

$$8\pi fe_1Y_2\left\{-\tfrac{1}{3}\rho_0r_1^2\left(1-\frac{r_1^2}{a^2}\right)+\tfrac{1}{10}\rho_1r_1^2+\tfrac{2}{35}\rho_1\frac{r_1^4}{a^2}-\tfrac{13}{90}\rho_1\frac{r_1^6}{a^4}\right\}. \tag{15}$$

Associate with Y_2 a number α between 0 and 1, and consider a redistribution of mass such that α increases by $\delta\alpha$. The matter at a place is replaced by matter from a place deeper by $r_1\phi_1Y_2\delta\alpha$, and its density is accordingly increased by

$$-r_1\phi_1Y_2\frac{d\rho}{dr_1}\delta\alpha=4e_1\rho_1\left(1-\frac{r_1^2}{a^2}\right)\frac{r_1^2}{a^2}Y_2\delta\alpha. \tag{16}$$

The part of U depending on r_1 only does not affect the work function, since the total mass is unaltered. Then the increase in the gravitational work function is

$$\begin{aligned}&32\pi f\alpha\,\delta\alpha\,.\,e_1^2\rho_1\iint Y_2^2\,d\omega\int_0^a\left\{-\tfrac{1}{3}\rho_0r_1^2\left(1-\frac{r_1^2}{a^2}\right)+\tfrac{1}{10}\rho_1r_1^2+\tfrac{2}{35}\rho_1\frac{r^4}{a^2}-\tfrac{13}{90}\rho_1\frac{r_1^6}{a^4}\right\}\\&\qquad\times\left(1-\frac{r_1^2}{a^2}\right)\frac{r_1^4}{a^2}dr_1=-\tfrac{128}{15}\pi^2f\alpha\,\delta\alpha e_1^2\rho_1(l_1^2+m_1^2)\cdot\tfrac{8}{693}a^5(\tfrac{1}{3}\rho_0-\tfrac{1}{5}\rho_1)\end{aligned} \tag{17}$$

and the work function for $\alpha=1$ is

$$W_1=-\frac{512}{3.15.693}\pi^2fe_1^2\rho_1a^5(\rho_0-\tfrac{3}{5}\rho_1)(l_1^2+m_1^2)=-\frac{16}{693}\frac{A_1}{a_1}g_1e_1^2\frac{\rho_1}{\rho_0-\frac{5}{7}\rho_1}(l_1^2+m_1^2), \tag{18}$$

since mean gravity at the surface of the core is

$$g_1=\tfrac{4}{3}\pi fa(\rho_0-\tfrac{3}{5}\rho_1). \tag{19}$$

We can write (18) as

$$W_1=-A_1\omega^2\epsilon''(l_1^2+m_1^2), \tag{20}$$

and ϵ'' is another small number.

4. *Work function due to the external field.*—We take the external potential to be $(c_1x+c_2y)z$. The corresponding work function in the displaced position is found to be

$$(A_{33}-A_{11})(c_1l+c_2m)+\left(\frac{a}{c}A_{33}-\frac{c}{a}A_{11}\right)(c_1l_1+c_2m_2) \tag{21}$$

and adding the contribution for rotation of the shell we have

$$W_2 = -(C-A)(c_1 l + c_2 m) + \epsilon' C_1 (c_1 l_1 + c_2 m_2). \tag{22}$$

The Lagrangian function is now the sum of T from (5) (the terms in $l_1^2 + m_1^2$ being omitted), W_1 and W_2.

5. *Values of* e_1, ϵ', ϵ''.—As we are attempting only a rough treatment it seemed that Bullen's original solution* would be adequate. But on inspection of this solution a slight numerical inconsistency was found. The solution for ρ is not far from the form adopted here, and as, for uniform composition, ρ_1/ρ_0 depends mostly on the velocity of longitudinal waves in the core, it can be regarded as well determined. All Bullen's trial values make it about 0·190. This makes I/Ma^2 very near 0·390, whereas he gets 0·395. Using 0·390 and interpolating between his solutions for the shell I get the density at depth 400 km. = 4·091 g./cm.^{3},

$$\left.\begin{aligned} M(\text{core}) &= 189{\cdot}7 \times 10^{25} \text{ g.}, \\ I(\text{core}) &= 8{\cdot}91 \times 10^{43} \text{ g./cm.}^2. \end{aligned}\right\} \tag{23}$$

η for the core boundary is now 0·076, as against Bullen's 0·04, and

$$e_1/e_0 = 0{\cdot}038. \tag{24}$$

The adjustment of course does not affect his determination of the ellipticity correction in seismology to the accuracy needed, since an accuracy of 1 part in 10 for this is quite adequate. With $e_0 + e_1 = 0{\cdot}00260$ this gives

$$\epsilon' = 0{\cdot}0000014. \tag{25}$$

Also

$$\epsilon'' = 2{\cdot}8 \times 10^{-8}. \tag{26}$$

The smallness of the numbers ϵ', ϵ'' does not prove that their effects are negligible, because small divisions occur in the solution.

These estimates ignore the inner core. This has little effect on I, but may increase M by something like 3 per cent. This will multiply ϵ' by about 2 and ϵ'' by about 4.

6. *Free periods.*—We put

$$l + im = \zeta, \qquad l_1 + im_1 = \zeta_1, \qquad c_1 + ic_2 = k, \tag{27}$$

with a time factor $e^{i\gamma t}$. Then the equations of motion are equivalent to

$$\left.\begin{aligned} &(\gamma+\omega)\{A\gamma - \omega(C-A)\}\zeta + (\gamma+\omega)(A_1\gamma + \epsilon' A_1 \omega)\zeta_1 = (C-A)k, \\ &(\gamma+\omega)(A_1\gamma + \epsilon' A_1\omega)\zeta + \{A_1\gamma^2 + \omega\gamma C_1(1+2\epsilon') - 2\epsilon'' A_1 \omega^2\}\zeta_1 = -\epsilon' C_1 k. \end{aligned}\right\} \tag{28}$$

There are two free periods with γ/ω small and two with it near -1. For the first pair, treat $(C-A)/C$, $(C_1 - A_1)/C_1$ and γ/ω as small quantities of the first order and neglect their squares and their products with ϵ' and ϵ''. Then to this order the solutions are

$$\frac{\gamma}{\omega} = 2\epsilon'', \qquad \frac{C_1(C-A) + 2AA_1\epsilon'' - 2\epsilon' A_1^2}{AC_1 - A_1^2}. \tag{29}$$

For the homogeneous core there is a zero solution, corresponding to a free steady displacement of the core with respect to the shell. We now find that gravity converts this into a free oscillation with a period of about 5×10^5 years. The second solution is the Eulerian nutation. It differs from its value for the homogeneous core by about 1 part in 10^4; the change is therefore negligible.

* K. E. Bullen, *M.N., Geophys. Suppl.*, **3**, 395–401, 1936.

As expected, one period makes γ/ω exactly -1. The other (corresponding to a resonance noted in Paper II) makes

$$\frac{\gamma}{\omega} = -1 - \frac{C(C_1 - A_1) + 2(\epsilon' + \epsilon'')A_1^2}{CA_1 - A_1^2}. \tag{30}$$

It is a retrograde motion in about 350 days, and the corrections again amount to about 1 part in 10^4.

7. *Forced motions.*—Except for periods very near the free periods, since the changes in the latter are so small, we can drop ϵ' and ϵ'' on the left sides of the equations of motion. The new feature is that the external field has a direct effect on the motion of the core relative to the shell. There are two interesting cases; if $\gamma = -\omega + n$, n/ω is small in both. In the first, the 19-yearly nutation, it is about $-\frac{1}{6800}$ and therefore small compared with $(C-A)/C$ and $(C_1 - A_1)/C_1$. In the second, the fortnightly and semi-annual nutations, it is about $+\frac{1}{14}$ or $+\frac{1}{180}$ and therefore larger than these two numbers. The correcting factor for the amplitude of ζ is, roughly,

$$1 + \frac{n}{\omega}\frac{A_1 C_1 \epsilon'}{(C-A)(C_1 - A_1 + A_1 n/w)}. \tag{31}$$

As there are two small divisors it looks as if this correction might be appreciable; but for the 19-yearly period it is about -3×10^{-6} and for the fortnightly one about $+4 \times 10^{-5}$. The effects of the changes of the coefficients on the left are even smaller.

The conclusion is that all effects of heterogeneity in the core are taken into account with sufficient accuracy if the core is taken as homogeneous and given its correct moments of inertia. Even if, as seemed possible in Section 5, the factors ϵ' and ϵ'' have been somewhat underestimated, this remains true. This is to be regarded simply as an analytical device, for a homogeneous core with the correct moment of inertia would have less than the correct mass.

8. *Outstanding discrepancy in the 19-yearly period.*—This analysis justifies the use in Paper I of the correct moments of inertia of the core. The effect on the amplitude of the nutation, with a rigid shell, was there estimated as -6 parts in 1000. In Paper II the data used made the moments of inertia of the core too large; but the important point now is that allowance for elasticity of the shell made a reduction from 9 parts to 6·6 parts in 1000. It seems probable, therefore, that with the correct treatment of the core and the same elasticity of the shell the effect would be about -4 parts in 1000. Again, in the solution for the variation of latitude I found $\phi = 0{\cdot}515\psi$, ϕ representing the elastic displacement at the surface and ψ that at the core boundary. For the nutation the ratio is 0·725. This indicates that distortion near the base of the shell is relatively more important in the variation of latitude than in the nutation, and therefore that it would be appropriate to use a lower rigidity in the latter. It appears possible that with a full treatment of the actual shell the effect might be as small numerically as -3 parts in 1000, making the theoretical amplitude about $9''{\cdot}200$ against the rigid body value of $9''{\cdot}227$. G. M. Clemence* has pointed out that in Spencer Jones's observational determination of $9''{\cdot}213$ (and in Jackson's previous one) the correction found was applied with the wrong sign, and that the data actually lead to $9''{\cdot}2066$. If these considerations are correct the observed value may agree

* G. M. Clemence, *Astr. Journ.*, **53**, 179, 1948.

better with the calculated value for a fluid core and elastic shell than with that for a rigid Earth; at any rate they are near enough for a full treatment to be worth while.

The fortnightly nutation has recently been determined from observations by H. R. Morgan. The amplitude for a rigid Earth would be 0″·088. Morgan * gets 0″·098, revising a preliminary determination that gave 0″·078. In this range a fluid core with a rigid shell would produce an increase of about $\frac{1}{8}$, so that Morgan's revised value is in good agreement.

Morgan has also made an analysis for the 19-yearly period, introducing a possible phase shift as an unknown ; it is small and doubtfully significant. I no longer think that imperfections of elasticity can produce a noticeable phase shift. Since the whole effect of the departures from perfect rigidity is expressed by a change of the coefficient by about 1 part in 400, and at the worst dissipation could only shift the phase of this part by 90°, the maximum phase shift for the nutation as a whole would be about 0°·2. The relevant tidal component has speed $-w+n$ relative to the Earth, and is therefore the lunar K_1, a diurnal, not a long-period, tide. For the semi-diurnal tide we can get the order of magnitude of the phase shift in the tide itself by attributing the whole of the tidal friction to the bodily tides, and it would be well under 1°. For the diurnal tide the shift will be of the same order of magnitude, and it is therefore unlikely that the resulting phase shift in the nutation will be over 0°·002.

160 *Huntingdon Road,*
Cambridge:
1950 *May* 28.

* Private communication.

STELLAR ABERRATION

J. G. Porter and D. H. Sadler

(Communicated by the Astronomer Royal)

(Received 1950 October 6)

Summary

A method is described for the routine calculation of the aberration day numbers, C and D, from the components of the Earth's velocity referred to the centre of gravity of the solar system. The presence of lunar terms in these day numbers gives rise to difficulties in checking the apparent places of stars at ten-day intervals, and two alternative methods are suggested for dealing with this problem.

---

1. *Introduction.*—At the meeting of the International Astronomical Union in Zürich in 1948, a number of questions concerning the volume *Apparent Places of Fundamental Stars* was discussed by Commission 4 (Ephemerides). The increasing need for greater accuracy and for consistency in the calculation of these apparent places led to the adoption of a recommendation:—

> " . . . that the Day Numbers C and D should be computed directly from the motion of the Earth referred to a suitable fixed frame of reference (instead of from multiples of the sine and cosine of the Sun's longitude as at present); . . . . It is further recommended that the terms in the aberration depending on the eccentricity of the Earth's orbit should continue to be omitted."

The correction for aberration, as computed at present in terms of the Sun's longitude, is not the true value; apart from other approximations it does not include the constant terms due to the eccentricity of the Earth's orbit. The true value may be computed from the ratios x'/V, y'/V, z'/V, where x', y', z' are the components of the Earth's velocity referred to the centre of gravity of the solar system, and V is the velocity of light; it includes not only the effect of lunar and planetary perturbations, but also the constant terms already referred to. These terms, which are constant for any given star, and which have always been omitted from the aberration corrections, may be considered as incorporated in the star's mean place. The removal of these constant terms, as recommended by the I.A.U., is clearly necessary, since their inclusion would necessitate a revision of the mean places of all stars.

These terms assume considerable importance in the case of photographic observations of planets and comets. As Cowell pointed out (1) as long ago as 1900, the position of the planet is antedated by the amount of its light-time and this affords a complete correction for aberration, including the terms depending on the eccentricity. The mean places of the stars to which the planet is referred already incorporate these terms, and an error may thus be produced which can

amount to $\kappa e = 0''\cdot342$. This appreciable source of error is removed in recent ephemerides, such as that of Pluto in the *Nautical Almanac* and *American Ephemeris*, which give astrometric places, i. e. mean places to which the constant terms have been applied. This type of ephemeris, which is immediately comparable with photographic observations, will also be given in future in these publications for the four minor planets Ceres, Pallas, Juno and Vesta.

2. *Formulae for day numbers C and D.*—The method of computing aberration corrections from the components of the Earth's velocity was first mentioned by Turner (**2**) in 1909, and the problem was discussed in greater detail by Plummer (**3**), who later (**4**) gave the first table of accurate values of C and D for the year 1910. In this early work the velocities were referred to the Sun as centre, while the effect of the planets Jupiter and Saturn was introduced by simple approximations. In routine calculations it is better to use the published values of the planetary coordinates, and the day numbers may be computed from the expressions

$$C + \text{constant term} = +y'/V, \quad D + \text{constant term} = -x'/V. \tag{1}$$

The value of V used in these equations must be derived from the accepted value of the aberration constant, $20''\cdot47$; introducing the expressions for the constant terms

$$C = +1189''\cdot80\,(y' + Ke\cos\pi\cos\epsilon), \quad D = -1189''\cdot80\,(x' + Ke\sin\pi), \tag{2}$$

in which π is the longitude of perihelion, e the eccentricity of the Earth's orbit, ϵ the obliquity of the ecliptic, x' and y' are measured in astronomical units per day, and K is the aberration constant divided by the factor 1189·80. It is to be noted that this factor is not consistent with modern values for the velocity of light, which would require a figure larger by about two units. Any future revision of the fundamental constant κ will necessitate a revision of the factor in (2). The constant terms may be evaluated (for equinox 1950·0) from the numerical quantities

$$e = 0\cdot016730, \qquad \pi = 282°\cdot081, \qquad \epsilon = 23°\cdot446,$$

leading to

$$Ke\cos\pi\cos\epsilon = +553\,.\,10^{-7}, \qquad Ke\sin\pi = -2815\,.\,10^{-7}. \tag{3}$$

These terms are not, in fact, constant, being subject to small changes in e and ϵ, but the variations have no significant effect over long periods of time.

Equations (2) may now be written

$$C = +1189''\cdot80\,(y' + 553)\,.\,10^{-7}, \qquad D = -1189''\cdot80\,(x' - 2815)\,.\,10^{-7}, \tag{4}$$

in which x' and y' are to be referred to the centre of gravity of the solar system and are in units of the seventh decimal of an astronomical unit per day. Now if

X, Y, Z are the solar coordinates referred to the Earth,

x_n, y_n, z_n are the planetary coordinates referred to the Sun,

then the coordinates of the Earth, referred to the centre of gravity of the whole system, will be

$$X_c = -X - \Sigma m x_n/(1 + \Sigma m), \tag{5}$$

where m represents planetary masses in terms of the Sun's mass, and similar expressions hold for Y_c and Z_c.

The values to be adopted for the masses of the planets are not critical, and in the present paper the values given in the volumes of *Planetary Coordinates* are used without change. The maximum effect of a planet on x' or y' due to the use of (5) is, in the usual notation, $kman = km/\sqrt{a}$, or, in units of the seventh decimal,

Mercury	0·04	Jupiter	72·0
Venus	0·50	Saturn	15·9
Earth	0·52	Uranus	1·7
Mars	0·04	Neptune	1·6

Since one unit in these values will only affect the fourth decimal of C or D, it is clear that Jupiter, Saturn, Uranus and Neptune alone need be considered. The denominator of (5), however, must contain the masses of all the planets, so that this equation may be written in the form

$$X_c = -X - \Sigma m' x_n, \tag{6}$$

where m' is now used to represent the planetary masses divided by the total mass 1·001345. The " reduced " masses to be used in this equation are thus

Jupiter	0·000953	Uranus	0·000044
Saturn	0·000285	Neptune	0·000052

The velocity components of the Earth, including all the planetary and lunar perturbations, may thus be obtained from the differences of X_c, Y_c and Z_c, and the aberration corrections are computed then from the usual equations:

$$\left.\begin{aligned} \cos\delta\,\Delta\alpha &= -\frac{x'}{V}\sin\alpha + \frac{y'}{V}\cos\alpha, \\ \Delta\delta &= -\frac{x'}{V}\sin\delta\cos\alpha - \frac{y'}{V}\sin\delta\sin\alpha + \frac{z'}{V}\cos\delta. \end{aligned}\right\} \tag{7}$$

Practical methods for computing the corrections in this form have been discussed by Zagar (**5**), whose tables for 1940 and 1941 (**6** and **7**) give three day numbers for use with the second of equations (7). The conversion of this equation into the usual form

$$\Delta\delta = Cc' + Dd'$$

may, however, be accomplished without any appreciable loss of accuracy.

There are three sources of error in replacing z' in (7) by $y' \tan\epsilon$: firstly, the lunar and planetary perturbations in the Sun's latitude, giving rise to a maximum error of about 10 in the seventh decimal, corresponding to 0″·0012 in the declination; secondly, the secular rotation of the ecliptic, giving rise to an error of about $\frac{1}{2}$ (number of years from 1950), or 0″·001 in the declination in about 20 years; finally, the inclinations of the planetary orbits whose contribution, as shown below, is negligible. With the usual notation, for a particular planet,

$$y'_n = \frac{k}{r\sqrt{a}}(B_y\cos E - A_y\sin E), \quad z'_n = \frac{k}{r\sqrt{a}}(B_z\cos E - A_z\sin E), \tag{8}$$

from which it follows that $z'_n - y'_n \tan\epsilon$ cannot exceed

$$\frac{k\sqrt{a}}{r}\sec\epsilon\sin i, \tag{9}$$

where i is the inclination to the ecliptic. The error is thus less than two units of the seventh decimal for Jupiter and even smaller for the other planets.

The desired standard of accuracy may therefore be attained with the usual formulae

$$\Delta\alpha = Cc + Dd, \qquad \Delta\delta = Cc' + Dd'. \tag{10}$$

3. *Calculation of day numbers C and D.*—The computation is divided naturally into two steps as follows:

(*a*) The daily differences of the Sun's X and Y lead to velocity components X' and Y'; taking third differences into account, and using central-difference notation,

$$X' = \mu(\delta - \tfrac{1}{6}\delta^3)X, \qquad Y' = \mu(\delta - \tfrac{1}{6}\delta^3)Y. \tag{11}$$

The second term in these expressions cannot exceed 10 units of the seventh decimal, and may be considered as determinable from the Sun's ephemeris for any year. These small terms may therefore be thrown, together with the constants of equations (3) and (4), into the second step, involving the reduction to the barycentre.

(*b*) The second step, like the first, involves mechanical differentiation. The quantities $\Sigma m' x_n$ and $\Sigma m' y_n$, which form the reduction to the barycentre in (6), are obtained from the heliocentric coordinates x_n and y_n of the planets (taken, for example, from *Planetary Coordinates*) at an interval of 100 days. These are multiplied by their respective "reduced" masses, the sums of these quantities are tabulated for each date, and from the differences the *daily* velocities are found at 50-day intervals. Denoting these values by $(mx)'$ and $(my)'$, and adding the small term in (11) and the constant terms in (4), the quantities

$$\Delta Y' = (my)' - \tfrac{1}{8}\mu\delta^3 Y - 553, \qquad \Delta X' = (mx)' - \tfrac{1}{8}\mu\delta^3 X - 2815 \tag{12}$$

may be formed at intervals of 50 days. The day numbers C and D can then be formed from the expressions

$$C = -1189''{\cdot}80\,(\mu\delta Y + \Delta Y'), \qquad D = +1189''{\cdot}80\,(\mu\delta X + \Delta X'), \tag{13}$$

which are now in a form suitable for machine working. In the case of D, for example, daily values of $2(\mu\delta X + \Delta X')$ are formed in one operation on a National machine by integration from second differences of X, with simultaneous interpolation of $\Delta X'$ to fiftieths. Multiplication by 594·90 then gives the required values of D, three decimals being retained in the final values of both C and D.

4. *Lunar terms in aberration corrections.*—Reference has already been made to the fact that C and D computed in this way contain small terms due to lunar perturbations. The presence of these terms causes no difficulty in a daily ephemeris, but the calculation of the apparent places of stars at every tenth transit (such as in *Apparent Places of Fundamental Stars*) will be difficult to check, since the higher differences fail to run smoothly. Occasional fourth differences exceeding 100 in units of the third decimal will be found in the ten-day values of C and D. However, it is possible to estimate their value at any given date with

some accuracy; the effect of lunar perturbations on the Earth's velocity may be shown to be approximately

$$\Delta X' = +mvp \sin \mathbb{C}, \qquad \Delta Y' = -mvq \cos \mathbb{C}, \tag{14}$$

where m is the mass of the Moon (Earth = 1), $\mathbb{C}$ is the Moon's mean longitude and v its mean velocity. The factors p and q are functions of the inclination and longitude of the node of the Moon's orbit, and have a range of values from 0·88 to 1·00. These equations may be written in the form of variations in C and D:

$$\Delta C = -0''{\cdot}0086\, q \cos \mathbb{C}, \qquad \Delta D = -0''{\cdot}0086\, p \sin \mathbb{C}. \tag{15}$$

They may be expressed, with sufficient accuracy, in units of the third decimal of a second of arc in the form

$$\Delta C = -9 \cos \mathbb{C}, \qquad \Delta D = -9 \sin \mathbb{C}. \tag{16}$$

Thus the variations in C and D are actually of the type

$$A \sin (B + \theta),$$

where θ is the mean motion of the Moon in 10 sidereal days, namely 131°·4. Now the fourth differences of this expression are

$$16A \sin^4 \tfrac{1}{2}\theta \sin (B + \theta),$$

being $16 \sin^4 \theta/2$, or approximately 11, times as great as the original function: their amplitude will thus be about 100. The variations in the apparent place caused by the lunar terms are thus

$$\Delta\alpha = c\Delta C + d\Delta D, \qquad \Delta\delta = c'\Delta C + d'\Delta D. \tag{17}$$

We may combine the first of these equations with (16) to give

$$\Delta\alpha = -0^s{\cdot}0006 \sec\delta \cos (\mathbb{C} - \alpha). \tag{18}$$

The maximum value of this expression is $0^s{\cdot}0012$ for a star of declination 60° and $0^s{\cdot}0035$ for a declination of 80°. For the declination, the second equation of (17) may be put in a similar form by the transformation

$$c' = r \cos s, \qquad d' = r \sin s, \tag{19}$$

so that

$$\Delta\delta = -0''{\cdot}009\, r \cos (\mathbb{C} - s), \tag{20}$$

in which r cannot exceed 1·09, so that $\Delta\delta$ has a maximum value of 0″·010.

The lunar terms, although small, thus affect the last figure retained in an ephemeris place and for the most accurate work must clearly be included. Interpolation of a ten-day ephemeris by ordinary methods, using second differences, provides adequate accuracy, in spite of the fact that the phase of the lunar terms changes by 131°·4 in the ten-day interval. For many purposes the inclusion of these small terms may be considered unnecessary, and it is then clearly simpler to remove the lunar terms given in (16) from C and D before computing the apparent place. The "smoothed" values of C and D so obtained

will give star places which can be checked in the usual way by differencing, while if the highest accuracy is required, the lunar terms can be added to the computed place by means of the corrections (18) and (20).

Alternatively, the computer may prefer to compute apparent places directly by means of the correct values of C and D, and use multiples of (18) and (20) to check the fourth differences within the limits normally imposed by rounding-off errors. A suggested method of tabulating the lunar terms and of employing these two methods is given below.

TABLE I

Day numbers C and D, 1956, for every tenth sidereal day

Date	True values				"Smoothed" values			
1956	C	δ^4C	D	δ^4D	C	δ^4C	D	δ^4D
	″		″		″		″	
Jan. 0·7	− 2·984	+52	+20·197	− 48	− 2·990	−14	+20·204	+28
10·7	6·213	+ 9	19·318	+108	6·214	−15	19·309	+ 8
20·7	9·249	−92	17·808	− 26	9·241	− 6	17·813	+31
30·6	11·966	+74	15·757	− 11	11·975	−26	15·759	+12
Feb. 9·6	14·330	−51	13·229	+ 93	14·326	− 7	13·221	+ 7
19·6	−16·233	−57	+10·277	− 76	−16·230	−19	+10·285	+14
29·6	17·618	+63	7·047	+ 35	17·627	−33	7·044	+ 2
Mar. 10·5	18·485	−89	3·609	+ 42	18·477	+ 1	3·605	− 5
20·5	18·771	− 2	+ 0·068	− 92	18·773	−26	+ 0·077	+ 4
30·5	18·502	+36	− 3·429	+ 65	18·507	−20	− 3·436	−15
Apr. 9·5	−17·706	−97	− 6·827	− 16	−17·697	− 1	− 6·826	− 6
19·4	16·375	+48	10·006	− 73	16·381	−22	10·000	− 6
29·4	14·598	− 3	12·862	+ 76	14·598	− 7	12·871	−23
May 9·4	12·416	−77	15·364	− 70	12·409	+ 1	15·358	− 7
19·3	9·873	+81	17·405	− 28	9·882	−22	17·403	−12
29·3	− 7·090	−43	−18·948	+ 67	− 7·084	+16	−18·955	−17
June 8·3	4·107	−34	19·984	−110	4·104	− 9	19·975	−14
18·3	− 1·007	+79	20·437	+ 33	− 1·015	−10	20·441	− 9
28·2	+ 2·093	−70	−20·341	+ 22	+ 2·101	+20	−20·345	−21

5. *Checking the lunar terms.*—The first of these methods will necessarily involve the publication of "smoothed" values of C and D which, by way of illustration, are given in Table I for part of the year 1956. The data are given at 0^h sidereal time for every tenth sidereal day, and the "smoothed" values have been obtained by the application of (16) to the true values. The Moon's mean longitude has been taken as 136°·6 on the first date, and increments of 131°·4 have been added for each subsequent entry. It would probably be simpler in practice to use a series of terms such as those given in Tables II and III, since it is not necessary to remove completely the oscillations in the fourth differences.

The star positions may then be computed in the normal manner, using the "smoothed" values of C and D; the aberration corrections computed in this

way are shown in the first columns of Table II for a typical star (FK3 No. 1397), one extra figure being retained in order to reduce the rounding-off errors. The lunar terms to be added to the smoothed values to give the final values are tabulated in the next columns of Table II and are taken from Tables III and IV. Table III gives the values of (15), (18) or (20) for four different amplitudes and for increments of 132° in the angle. The four amplitudes chosen (0·9, 3, 6 and 9) are sufficient to cover all possible cases, and the use of 132° to represent the motion in ten days is sufficiently close to the truth to give ample accuracy, while having the advantage of giving a series recurring after 30 terms; the unit is the third decimal in all cases. Table IV gives the series and number of the term in Table III to be used to represent the correction on the first date of the year's ephemeris. Subsequent corrections at intervals of ten sidereal days are then given by succeeding terms of the same series, taken in the order printed, and repeating from the first term when the thirtieth term is reached. Table IV must not be interpolated; it is entered with the nearest hour of R.A. and the nearest tenth degree of declination, the intervals having been chosen so that there is very little divergence between neighbouring terms. It will be noticed that series P is to be used for the R.A. corrections for stars with declinations less than 60°; for stars nearer to the poles it is customary to drop the third decimal in the R.A. and series Q is to be used. The declination corrections have a zero value at 6^h, $+23°$ or 18^h, $-23°$ and have a maximum value of 9·8, but the four ranges of amplitude given have been selected to cover these values with a minimum of error. Since the Moon's longitude changes by 132°·7 in one Julian year, these tables may be used for future years by increasing the numbers of Table IV by unity for each year after 1956. This process may continue for some fifteen years without the necessity of a revision.

For star No. 1397 (R.A. $15^h\ 05^m$; Dec. $+54°\ 45'$) it is seen that the R.A. corrections have P13 for their initial term, while those in declination commence with S15. The application of these corrections, followed by rounding off, gives the final values in Table II. These may be compared with the true values in the following columns, the latter having been computed directly from the true values of *C* and *D* in Table I.

The second method is also illustrated in Table II, where the computed aberration corrections are differenced. The oscillations in the fourth difference are compared directly with the terms of Table III, commencing as before with P13 and S15, but noting that the terms now represent units of the *second* decimal, since they refer to the fourth differences, approximately 10 times the function values. The example illustrates the order of agreement which is obtained, and which usually comes well within the accepted limits of six units in the fourth difference; the signs of the differences are indicated with some certainty.

The error involved in the use of these tables is very small. The discrepancy between the true motion of 131°·4 in ten days, and the assumed value of 132°, may give rise to a divergence from the correct value of the longitude at the end of the year of about 23°. By commencing the series with a value of 127°, instead of the true value of 136°·6, the errors are distributed over the year and do not exceed $0^s·0003$ in R.A. (at 60° declination) or 0″·004 in declination; they can be ignored. The errors due to the use of an approximate amplitude are also negligible.

TABLE II

Aberration corrections for FK3 star No. 1397

$c = -0.07993$, $d = -0.08333$, $c' = +0.8398$, $d' = -0.5651$

Date		Right ascension						Declination					
1956		Smooth $\Delta\alpha$	Corr.	Final value	True $\Delta\alpha$	δ^4	Table	Smooth $\Delta\delta$	Corr.	Final value	True $\Delta\delta$	δ^4	Table
		s		s	s			"		"	"		
Jan.	0·7	−1·4456	0	−1·446	−1·446	− 3	0	−13·928	+9	−13·92	−13·92	+ 3	+9
	10·7	1·1133	−7	1·114	1·114	− 5	−7	16·130	−5	16·13	16·13	− 2	−5
	20·7	0·7466	+9	0·746	0·746	+ 4	+9	17·827	−2	17·83	17·83	− 9	−2
	30·6	−0·3568	−5	−0·357	−0·357	+ 1	−5	18·962	+8	18·95	18·95	+ 9	+8
Feb.	9·6	+0·0427	−2	+0·042	+0·042	− 9	−2	19·502	−9	19·51	19·51	−11	−9
	19·6	+0·4397	+8	+0·440	+0·441	+14	+8	−19·442	+4	−19·44	−19·44	+ 1	+4
	29·6	0·8216	−9	0·821	0·821	− 9	−9	18·784	+4	18·78	18·78	+ 1	+4
Mar.	10·5	1·1763	+4	1·177	1·177	+ 4	+4	17·554	−9	17·56	17·56	− 8	−9
	20·5	1·4941	+4	1·494	1·495	+ 7	+4	15·809	+8	15·80	15·80	+ 5	+8
	30·5	1·7658	−9	1·765	1·765	− 6	−9	13·600	−2	13·60	13·60	− 2	−2
Apr.	9·5	+1·9837	+8	+1·984	+1·984	+ 6	+8	−11·005	−5	−11·01	−11·01	− 5	−5
	19·4	2·1431	−2	2·143	2·143	+ 4	−2	8·106	+9	8·10	8·10	+ 6	+9
	29·4	2·2400	−5	2·240	2·239	− 6	−5	4·986	−7	4·99	4·99	− 5	−7
May	9·4	2·2724	+9	2·273	2·273	+12	+9	− 1·742	0	− 1·74	− 1·74	+ 1	0
	19·3	2·2409	−7	2·240	2·240	− 6	−7	+ 1·536	+7	+ 1·54	+ 1·54	+ 5	+7
	29·3	+2·1467	0	+2·147	+2·147	0	0	+ 4·762	−9	+ 4·75	+ 4·75	− 6	−9
June	8·3	1·9935	+7	1·994	1·995	+11	+7	7·841	+5	7·85	7·84	+ 3	+5
	18·3	1·7855	−9	1·785	1·785	− 9	−9	10·699	+2	10·70	10·70	+ 5	+2
	28·2	+1·5284	+5	+1·529	+1·529	+ 5	+5	+13·261	−8	+13·25	+13·25	− 8	−8

TABLE III

Lunar terms in aberration corrections

Term	P	Q	R	S	Term	P	Q	R	S
1	+0·5	+2	+4	+5	16	−0·5	−2	−4	−5
2	+0·2	+1	+1	+2	17	−0·2	−1	−1	−2
3	−0·8	−3	−5	−8	18	+0·8	+3	+5	+8
4	+0·9	+3	+6	+9	19	−0·9	−3	−6	−9
5	−0·4	−1	−3	−4	20	+0·4	+1	+3	+4
6	−0·4	−1	−2	−4	21	+0·4	+1	+2	+4
7	+0·9	+3	+6	+9	22	−0·9	−3	−6	−9
8	−0·8	−3	−5	−8	23	+0·8	+3	+5	+8
9	+0·2	+1	+1	+2	24	−0·2	−1	−1	−2
10	+0·5	+2	+3	+5	25	−0·5	−2	−3	−5
11	−0·9	−3	−6	−9	26	+0·9	+3	+6	+9
12	+0·7	+2	+5	+7	27	−0·7	−2	−5	−7
13	0·0	0	0	0	28	0·0	0	0	0
14	−0·7	−2	−4	−7	29	+0·7	+2	+4	+7
15	+0·9	+3	+6	+9	30	−0·9	−3	−6	−9

The entries in the above table are in units of the third decimal.

TABLE IV

First terms in right ascension and declination for 1956

R.A.	Right ascension	Declination									R.A.
		0°	10°	20°	30°	40°	50°	60°	70°	80°	
h	P or Q										h
0	12	Q12	Q20	Q28	R17	R17	R 6	S 6	S25	S25	0
1	1	Q12	Q20	Q28	R17	R 6	R25	S14	S14	S 3	1
2	9	Q12	Q20	Q28	Q 6	R14	R14	R 3	S 3	S22	2
3	28	Q12	Q20	Q17	Q25	Q 3	R22	R22	S11	S11	3
4	17	Q12	Q20	Q17	Q 3	Q11	R11	R30	R30	S19	4
5	6	Q12	Q 1	P28	Q30	Q19	Q19	R 8	R 8	S 8	5
6	14	Q12	Q12	P12	P27	Q27	Q27	R27	R27	S27	6
7	3	Q12	Q23	P26	Q13	Q24	Q 5	R 5	R 5	S 5	7
8	22	Q12	Q23	Q 7	Q10	Q 2	R13	R24	R24	S24	8
9	11	Q12	Q 4	Q26	Q29	Q21	R21	R 2	S 2	S13	9
10	19	Q12	Q 4	Q26	Q18	R29	R10	R21	S21	S21	10
11	8	Q12	Q 4	Q26	R 7	R18	R29	R29	S10	S10	11
12	27	Q12	Q 4	R15	R26	R 7	R18	S18	S29	S29	12
13	16	Q12	Q23	R15	R15	R26	S 7	S 7	S 7	S18	13
14	24	Q12	R23	R 4	R15	S15	S26	S26	S26	S26	14
15	13	Q12	R23	R 4	R 4	S 4	S15	S15	S15	S15	15
16	2	Q12	R23	R23	R23	S23	S 4	S 4	S 4	S 4	16
17	21	Q12	R12	R12	R23	S23	S23	S23	S23	S23	17
18	29	Q12	R12	R12	R12	S12	S12	S12	S12	S12	18
19	18	Q12	R 1	R 1	R 1	S 1	S 1	S 1	S 1	S 1	19
20	7	Q12	R 1	R 1	R20	S20	S20	S20	S20	S 9	20
21	26	Q12	R 1	R20	R20	S 9	S 9	S 9	S 9	S28	21
22	4	Q12	R20	R20	R 9	S28	S28	S28	S17	S17	22
23	23	Q12	R20	R 9	R28	S28	S17	S17	S 6	S 6	23

For corrections in right ascension, use series P for all stars having declinations less than 60°, and series Q for stars with declinations from 60° to 80°.

For negative declinations, use R.A. $\pm 12^h$ as argument for the corrections in declination.

For other years, increase the numbers in the above table by unity for each year after 1956.

The second of the two methods described is more accurate and more direct, and should be used for systematic computation of apparent places of stars unless the method of calculation used relies on the smoothness of the differences. In this case, the first method offers a simple alternative.

H.M. Nautical Almanac Office,
The Royal Greenwich Observatory,
Herstmonceux Castle,
Sussex :
1950 *October* 4.

References

(1) P. H. Cowell, *The Observatory*, **23**, 448, 1900.
(2) H. H. Turner, *M.N.*, **69**, 413, 1909.
(3) H. C. Plummer, *M.N.*, **69**, 414, 1909.
(4) H. C. Plummer, *M.N.*, **70**, 80, 1909.
(5) F. Zagar, *Mem. Soc. Astr. Ital.*, **12**, 1, 1939.
(6) F. Zagar, *Mem. R. Acc. Sci. Bologna* (ix), **7**, 1939.
(7) F. Zagar, *Mem. R. Acc. Sci. Bologna* (ix), **8**, 1940.

ON THE EXPULSION OF CORPUSCULAR STREAMS BY SOLAR FLARES

F. D. Kahn

(Received 1950 July 8)

Summary

A value is found for the minimum momentum density in a corpuscular stream which has been emitted from a flare and which causes a terrestrial magnetic storm. It is shown that radiation pressure alone will always be insufficient to expel such a stream from the Sun.

---

1. *Introduction.*—Some twenty years ago Chapman and Ferraro (1) developed the corpuscular theory of magnetic storms, which is now generally accepted. They showed that terrestrial magnetic disturbances should take place whenever a cloud of particles emitted by the Sun travels past the Earth. In the case of the irregularly occurring magnetic storms, which are strongly associated with solar flares (*cf.* Newton (2)), it must be supposed that the particles are emitted by the direct action of the flares themselves. From the observed average interval between the two phenomena it is commonly deduced that the particles have speeds of between 1000 and 1600 km./sec.

Kiepenheuer (3) has proposed that the radiation pressure due to the flare may cause the expulsion of the cloud. This suggestion has also been subsequently made by Hoyle (4) and by the author (5). However, it will be shown in this paper that the momentum which can be communicated by radiation alone to the nearby particles will always be insufficient to expel a stream dense enough for a storm of observed intensity.

2. *The required momentum density of the stream.*—To obtain a workable model of the expulsion it was assumed in a previous paper (5) that the particles are emitted radially from the surface of the flare, here taken to be the cap of a sphere of radius b. The flare is situated in the solar atmosphere and the emission continues from time $t=0$ until $t=\tau_1$. Since storms always last much longer than the associated flares it was supposed that the velocity of emission is highest at the peak of the flare and then falls off gradually, thus giving a longitudinal expansion to the stream. With these assumptions the density near the front of a stream, t seconds after the flare peak, is given by

$$n(t)=\frac{b^2N(0)\tau_1}{v_0^2(v_0-v_1)t^3}, \qquad \text{when } t>\tau_1,$$

where

b = hypothetical radius of flare (2×10^9 cm.),
$N(0)$ = rate of emission per unit area of flare,
τ_1 = duration of flare (10^3 sec.),
v_0 = velocity of emission at flare peak ($1{\cdot}6\times10^8$ cm./sec.),
v_1 = velocity of emission at end of flare (10^8 cm./sec.).

(This formula was obtained in (5), Section 3.32. The values given in brackets in the list of symbols are typical, and will be adopted in the subsequent working.)

If $\bar{m}$ is the average mass of the particles, the momentum density near the front of the stream is given by

$$F = n(t)\bar{m}v_0^2 = \frac{b^2 N(0)\bar{m}\tau_1}{(v_0 - v_1)t^3}, \qquad \text{when } t > \tau_1.$$

The momentum density at the emitting area is $F_0 = N(0)\bar{m}v_0$, hence

$$F = \frac{b^2\tau_1 F_0}{v_0(v_0 - v_1)t^3} = \frac{4 \times 10^5 F_0}{t^3}.$$

When the storm reaches the Earth, $t \sim 10^5$ sec., and

$$F = 4 \times 10^{-10} F_0.$$

Chapman and Bartels (**6**) give an estimate of the minimum value of F, sufficient for a magnetic storm. They find that the least possible momentum density is that of a stream containing 10 H-atoms per c.c. and travelling at $1{\cdot}6 \times 10^8$ cm./sec. Thus, if m_H is the mass of a hydrogen atom,

$$F \geqslant 10 m_H v_0^2 = 4 \times 10^{-7} \text{ dynes/sq. cm.}$$

and

$$F_0 \geqslant 10^3 \text{ dynes/sq. cm.}$$

The rate at which momentum is given to the stream by the flare must then exceed 10^3 dynes/sq. cm.

This is not a very large value, but nevertheless it will be shown to exceed the radiation pressure which the flare can exert. A much smaller value is required by Hoyle, who assumes that particles are emitted radially from the *Sun* rather than radially from the *flare*, and who neglects the longitudinal expansion of the stream. On this model the density on emission can be much lower, but, since a flare subtends only a small solid angle at the centre of the Sun, the resulting emission is confined within a very narrow cone. Now even a flare well removed from the centre of the Sun's disk can cause a magnetic storm, so that we need to have cones of emission wider than is supposed on Hoyle's model.

3. *The mechanism of radiation pressure.*—There are two ways in which radiation pressure can act on the particles :

1. The atoms may absorb resonance radiation coming from the flare, and re-emit at random.

2. The atoms may be ionized by radiation coming from the flare.

In either case the absorption of a photon of wave-length λ gives an impulse h/λ away from the source.

3.1. *The resonance process.*—Consider an atom with a resonance line at wave-length λ_0 cm. Let the atom be exposed to a field of radiation contained within a solid angle Ω at P and let it have a velocity v away from the field. Light arriving at P within a small cone of solid angle $d\Omega$ around the line RP ($\angle \text{RPO} = \theta$) can be absorbed by the particle if its wave-length is

$$\lambda = \lambda_0\left(1 - \frac{v}{c}\cos\theta\right)$$

or if

$$\Delta\lambda = \lambda_0 \frac{v}{c}\cos\theta,$$

and the particle will be raised to an excited state. Each photon coming along RP has momentum h/λ, where h is Planck's constant, and the component of this along

OP will be $h \cos\theta/\lambda$. If the emitting region is symmetrical about OP, the sideways components will cancel out.

The atoms are accelerated to a final speed v_0 and the width of the spectral band in which radiation coming from the direction RP can be absorbed is given by

$$\Delta\lambda_0 = \lambda_0 \frac{v_0}{c} \cos\theta \leqslant \lambda_0 \frac{v_0}{c}.$$

The increase in outward momentum which is given by each absorption is approximately $h \cos\theta/\lambda_0 \leqslant h/\lambda_0$, and in order that a group of atoms may gain momentum p_0 the total number of absorptions and re-emissions must exceed $p_0\lambda_0/h$. Now the rate of gain of momentum of the stream near the flare is at least 10^3 dynes/sq. cm.; if this is entirely due to radiation pressure the rate of absorptions and re-emissions above a unit area of flare has to be greater than $10^3\lambda_0/h$ per sq. cm. per sec.

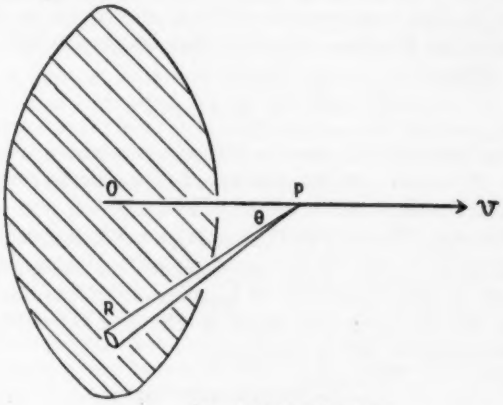

FIG. 1.—*The radiation field at P.*

Let I_λ photons/cm./sq. cm./sec. be the intensity of the radiation emitted by the flare near λ_0 cm. wave-length. The maximum number of absorptions over a unit area of the flare within a band of width $\Delta\lambda_0$ is then

$$I_\lambda \Delta\lambda_0 = I_\lambda \frac{\lambda_0 v_0}{c} \text{ photons/sq. cm./sec.}$$

Hence, if radiation pressure is the *sole* cause of the expulsion,

$$I_\lambda \frac{\lambda_0 v_0}{c} \geqslant 10^3 \frac{\lambda_0}{h},$$

or

$$I_\lambda \geqslant 10^3 \frac{c}{h v_0} = 3 \times 10^{31} \text{ photons/cm./sq. cm./sec.},$$

if we adopt the values

$$h = 6{\cdot}6 \times 10^{-27} \text{ erg.sec.}, \quad c = 3 \times 10^{10} \text{ cm./sec.}, \quad v_0 = 1{\cdot}6 \times 10^8 \text{ cm./sec.}$$

Where the absorbing atoms have a resonance doublet such as the H and K lines of *Ca* II the minimum intensity need have only half this value.

It will be shown that I_λ is much greater than the intensity of radiation to be expected from the flare, whichever group of atoms we choose to consider. Thus Partridge (7) has found that the intensity near the H and K lines is of the same

order as black-body radiation at 6000 deg. K.—it may be up to five times as intense. In full radiation the intensity $\mathfrak{J}$ is given by

$$\mathfrak{J}(\nu)\,d\nu = \frac{8\pi\nu^2}{c^2}\exp(-h\nu/kT)\,d\nu,$$

or

$$\mathfrak{J}(\lambda)\,d\lambda = \frac{8\pi c}{\lambda^4}\exp(-hc/\lambda kT)\,d\lambda,$$

or

$$\mathfrak{J}(\lambda) = 7{\cdot}6\times 10^{26}\ \text{photons/cm./sq. cm./sec.}$$

This is only 5×10^{-5} of the required least value of the intensity, and, at best, H and K radiation pressure fails by a factor of $2{\cdot}5\times 10^{-4}$. In contrast, this pressure is strong enough on Hoyle's model.

Although there are, of course, no experimental data about radiation at $\lambda = 1215$ A. it may be inferred that the $L\alpha$ line is also insufficiently strong for the expulsion. To be effective the rate of absorption of $L\alpha$ photons in a band of width $d\lambda$ above the flare must exceed $3\times 10^{31}\,d\lambda$ photons/sq. cm./sec. and so the rate of absorption by H atoms with velocities between v and $v+dv$ exceeds $3\times 10^{31}\lambda_0\,dv/c$, where

$$\frac{d\lambda}{\lambda_0} = \frac{dv}{c}, \qquad \lambda_0 = 1215\ \text{A.}$$

Each absorption raises an H atom to the $2p$ state whose natural lifetime is $1{\cdot}6\times 10^{-9}$ sec. It follows that the number of $H(2p)$ atoms over a unit area of flare with velocities in the range $(v, v+dv)$ will be

$$3\times 10^{31}\times 1{\cdot}6\times 10^{-9}\lambda_0\,dv/c \sim 5\times 10^{22}\lambda_0\,dv/c,$$

unless there is some process which de-populates the excited state at a rate comparable with or faster than that of spontaneous transitions to the ground state. Each of the $2p$ atoms can absorb in $H\alpha$ light ($\lambda_1 = 6563$ A.) where the absorption cross-section is, after Unsöld (**8**),

$$\alpha_\lambda = \frac{\pi e^2\lambda_1^2}{mc^2}f = 2{\cdot}1\times 10^{-21}\ \text{cm.}^2.$$

Here e = electronic charge, m = electronic mass, c = velocity of light, f = oscillator strength of the transition, λ_1 = wave-length of $H\alpha$.

The atoms with velocities between v and $v+dv$ absorb over a band of width $d\lambda = \lambda_1\,dv/c$ and the optical depth of the cloud for $H\alpha$ light becomes, at least,

$$\alpha_\lambda\times 5\times 10^{22}\times\frac{\lambda_0}{\lambda_1} = 19, \qquad (\lambda_0/\lambda_1 = \tfrac{5}{27}).$$

The cloud of corpuscles is likely to have a great optical depth for $L\alpha$ light and an $L\alpha$ photon may be absorbed and re-emitted many times within the stream, although only the first absorption contributes to the momentum. The density of $H(2p)$ atoms should thus be larger, and the estimate for the $H\alpha$ optical depth should be too low.

With such a great optical depth the cloud should cause a far greater asymmetry in the $H\alpha$ emission of the flare than is commonly found. A rough comparison of the red and blue wings of the $H\alpha$ line, as observed by Ellison (**9**), shows that the excess absorption on the blue wing is about 15 per cent. This is due to a cloud, with an optical depth of the order 0·15, receding from the flare. If the radiation pressure theory is to be maintained we must find a process which reduces the estimated density of $H(2p)$ atoms by a factor of 10^2.

The cloud is too tenuous for collisional de-activation to be important, but it might be thought that ionization of $H(2p)$ atoms by radiation of the Balmer

continuum is fast enough. According to Unsöld (**10**) the total oscillator strength of the transition $2p \rightarrow$ continuum is $f = 0{\cdot}19$, and the total absorption coefficient for light of wave-length $\lambda \leqslant 3647$ A. becomes $\alpha_\nu = (\pi e^2/mc)f$ (it is more convenient here to use the absorption coefficient per unit *frequency* interval) or

$$\alpha_\nu = 5{\cdot}0 \times 10^{-3}.$$

In order that the removal of $2p$ atoms may be sufficiently fast we require 6×10^{10} ionizations per $H(2p)$ atom per second; if I_ν is the maximum intensity of the flare beyond the Balmer limit $\alpha_\nu I_\nu \geqslant 6 \times 10^{10}$,

$$\text{or } I_\nu \geqslant 1{\cdot}2 \times 10^{13} \text{ photons per unit frequency interval/sq. cm./sec.}$$

This is about 4×10^5 times the intensity of a black body at 6000 deg. K. at the Balmer limit, and is by many orders higher than the emission of a flare in this part of the spectrum. The low observed density of H atoms in the $2p$ state shows, therefore, that $L\alpha$ radiation pressure cannot be the cause of the expulsion.

3.2. *The ionizing process.*—Pressure is exerted by ionizing radiation in much the same way as by resonance radiation, but an essential difference between the two processes is that the ions here formed have to recombine with electrons before they can again be acted on by photons. The rate of recombination enables us to fix an upper limit to the effectiveness of radiation pressure. Here it is best to investigate the acceleration of the cloud by the radiation, and the previous model of the emission must be abandoned.

To take the best possible case, consider a cloud of pure hydrogen. Let a typical unit volume of it contain $n(1-x)$ H atoms, nxH^+ ions and nx electrons. If Δ is the total recombination coefficient of H^+ ions to H atoms, the rate of recombination becomes $\Delta n^2x^2 < \Delta n^2$. For equilibrium Δn^2x^2 is also the maximum rate of ionization of H atoms, and since an ionization by light of wave-length λ transmits, on the average, an impulse h/λ, the maximum rate of communication of momentum to the group becomes $\Delta n^2 h/\lambda$. In a time dt an upper limit to the increase dv in the velocity of the group is given by

$$m_H n\, dv \leqslant \frac{\Delta n^2 h}{\lambda}\, dt$$

or

$$dv \leqslant \frac{\Delta n h}{m_H \lambda}\, dt = 3{\cdot}3 \times 10^{-10} n\, dt,$$

where $\lambda = 900$ A. $= 9 \times 10^{-6}$ cm. (a typical value),

$\Delta = 7 \times 10^{-13}$ cm.^{3}/sec. (*cf.* (**5**), Section 4.32, Table II).

The acceleration produces a longitudinal expansion so that, while the cloud is near the flare, the particle density will decrease faster than by an inverse square law, or $n < \mathfrak{N} b^2/r^2$.

Here $\mathfrak{N}$ = density at the emitting area, b = radius of flare, r = distance from flare centre.

The front of the cloud is accelerated to a final velocity v_0 in time τ_1, while the acceleration decreases with increasing distance from the flare; if v is the velocity t sec. after the emission,

$$\frac{v}{t} \geqslant \frac{v_0}{\tau_1}, \qquad \text{if } t \leqslant \tau_1.$$

At a time t the group will be $r-b$ cm. from the surface of the flare, and so

$$r - b = \int_0^t v\, dt \geqslant \int_0^t \frac{v_0}{\tau_1} t\, dt = \tfrac{1}{2} v_0 t^2/\tau_1.$$

Hence

$$dv \leqslant \frac{\Delta nh}{m_H \lambda}\, dt$$
$$\leqslant 3{\cdot}3 \times 10^{-10}\, \mathfrak{N} b^2/r^2\, dt$$
$$\leqslant \frac{3{\cdot}3 \times 10^{-10}\, \mathfrak{N} b^2}{(b + \frac{1}{2}v_0 t^2/\tau_1)^2}\, dt.$$

With the substitution $\tan\theta = t\sqrt{(v_0/2b\tau_1)}$ we find

$$\int_0^{v_0} dv \leqslant 3{\cdot}3 \times 10^{-10}\, \mathfrak{N} \sqrt{\left(\frac{2b\tau_1}{v_0}\right)} \int_0^{\tan^{-1}\sqrt{(v_0\tau_1/2b)}} \cos^2\theta\, d\theta,$$
$$\leqslant 3{\cdot}3 \times 10^{-10}\, \mathfrak{N} \sqrt{\left(\frac{2b\tau_1}{v_0}\right)} \cdot \frac{\pi}{4},$$

since $\tan^{-1}\sqrt{(v_0\tau_1/2b)} < \pi/2$.

Insertion of numerical values gives

$$v_0 \leqslant 4 \times 10^{-8}\, \mathfrak{N}.$$

Now we require that $v_0 = 1{\cdot}6 \times 10^8$ cm./sec., and this implies that

$$\mathfrak{N} \geqslant 4 \times 10^{15}.$$

Thus a cloud can be expelled by radiation of the Lyman continuum only if its initial density exceeds 4×10^{15} particles per c.c. However intense the radiation may be, expulsion cannot take place in more tenuous clouds, since the rate of recombination could not keep pace with the required rate of photo-ionization. But the density of the solar atmosphere near the flare is much less than 4×10^{15} particles per c.c. and this process also fails by some orders of magnitude.

It seems hard to think of any other way in which radiation pressure could possibly be effective, and some entirely different mechanism of expulsion must be found. This should not prove too difficult, for the required excess pressure near the flare is only of the order of 10^3 dynes per sq. cm.

Acknowledgments

I should like to thank Professor S. Chapman, my former supervisor, and Professor H. H. Plaskett for their encouragement and advice during the preparation of this paper. Some of the text is contained in a thesis for which the degree of Doctor of Philosophy was awarded by the University of Oxford.

Department of Mathematics,
The University,
Manchester, 13:
1950 *June* 30.

References

(1) S. Chapman and V. C. A. Ferraro, *Terr. Mag. Atmos. Elec.*, **36**, 77, 171, 1931.
(2) H. W. Newton, *M.N.*, **103**, 244, 1943.
(3) K. O. Kiepenheuer, *Z. f. Ap.*, **15**, 53, 1937.
(4) F. Hoyle, *Some Recent Researches in Solar Physics*, Cambridge, 1949, ch. 6.
(5) F. D. Kahn, *M.N.*, **109**, 324, 1949.
(6) S. Chapman and J. Bartels, *Geomagnetism*, Vol. II, Oxford, 1940, ch. 24.
(7) A. B. Partridge, *The Observatory*, **67**, 62, 1947.
(8) A. Unsöld, *Physik der Sternatmosphären*, ch. 9.
(9) M. A. Ellison, *M.N.*, **109**, 3, 1949.
(10) A. Unsöld, *Physik der Sternatmosphären*, p. 187.

AN INVESTIGATION INTO THE POSSIBILITY OF OBSERVING STREAMS OF CORPUSCLES EMITTED BY SOLAR FLARES, II

F. D. Kahn

(Received 1950 July 8)

Summary

The ionization in a stream of solar corpuscles is re-calculated by means of two equations derived in a previous paper (*M.N.*, **109**, 324, 1949). The new values differ somewhat from those given there; in particular the *Ca* II content is found to be rather lower. This would make the spectroscopic detection of the stream even harder.

---

1. *Introduction.*—The physical state of a cloud of corpuscles emitted by a solar flare has been discussed in a previous paper (1).* A simple model of the emission from a flare was used to calculate the variation of particle density in a typical stream. It was found that

$$n(t)=\frac{4\times 10^{k+5}}{t^3} \qquad \text{(I, Section 3.32 (9))},$$

where $n(t)$ = density near the front of the stream at time t,
t = lapse of time from instant of emission,
10^k = density near the emitting area.

This formula holds approximately when $t>\tau_1$, the duration of the flare.

The equations of ionization by solar radiation after the end of the flare were shown to be

$$\frac{dx}{dt}=\beta\gamma_1(1-x)-\Delta n x^2 \qquad \text{(I, Section 4.33 (5))} \qquad (1)$$

for hydrogen, and

$$\frac{dx'}{dt}=\beta\gamma_1'(1-x')-\Delta' n_e x' \qquad \text{(I, Section 4.33 (6))} \qquad (2)$$

for any other elements present. Here

β = dilution factor of solar radiation,
x = proportional ionization of the element,
γ_1 = ionization coefficient from *ground* state,
Δ = total recombination coefficient,
n_e = electron density.

The unprimed symbols x, γ_1 and Δ refer to hydrogen, the primed symbols to any other element.

Owing to the great abundance of hydrogen it is permissible to assume that the combined density of H atoms and H^+ ions is approximately equal to n, the particle density, and that $n_e\sim nx$. When equation (1) has been solved to find n_e the solution may be used in (2) for the state of some other, less abundant,

* This paper will be referred to as I in the text.

elements. The ionization of sodium and of calcium was found to be of particular interest in Paper I, for *Na* I, *Ca* I and *Ca* II have good resonance lines which may make the cloud detectable in absorption.

Since some rather crude approximations were used in Paper I for the solution of equations (1) and (2) we shall give a better treatment of them here.

2. *The ionization of the cloud* during *the flare*.—Before going on to solve the equations we must know the ionization of various elements in the stream when the flare ends. Observational evidence will help to find this. During the flare the ionization of any part of the stream will not tend to change. Near the emitting area the particle density in the stream will diminish as the inverse square of the distance from the flare (I, Section 3.31) in the same way as the intensity of the radiation received. Thus ionization and recombination will remain balanced at this time.

Solar flares are known to emit the *He* resonance line ($\lambda = 584$ A.) and are thought to be rich in radiation of the Lyman continuum, and thus the hydrogen will be highly ionized early on. In the later working the typical values assumed will range from 80 to 99 per cent ionization of *H*.

Both *Na* I and *Ca* I have low ionization potentials ($\chi = 5{\cdot}12$ e.V. and $6{\cdot}09$ e.V., respectively) and may be expected to be almost entirely absent. *Ca* II is harder to ionize; here observational evidence must be used to fix a lower limit to the ratio [*Ca* III]:[*Ca* II]. If there were much *Ca* II present we should expect the H and K emission lines of the flare to show an asymmetry similar to that observed for the *Hα* line by Ellison (**2**). Partridge (**3**) has failed to find such an asymmetry for the H and K lines, and so there can be little absorption over the flare.

Suppose that 10^k is the density of the stream on emission, then the number of corpuscles in a unit column along the line of sight from the Earth to the flare will be $\mathcal{N}$, say, where

$$\mathcal{N} \sim \int_b^\infty 10^k \frac{b^2}{r^2}\, dr = 10^k b = 2 \times 10^{k+9}.$$

Here b = radius of model flare $= 2 \times 10^9$ cm.

On Strömgren's composition (quoted in I, Section 4.1, Table I) this contains a total number of *Ca* ions (*Ca* II or *Ca* III) equal to

$$2 \times 10^{k+9} \times 1{\cdot}6 \times 10^{-6} = 3{\cdot}2 \times 10^{k+3}.$$

Since the ratio [*Ca* III]:[*Ca* II] $= x' : 1 - x'$, the number of *Ca* II ions per unit column becomes $3{\cdot}2 \times 10^{k+3}(1 - x')$. These ions may have a velocity spread of up to 1600 km./sec. owing to the longitudinal expansion of the cloud, and their absorption band will extend over a width of 22 A., or less. The number of *Ca* II ions per cm. spectral width in the column is then at least $1{\cdot}5 \times 10^{k+10}(1 - x')$. Figures given by Unsöld (**4**) show that 10^{20} *Ca* II ions per cm. width in a unit column cause about 10 per cent absorption, and in the case of the H and K lines the depth must be of this order, or less, thus

$$1{\cdot}5 \times 10^{k+10}(1 - x') \leqslant 10^{20},$$

or

$$(1 - x') \leqslant 7 \times 10^{9-k}.$$

We find the following minimum values for the ionization of *Ca* II while the flare is in progress.

TABLE I

Minimum ionization of Ca II during a flare in some typical clouds

	x'
$k=11$	0·93
$k=12$	0·993
$k=13$	0·9993

Now the anomalous absorption by *Ca* II ions should be strongest directly over the emitting area. During the flare no effect is visible here, by Partridge's result, and it is useless to search for absorption on other parts of the Sun's disk. A stream in which there is little recombination later will remain invisible even when the flare has ended.

3. *The solution of the equations for ionization* after *the flare.* (*a*) *The solution for hydrogen.*—The flare ends when $t=\tau_1$ and at later times the front of the cloud will be several solar radii removed from the Sun. We may then take $\beta=a^2/4v_0^2t^2$, where

$a=$ radius of Sun, $v_0=$ velocity of the front of the cloud.

Inserting this and the expression for $n(t)$ into equation (1) gives

$$\frac{dx}{dt}=\frac{a^2\gamma_1(1-x)}{4v_0^2t^2}-\frac{4\times10^{k+5}\Delta x^2}{t^3}.$$

We put $T=t/\tau_1$ and find

$$\frac{dx}{dT}=\frac{a^2\gamma_1(1-x)}{4v_0^2\tau_1T^2}-\frac{4\times10^{k+5}\Delta x^2}{\tau_1^2T^3}$$

$$=\frac{A(1-x)}{T^2}-\frac{Bx^2}{T^3}. \qquad (3)$$

The initial condition is that $x=x_1$ when $t=\tau_1$, or $T=1$. Adoption of the numerical values

$$\left.\begin{aligned}&a=7\times10^{10}\text{ cm.},\quad v_0=1{\cdot}6\times10^8\text{ cm./sec.},\quad \tau_1=10^3\text{ sec.},\\&\gamma_1=1{\cdot}2\times10^{-3}\text{ sec.}^{-1}\\&\Delta=7\times10^{-13}\text{ cm.}^3\text{/sec.}\end{aligned}\right\}\ \textit{cf.}\ \text{I, Section 4.32, Table II.}$$

gives

$$A=5{\cdot}7\times10^{-2},\quad B=2{\cdot}8\times10^{k-13}.$$

The cloud reaches the Earth when $t\sim10^5$ sec., or $T\sim10^2$.

There is a simple method of approximating to the value of x which allows some insight into the physics of the problem. With the initial condition that $x=x_1$ when $T=1$, the solution of (3) for any $T>1$ lies between the solutions Y, y of (4) and (5), where

$$\frac{dY}{dT}=\frac{A(1-Y)}{T^2},\qquad Y=x_1\text{ when }T=1, \qquad (4)$$

$$\frac{dy}{dT}=-\frac{By^2}{T^3},\qquad y=x_1\text{ when }T=1. \qquad (5)$$

In other words x will be overestimated or underestimated according as photo-ionization or recombination is neglected.

To prove that $Y>x$ we write (3) and (4) in the form

$$\frac{d}{dT}(xe^{-A/T}) = \frac{A}{T^2}e^{-A/T} - \frac{Bx^2}{T^3}e^{-A/T},$$

$$\frac{d}{dT}(Ye^{-A/T}) = \frac{A}{T^2}e^{-A/T} \geqslant \frac{d}{dT}(xe^{-A/T}).$$

Thus $Ye^{-A/T} \geqslant xe^{-A/T} + \text{constant}$, for $T \geqslant 1$. When $T=1$, $Y=x=x_1$, so that, for $T>1$, $Y>x$.

Similarly $x>y$.

The equations (4) and (5) integrate to give

$$Y = 1-(1-x_1)e^{-A(1-1/T)}, \tag{6}$$

$$y = \left\{\frac{1}{x_1} + \frac{B}{2}\left(1-\frac{1}{T^2}\right)\right\}^{-1}. \tag{7}$$

The hydrogen will never be completely ionized or completely recombined, for Y steadily increases and tends to $Y_\infty = 1-(1-x_1)e^{-A}$, while y steadily decreases and tends to $y_\infty = \left(\frac{1}{x_1}+\frac{B}{2}\right)^{-1}$.

If A is small it can be shown that $(x-y)$ will remain small and at any given time x, the ionization, will lie close to y, the lower limit. To prove this we subtract equation (5) from equation (3) to find

$$\frac{d}{dT}(x-y) = \frac{A(1-x)}{T^2} - \frac{B}{T^3}(x^2-y^2).$$

With $x>y>y_\infty$ it follows that

$$\frac{d}{dT}(x-y) < \frac{A(1-y_\infty)}{T^2} - \frac{B}{T^3}(x-y)(x+y)$$

$$< \frac{A(1-y_\infty)}{T^2} - \frac{2By_\infty}{T^3}(x-y).$$

This may be re-written as

$$\frac{d}{dT}\{(x-y)e^{-By_\infty/T^2}\} < \frac{A(1-y_\infty)}{T^2}e^{-By_\infty/T^2},$$

which gives on integration (with $x-y=0$ when $T=1$),

$$(x-y)e^{-By_\infty/T^2} < \frac{A(1-y_\infty)}{\sqrt{By_\infty}}\frac{\sqrt{\pi}}{2}\left\{\operatorname{erf}\sqrt{By_\infty} - \operatorname{erf}\frac{\sqrt{By_\infty}}{T}\right\}. \tag{8}$$

But in the interval $0 \leqslant u \leqslant u_0$ the maximum value of

$$f(u) = e^{u^2}(\operatorname{erf} u_0 - \operatorname{erf} u)$$

occurs for $u=0$. Applying this result to (8), with $u^2 = By_\infty/T^2$,

$$x-y < \frac{A(1-y_\infty)}{\sqrt{By_\infty}}\frac{\sqrt{\pi}}{2}\operatorname{erf}\sqrt{By_\infty}. \tag{9}$$

In the most unfavourable case to be considered $B=2\cdot8$, $x_1=0\cdot80$ and $y_\infty=0\cdot37$; this will give the largest value of $(x-y)$. Here $By_\infty\sim1$, and

$$x-y<A(1-0\cdot37)\frac{\sqrt{\pi}}{2}\operatorname{erf}1$$

or

$$x-y<0\cdot027.$$

This is a small margin of error, considering the nature of the problem. The table below gives the values of the ionization of hydrogen to be expected at two typical times, in clouds of different densities.

TABLE II

The ionization of hydrogen at two typical times after the end of the flare. $t\sim10^5$ sec. corresponds to the time when the stream reaches the Earth

Initial ionization	Time (sec)	Distance from Sun (cm.)	$k=10$	$k=11$	$k=12$	$k=13$
0·80	2×10^3	$3\cdot2\times10^{11}$	0·80	0·79	0·74	0·44
	10^5	$1\cdot5\times10^{13}$	0·80	0·79	0·72	0·37
0·90	2×10^3	$3\cdot2\times10^{11}$	0·90	0·89	0·83	0·47
	10^5	$1\cdot5\times10^{13}$	0·90	0·89	0·80	0·40
0·99	2×10^3	$3\cdot2\times10^{11}$	0·99	0·99	0·90	0·50
	10^5	$1\cdot5\times10^{13}$	0·99	0·99	0·87	0·41

With the formula $n(t)=4\times10^{k+5}/t^3$ for the density near the front of the stream we find the following values for n_e, the electron density.

TABLE III

The electron density at two typical times after the end of the flare for streams of various densities

Initial ionization	Time (sec.)	Distance from Sun (cm.)	Electron density (cm.$^{-3}$) $k=10$	$k=11$	$k=12$	$k=13$
0·80	2×10^3	$3\cdot2\times10^{11}$	$4\cdot0\times10^5$	$4\cdot0\times10^6$	$3\cdot7\times10^7$	$2\cdot2\times10^8$
	10^5	$1\cdot5\times10^{13}$	3·2	$3\cdot2\times10$	$2\cdot9\times10^2$	$1\cdot5\times10^3$
0·90	2×10^3	$3\cdot2\times10^{11}$	$4\cdot5\times10^5$	$4\cdot5\times10^6$	$4\cdot2\times10^7$	$2\cdot4\times10^8$
	10^5	$1\cdot5\times10^{13}$	3·6	$3\cdot6\times10$	$3\cdot2\times10^2$	$1\cdot6\times10^3$
0·99	2×10^3	$3\cdot2\times10^{11}$	$5\cdot0\times10^5$	$4\cdot9\times10^6$	$4\cdot5\times10^7$	$2\cdot5\times10^8$
	10^5	$1\cdot5\times10^{13}$	4·0	$3\cdot9\times10$	$3\cdot5\times10^2$	$1\cdot6\times10^3$

(*b*) *The ionization of sodium and calcium.*—Some estimates for the ionization and recombination coefficients of *Na* I and *Ca* II were given in Paper I (Section 4.32, Table II). Since then Ditchburn and Jutsum (**5**) have measured the continuous absorption coefficient for sodium. Their experimental results show it to be only about 70 per cent of Rudkjøbing's calculated value (**6**), which

was assumed in Paper I. Further, rocket spectra taken at White Sands (**7**) have established that the intensity of solar radiation near the head of the sodium continuum ($\lambda\sim2400$ A.) is only about one-tenth that of a black body at 6000 deg. K. In this way the estimate of γ_1' for *Na* I is reduced to $2{\cdot}6\,\text{sec.}^{-1}$. Even so this is a high value compared with that for hydrogen and, as before, we conclude that the sodium will remain highly ionized at all times.

From data given by Bates and Massey (**8**) we find that for *Ca* I $\Delta'=2\times10^{-13}\,\text{cm.}^3/\text{sec.}$ and $\gamma_1'=1{\cdot}5\,\text{sec.}^{-1}$, if the solar radiation is only 10 per cent of full black-body intensity near the *Ca* I continuum ($\lambda\sim2020$ A.) Once again, neutral calcium will be very rare, and it remains only to evaluate the relative densities of *Ca* II and *Ca* III.

According to (2) the equation of ionization of calcium becomes

$$\frac{dx'}{dt}=\frac{a^2\gamma_1'(1-x')}{4v_0^2t^2}-\Delta' n_e x'.$$

Now in Paper I we saw that $\gamma_1'=7{\cdot}4\times10^{-4}\,\text{sec.}^{-1}$, and $\Delta'=2\times10^{-13}\,\text{cm.}^3/\text{sec.}$; writing $T=t/\tau_1$ gives

$$\frac{dx'}{dT}=\frac{3{\cdot}7\times10^{-2}(1-x')}{T^2}-2\times10^{-13}\tau_1 n_e x'.$$

The first term on the right-hand side is small and so

$$\frac{dx'}{dT}\sim-2\times10^{-13}\tau_1 n_e x'. \tag{10}$$

In the same way the equation of ionization of hydrogen may be written

$$\frac{dx}{dT}\sim-7\times10^{-13}\tau_1 n_e x. \tag{11}$$

Division of (10) by (11) gives

$$\frac{dx'}{dx}\sim\frac{2}{7}\frac{x'}{x}$$

or

$$\frac{x'}{x_1'}\sim\left(\frac{x}{x_1}\right)^{2/7}. \tag{12}$$

Now x' and x_1' denote the ionization of the *Ca* II present at time t and at time τ_1, respectively, and the ratio $x':x_1'$ is a measure of the importance of the recombination of *Ca* III to *Ca* II. In clouds for which $k\leqslant11$, $x:x_1$ remains approximately unity (see Table II), hence also $x':x_1'\sim1$, and there will be little change in the ionization of calcium. There is sensible recombination in denser clouds, and some typical values of x' are given in Table IV. Here we know that $x_1'\sim1$, by the results in Table I.

The abundance of *Ca* II ions in the cloud may now be found. As in Paper I, Section 4.4, two different compositions are assumed for the stream.

(*c*) *Observation of the anomalous absorption.*—There is effectively no recombination when $k\leqslant11$, and such thin streams will remain invisible in calcium light both during and after the flare. It may be possible to observe denser streams of corpuscles and, using the same working as in Paper I, Section 4.4, we find the following values for the probable depth of the absorption band at two representative times.

TABLE IV

Ionization of Ca II at two typical times after the end of the flare

Initial ionization of hydrogen	Time (sec.)	Distance from Sun (cm.)	Ionization of *Ca* II $k=12$	$k=13$
0·80	2×10^3	$3{\cdot}2\times10^{11}$	0·98	0·84
	10^5	$1{\cdot}5\times10^{13}$	0·97	0·80
0·90	2×10^3	$3{\cdot}2\times10^{11}$	0·98	0·83
	10^5	$1{\cdot}5\times10^{13}$	0·97	0·79
0·99	2×10^3	$3{\cdot}2\times10^{11}$	0·97	0·82
	10^5	$1{\cdot}5\times10^{13}$	0·96	0·78

TABLE V

The expected abundance of Ca II ions at two typical times after the end of the flare for clouds of two different densities

Initial ionization of hydrogen	Time (sec.)	Distance from Sun (cm.)	Density of *Ca* II ions in the cloud Composition A $k=12$	Composition A $k=13$	Composition B $k=12$	Composition B $k=13$
0·80	2×10^3	$3{\cdot}2\times10^{11}$	$1{\cdot}5\times10^3$	$1{\cdot}2\times10^5$	1·6	$1{\cdot}3\times10^2$
	10^5	$1{\cdot}5\times10^{13}$	$1{\cdot}8\times10^{-2}$	1·2	$1{\cdot}9\times10^{-4}$	$1{\cdot}3\times10^{-3}$
0·90	2×10^3	$3{\cdot}2\times10^{11}$	$1{\cdot}5\times10^3$	$1{\cdot}3\times10^5$	1·6	$1{\cdot}4\times10^2$
	10^5	$1{\cdot}5\times10^{13}$	$1{\cdot}8\times10^{-2}$	1·3	$1{\cdot}9\times10^{-4}$	$1{\cdot}4\times10^{-3}$
0·99	2×10^3	$3{\cdot}2\times10^{11}$	$2{\cdot}3\times10^3$	$1{\cdot}4\times10^5$	2·4	$1{\cdot}5\times10^2$
	10^5	$1{\cdot}5\times10^{13}$	$2{\cdot}4\times10^{-2}$	1·4	$2{\cdot}5\times10^{-4}$	$1{\cdot}5\times10^{-3}$

A on Unsöld's composition, B on Strömgren's composition, } quoted in I, Section 4.1, Table I.

TABLE VI

Percentage depth of absorption near the H *and* K *lines of calcium after a flare, for dense clouds*

Initial ionization of hydrogen	Time (sec.)	Distance from Sun (cm.)	Percentage depth of absorption Composition A $k=12$	Composition A $k=13$	Composition B $k=12$	Composition B $k=13$
0·80	2×10^3	$3{\cdot}2\times10^{11}$	89	99+	—	20
	10^5	$1{\cdot}5\times10^{13}$	—	1	—	—
0·90	2×10^3	$3{\cdot}2\times10^{11}$	89	99+	—	21
	10^5	$1{\cdot}5\times10^{13}$	—	1	—	—
0·99	2×10^3	$3{\cdot}2\times10^{11}$	96	99+	—	22
	10^5	$1{\cdot}5\times10^{13}$	—	—	—	—

Values of less than 1 per cent are denoted by a dash.

The new values for the depth of absorption are rather lower than those found in the earlier paper (Section 4.4, Table VI). Even dense clouds for which $k = 12$ can remain permanently invisible and so the chance of observing the absorption becomes very small.

Acknowledgments

Thanks are due to Professor S. Chapman and to Professor H. H. Plaskett for their encouragement and advice while this paper was being prepared. Some of the work was carried out during the tenure of a D.S.I.R. grant and of the Skynner Senior Studentship in Astronomy at Balliol College. The paper forms part of a thesis for which the degree of Doctor of Philosophy was awarded by the University of Oxford.

Department of Mathematics,
The University, Manchester, 13:
1950 *June* 30.

References

(1) F. D. Kahn, *M.N.*, **109**, 324, 1949.
(2) M. A. Ellison, *M.N.*, **109**, 3, 1949.
(3) A. B. Partridge, *The Observatory*, **67**, 62, 1947.
(4) A. Unsöld, *Physik der Sternatmosphären*, chs. 8 and 9.
(5) R. W. Ditchburn and P. J. Jutsum, *Nature*, **165**, 724, 1950.
(6) M. Rudkjøbing, *Meddelelser Kobenhaven Obs.*, **18**, 1, 1940.
(7) E. Durand, J. J. Oberly and R. Tousey, *Ap. J.*, **109**, 1, 1949.
(8) D. R. Bates and H. S. W. Massey, *Proc. Roy. Soc.* A, **177**, 329, 1941.

AN ATTEMPT TO EXPLAIN THE POLARIZATION IN $H\alpha$ AND D_3 FOR PROMINENCES

H. Zanstra

(Received 1950 July 29)

Summary

Using Heisenberg's theory as developed by Öhman for problems of this kind, it is shown that, for the line $H\alpha$, the hydrogen atom acts as a space oscillator for 35 per cent of the incident energy, and as an isotropic scatterer for the remaining 65 per cent. For the D_3 line of neutral helium the figures are 36 and 64 per cent.

For the photospheric radiation an approximate value for the coefficient of darkening $\beta_1 = 0{\cdot}67$ is derived for the centre of $H\alpha$ from Abbot's observations and Evans' residual intensities. For the D_3 line a value $\beta_1 = \beta = 1{\cdot}36$ is adopted. The theory, given for a prominence of small total optical depth, predicts for the emission a degree of polarization of 1·6 per cent at the photosphere, and 7·5 per cent at an altitude of 50,000 km., as compared with Lyot's observed values of 0·8 to 1·2 per cent in general. For the D_3 emission the theory gives 2·6 per cent at the photosphere and 8·4 per cent at an altitude of 50,000 km., as compared with the observed 0·9 to 1·5 per cent. The excess of the theoretical above the observational effect may in part be attributed to other processes of excitation like fluorescence and ionization and re-combination. The fact that the plane of vibration is not parallel to the solar limb, but shows deviations lying between 0° and 30° for $H\alpha$ and 0° and 40° for D_3, is not explained by the simple theory.

---

1. *Introduction.*—The following is an attempt to explain the polarization of emission lines of $H\alpha$ and D_3 in prominences, observed by Lyot.* The necessary theory was largely developed by Öhman† making use of Heisenberg's theory of polarization‡ for resonance or fluorescence under incident light. He also expected polarization in prominence emission lines, but only for the part of the prominence which is well above the photosphere, since he did not think of the effect of darkening towards the limb on the incident photospheric light. Actually this limb darkening results in a preponderance of light leaving the photosphere normally as compared with that for larger angles θ with the normal and this may result in a polarization of the light scattered by the lowest part of the prominence as well. So there are two effects intermixed: that of the limb darkening and that due to the elevation of the prominence above the photospheric surface. Effectively they both increase the intensity of that part of the radiation leaving the photosphere normally. If now for instance an atom of the prominence acts like a classical oscillator, it is easily seen that the scattered light would be partly polarized, there being a preponderance of electrical vibrations parallel to the limb. As Öhman pointed out and illustrated, Heisenberg's theory also enables us to work out the polarization for other types of lines, as in our case the hydrogen line $H\alpha$ and the line D_3, λ 5875·61, $2^3P - 3^3D$ of neutral helium. In Section 2 Heisenberg's

* B. Lyot, *Comptes Rendus*, **198**, 250, 1934; *Bull. Soc. Astr. de France*, **51**, 203, 1937.

† Y. Öhman, *M.N.*, **89**, 479, 1924.

‡ W. Heisenberg, *Zeit. f. Physik*, **31**, 617, 1925.

theory is applied to these two lines. The atom can partly be considered as an oscillator vibrating along the electric light vector and thus re-emitting polarized radiation, and partly as an isotropic scatterer re-emitting unpolarized radiation uniformly in all directions, and the fraction of oscillator scattering and isotropic scattering is computed.

In Section 3 the polarization for prominence material close to the solar surface, which is due to limb darkening only, is considered, assuming a small total optical depth of the prominence in the spectral line. In Section 4 the general case of polarization due to the combined effect of limb darkening and elevation above the photosphere is treated, likewise for small optical depth, using Minnaert's formulae, originally derived for scattering of photospheric light by free electrons, but applying equally well to oscillator scattering of a spectral line. The result of the theory is contained in Table IV and this theoretical degree of polarization turns out to be stronger than the values observed by Lyot. Section 5 contains a remark regarding the derivation of Section 2.

2. *Representation of an atom by a classical oscillator plus an isotropic scatterer, worked out for Hα and D_3.*—Heisenberg considers a beam of plane polarized light incident on an atom or ion of any type in any state and capable of exciting this to a higher state by absorption of a certain line. In order to investigate the polarization, he introduces a magnetic field in the direction of the electric vector of the incident beam. This magnetic field is not actually there, but merely serves as an artifice by means of which the various directions of vibration of the scattered light can be predicted. He then shows, from considerations akin to the correspondence principle, that this auxiliary magnetic field does not alter the vibrations of the atom, apart from the slight shifts in frequency due to the Zeeman effect, so that the degree of polarization remains the same. The excitation to the higher state, viz. to the Zeeman components of which it consists, takes place exclusively by the vibrations parallel to the electric vector, that is the π transitions for which $\Delta M = 0$, M being the magnetic quantum number. When however the atom falls back to its original or to any other state, he assumes, following Breit, or Gaviola and Pringsheim, that the emission is entirely spontaneous, and so contains the various π and σ components with the relative intensities predicted for the Zeeman effect. If now one lets the magnetic field approach to zero, the various π and σ components tend to the same frequency, but their intensities and directions of vibration are not altered, so that one finally knows the degree of polarization if no magnetic field is present.

As a preparation to Table I, Heisenberg's procedure is illustrated in Fig. 1A for the line $^2S_{\frac{1}{2}} - {}^2P_{1\frac{1}{2}}$ of a doublet. Upon application of the auxiliary magnetic field along the light vector $\bar{E}$ (Fig. 1B), the lower state $J' = \frac{1}{2}$ is split up into the components with magnetic quantum numbers $M' = -\frac{1}{2}$ and $+\frac{1}{2}$, and the upper state $J'' = 1\frac{1}{2}$ into components with $M'' = -1\frac{1}{2}$, $-\frac{1}{2}$, $+\frac{1}{2}$ and $+1\frac{1}{2}$. Only the π components $\Delta M = 0$ are absorbed, so that only $M'' = -\frac{1}{2}$ and $+\frac{1}{2}$ are excited. Upon return to the lower state, the two π components of total intensity $i_\pi = 2 + 2 = 4$ and the right-hand and left-hand σ components, each of intensity $i_\sigma = 1$, are re-emitted, the latter being observed along the field so that they have their maximum strength.*

* In general, the total intensity of all π components viewed perpendicular to the field will be termed i_π and of all right-hand circular components or all left-hand circular components viewed along the field i_σ. Some authors define the intensities of the σ components as those observed in the direction perpendicular to the field, that is the y or x direction in Fig. 1B. If this is done, the intensities in Fig. 1A should be halved.

For the purpose of linear polarization, one may replace the two right-hand and left-hand circularly polarized vibrations σ_1 and σ_2, each of strength $i_\sigma = 1$, by two linearly polarized vibrations i_σ, perpendicular to each other and in the plane of the formerly circular motion, as is shown in Fig. 1B (see Section 5). Consider first Heisenberg's case of a plane polarized wave incident along the x-axis and vibrating in the z direction. When observed along the y-axis, the degree of polarization will be $(i_\pi - i_\sigma)/(i_\pi + i_\sigma) = \frac{3}{5} = 60$ per cent. A space oscillator on the other hand would vibrate entirely along $\bar{E}$ and thus only have the π component, and a polarization of 100 per cent seen along the y-axis.

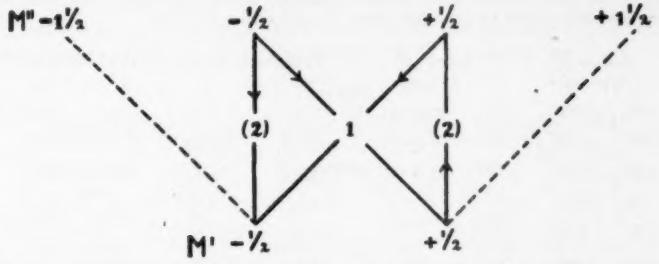

FIG. 1A.—*Zeeman pattern for the transition $J' = \frac{1}{2}$ to $J'' = 1\frac{1}{2}$. M' and M'' are the magnetic quantum numbers of lower and higher states. The intensities of the σ components (viewed along the field) and of the π components (in brackets) are indicated.*

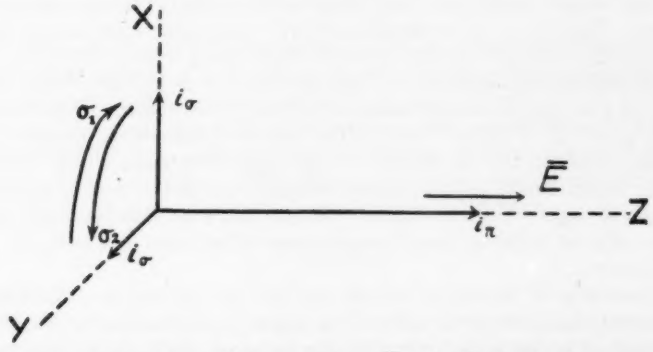

FIG. 1B.—*Intensities of the three vibrations. $\bar{E}$ is the vibrating electric vector.*

The total intensity of the three vibrations is $i_\pi + 2i_\sigma$, so that the *fractional intensity of the π and σ component* is

$$\frac{i_\pi}{i_\pi + 2i_\sigma} \quad \text{and} \quad \frac{i_\sigma}{i_\pi + 2i_\sigma}, \tag{1}$$

which yields $4/(4+2) = \frac{2}{3}$ and $1/(4+2) = \frac{1}{6}$ for the line under consideration.*

* In the above example, the intensities of all π components are the same, viz. 2. When these π components differ in intensity, as is the case for $^2P_{1\frac{1}{2}} - {}^2D_{1\frac{1}{2}}$ and $^2P_{1\frac{1}{2}} - {}^2D_{2\frac{1}{2}}$ of Table I and all lines but the first of Table II, each absorbed π intensity is re-distributed amongst the π and σ emissions from the state excited by it. The intensities of the Zeeman pattern then serve for the absorbed π intensities as well as for the ratios of the re-emitted π and σ intensities.

This is shown in the sixth row, columns 3 and 4, of Table I for the line $2^2S_{\frac{1}{2}}-3^2P_{1\frac{1}{2}}$ of $H\alpha$. Exactly the same applies to the line of the next row $2^2P_{\frac{1}{2}}-3^2D_{1\frac{1}{2}}$ which, though not belonging to the same doublet as $2^2S_{\frac{1}{2}}-3^2P_{\frac{1}{2}}$, coincides with it, as is indicated by the bracket. In the fine structure of $H\alpha$ this composite line has the theoretical intensity 7·08 of the second column, so that finally $i_\pi = 4{\cdot}72$ and $i_\sigma = 1{\cdot}18$, given in the last two columns, in the intensity unit of column 2, which is common to all lines of the whole fine structure.

TABLE I

Polarization of Hα, λ6562·79

(The values of the intensities i_π and i_σ (Fig. 1B) are first obtained for each line of the structure and then added to get their value for the whole line $H\alpha$.)

Lines of fine str.	Int. f. str. $i_\pi+2i_\sigma$	Fractional int. π	σ	Int. i_π	Int. i_σ
$2^2P_{1\frac{1}{2}}-3^2S_{\frac{1}{2}}$	0·2	1/3	1/3	$0{\cdot}0_7$	$0{\cdot}0_7$
$2^2P_{1\frac{1}{2}}-3^2D_{1\frac{1}{2}}$	1·0	41/75	17/75	$0{\cdot}5_5$	$0{\cdot}2_3$
$2^2P_{1\frac{1}{2}}-3^2D_{2\frac{1}{2}}$	9·0	13/25	6/25	$4{\cdot}6_8$	$2{\cdot}1_6$
$2^2S_{\frac{1}{2}}-3^2P_{\frac{1}{2}}$	1·14	1/3	1/3	$0{\cdot}3_8$	$0{\cdot}3_8$
$2^2P_{\frac{1}{2}}-3^2S_{\frac{1}{2}}$		1/3	1/3		
$2^2S_{\frac{1}{2}}-3^2P_{1\frac{1}{2}}$	7·08	2/3	1/6	$4{\cdot}7_2$	$1{\cdot}1_8$
$2^2P_{\frac{1}{2}}-3^2D_{1\frac{1}{2}}$		2/3	1/6		
Line $H\alpha$	18·42			$10{\cdot}4_0$	$4{\cdot}0_2$

The other lines of Table I need but little elucidation, since the same procedure was followed. The lines are all arranged in column 1 according to increasing frequency, the separation between the two strongest lines being 0·3285 cm.$^{-1}$ or 0·1415 A., the same as would be produced by a Doppler shift of 6·45 km./sec. The intensities of column 2 are the theoretical intensities of the fine structure. They were taken from a paper by Williams* who gives various literature references, and are naturally based on the occupation of the upper levels according to statistical weights, which should approximately be applicable to our case of excitation by photospheric light. For the Zeeman patterns and intensities needed, the reader may be referred to the current formulae and tables given in Candler†, Vol. II, pp. 108 to 120.

All intensities of the second and the last two columns are now added and yield the desired i_π and i_σ for the line $H\alpha$. The degree of polarization for $H\alpha$ in Heisenberg's case of observations perpendicular to an incident plane polarized beam becomes $(10{\cdot}4_0-4{\cdot}0_2)/(10{\cdot}4_0+4{\cdot}0_2)=0{\cdot}44$. We shall use the result in a different form. According to Fig. 1B, we may replace the intensities by three intensities i_σ along the three axes and one intensity $i_\pi-i_\sigma$ along the z-axis, viz. the direction of $\bar{E}$. Thus the atom may be replaced by *a space oscillator and an isotropic scatterer*, the energies scattered being the fractions of the absorbed energy

$$\frac{i_\pi-i_\sigma}{i_\pi+2i_\sigma} \quad \text{and} \quad \frac{3i_\sigma}{i_\pi+2i_\sigma}, \tag{2}$$

* *Cf.* R. C. Williams, *Phys. Rev.*, **54**, 558, 1928. For the most recent literature the reader may be referred to H. Kuhn and G. W. Series, *Proc. Roy. Soc.*, **202**, 127, 1950.

† *Cf.* A. C. Candler, *Atomic Spectra*, Cambridge, 1937. A diagram for the fine structure of $H\alpha$ is found in Vol. I, p. 42, Fig. 3·17.

in general, or numerically for $H\alpha$: 35 per cent scattered by space oscillators and 65 per cent scattered isotropically. *The ratio of the absorption coefficient σ′ of oscillator scattering to σ for isotropic scattering* becomes, in general,

$$\frac{\sigma'}{\sigma} = \frac{i_\pi - i_\sigma}{3i_\sigma}, \tag{3}$$

or, in the case of $H\alpha$,

$$\frac{\sigma'}{\sigma} = 0{\cdot}53. \tag{3a}$$

For the polarization of D_3 of neutral helium, we have Table II which has been obtained in the same way as Table I for hydrogen. The case is somewhat simpler than for hydrogen lines, since the line represents only one multiplet, so that the intensities of each component line contained in the second row can be obtained from formulae or tables as given in Candler *, Vol. II, pp. 94 to 101.

TABLE II

Polarization of the D_3 line of HeI $\begin{cases} \lambda 5875{\cdot}618 : 2^3P_{2,1} - 3^3D_{3,2,1} \\ \lambda 5875{\cdot}960 : 2^3P_0 - 3^3D_1 \end{cases}$

Component lines	Int. $i_\pi + 2i_\sigma$	Fractional int. π	Fractional int. σ	Int. i_π	Int. i_σ
$2^3P_0 - 3^3D_1$	23·8	1	0	23·8	0·0
$2^3P_1 - 3^3D_1$	17·9	1/2	1/4	$8{\cdot}9_5$	$4{\cdot}4_7$
$2^3P_2 - 3^3D_1$	1·2	17/50	33/100	$0{\cdot}4_1$	$0{\cdot}4_0$
$2^3P_1 - 3^3D_2$	53·6	17/30	13/60	$30{\cdot}3_6$	$11{\cdot}6_2$
$2^3P_2 - 3^3D_2$	17·9	17/30	13/60	$10{\cdot}1_4$	$3{\cdot}8_8$
$2^3P_2 - 3^3D_3$	100·0	259/525	133/525	49·4	25·3
D_3 line	214·4			123·1	45·7

The total intensities i_π and i_σ for the whole D_3 line are again given at the bottom of the table. The degree of polarization for an incident plane polarized beam observed perpendicularly would become $(123{\cdot}1 - 45{\cdot}7)/(123{\cdot}1 + 45{\cdot}7) = 0{\cdot}46$. If instead of this we replace the atom by a space oscillator and an isotropic scatterer, formula (2) leads to 36 per cent and 64 per cent of the incident energy respectively scattered in these two ways. The ratio of the absorption coefficients σ′ for oscillator scattering and σ for isotropic scattering (3) becomes

$$\frac{\sigma'}{\sigma} = 0{\cdot}56 \tag{3b}$$

for the D_3 line.

Strictly speaking, one should take the Zeeman components of the hyperfine structure, and this results in a reduction of the theoretical polarization for $H\alpha$.† However, for helium the nuclear spin is zero and consequently the D_3 line has no hyperfine structure, so that the computation for this line is quite correct.

3. *The effect of limb darkening: theoretical polarization of Hα and D_3 for low prominence material.*—We now proceed to the theoretical excitation of a prominence by photospheric radiation, but assume the prominence material to be close to the solar surface, so that only the effect of limb darkening but not the effect of elevation comes in.

For the continuous background of the photospheric spectrum at $H\alpha$ λ6562·82, the coefficient of darkening $\beta = 1{\cdot}20$ follows from Abbot's observations of intensity

* *Loc. cit.*

† A. G. C. Mitchell and M. W. Zemansky, *Resonance Radiation and Excited Atoms*, Cambridge, 1934, p. 283.

$I(\theta)$ at $\cos\theta = 1$ and 0·312, or $\beta = 0{\cdot}91$ from the observations at $\cos\theta = 1$ and 0·661 (*cf. M.N.*, **101**, 250, Fig. 2, 1941). For the excitation of $H\alpha$ in prominences one should take the photospheric intensity $I_1(\theta)$ at the centre of $H\alpha$. There might be a displacement due to Doppler effect but, for instance, for 10 km./sec. this would be only 0·2 A., and presumably not carry one far away from the core. If r be the residual intensity at the centre of $H\alpha$, expressed in units of the continuous background, we have for I_1 and the corresponding coefficient of darkening β_1,

$$I_1(\theta) = I(\theta) r(\theta), \tag{4}$$

$$\frac{I_1(\theta)}{I_1(0)} = \frac{1 + \beta_1 \cos\theta}{1 + \beta_1} = 1 - \frac{\beta_1}{1 + \beta_1}(1 - \cos\theta). \tag{5}$$

For $r(\theta)$ we use the values determined by Evans* in the second row of Table III for the cos θ of the first row. These are reduced to $r(\theta)/r(0)$ in the third row.

TABLE III

Centre of Hα: Values of $I_1(\theta)/I_1(0)$

	$\cos\theta = 1{\cdot}000$	0·741	0·364	0·303	0·229
Evans	$r(\theta) = 0{\cdot}179$	0·230	0·224	0·211	0·245
	$r(\theta)/r(0) = 1{\cdot}00$	1·29	1·25	1·18	1·37
	$I(\theta)/I(0) = 1{\cdot}000$	0·875	0·658	0·616	0·560
Abbot	$I_1(\theta)/I_1(0) = 1{\cdot}00$	1·13	0·82	0·73	0·77

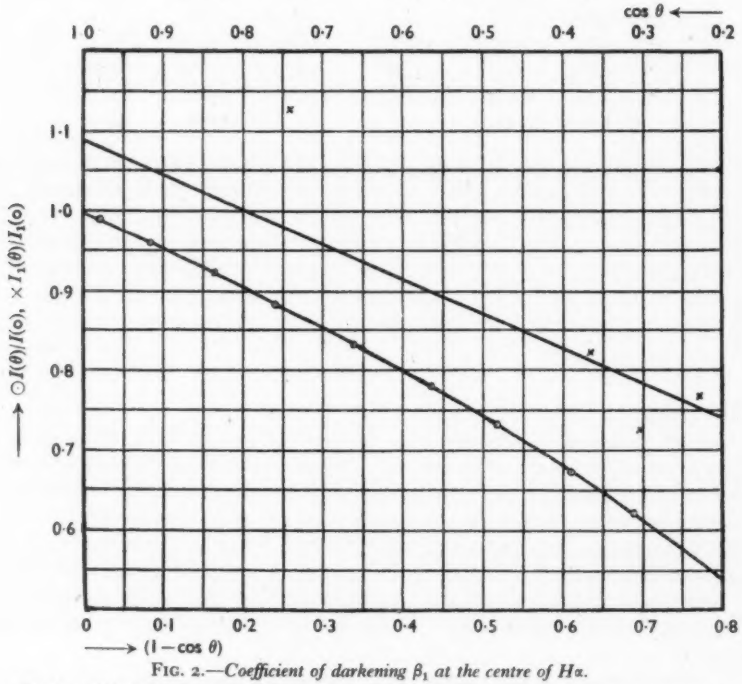

FIG. 2.—*Coefficient of darkening β_1 at the centre of Hα.*

Circles: Abbot's observations, reduced to the crosses by means of Evans' residual intensities. Straight line: Least squares solution for determination of β_1.

Erratum: A further cross should have been plotted at cos $\theta = 1{\cdot}000$ and $I_1(\theta)/I_1(0) = 1{\cdot}00$

* D. S. Evans, *M.N.*, **100**, 156, 1940, Table XIII.

Abbot's observations of $I(\theta)/I(0)$* are plotted in Fig. 2 as circles, from which plot the values of the fourth row are obtained. By multiplying them by the previous row the desired values of $I_1(\theta)/I_1(0)$ are obtained, given in the last row of Table III and represented by crosses in Fig. 2. Evans remarks that the experimental error in r is of the order of 3 per cent. The scatter of the three crosses on the right is therefore largely experimental, while the maximum indicated by the second cross is probably real. However, we wish to use the linear relation (5), which can formally be done by introducing, for $\theta = 0$, the value $\overline{r(0)}$ instead of the measured $r(0)$, so that equation (5) assumes the form

$$\frac{I_1(\theta)}{I_1(0)} = \frac{\overline{r(0)}}{r(0)}\left[1 - \frac{\beta_1}{1+\beta_1}(1-\cos\theta)\right], \tag{6}$$

realizing that the difference $\overline{r(0)} - r(0)$ may only partly be an observational error.

A least squares solution of (6) with the variables $I_1(\theta)/I_1(0)$ and $1-\cos\theta$ yields the straight line of Fig. 2 with

$$\frac{\overline{r(0)}}{r(0)} = 1{\cdot}09 \quad \text{and} \quad \beta_1 = 0{\cdot}67, \tag{6a}$$

for $H\alpha$.

Thus β_1 for the line centre is smaller than the corresponding β of the adjoining continuous background.

Now consider the theoretical effect to be expected for a prominence near the photosphere having a small optical depth in $H\alpha$. The radiation observed emerges at an angle $\theta = 90°$ with the normal to the photosphere. This case of scattering material close to the photospheric surface was worked out by the writer.† We introduce σ', the coefficient of scattering per cm. by space oscillators, and σ, the same quantity for the radiation scattered isotropically.

Then the intensity of the oscillator radiation which is emitted by 1 cm.^{3} of the prominence has the components ϵ'_L with the electric vector parallel to the solar surface and ϵ'_R along the radius, given by

$$\epsilon'_L = \epsilon'_r = 2\frac{I_1(0)}{(1+\beta_1)}\sigma'(\tfrac{1}{2} + \tfrac{9}{32}\beta_1), \tag{7}$$

$$\epsilon'_R = \epsilon'_l = 2\frac{I_1(0)}{(1+\beta_1)}\sigma'(\tfrac{1}{2} + \tfrac{9}{32}\beta_1 - \tfrac{3}{32}\beta_1 \sin^2\theta)$$

$$= 2\frac{I_1(0)}{(1+\beta_1)}\sigma'(\tfrac{1}{2} + \tfrac{6}{32}\beta_1). \tag{8}$$

These are the formulae (4) and (5) of our former paper expressed in our present notation. The suffixes r and l mean that the plane of *polarization* is radial or parallel to the limb, but we now generally prefer to use the planes of *vibration* indicated by the capitals L and R. It should be remembered that a vibration parallel to the limb can also be indicated by its plane of polarization perpendicular to the limb.

The intensity of isotropic radiation has the two equal components ϵ_L and ϵ_R whose intensity is given by

$$\epsilon_L = \epsilon_R = \tfrac{1}{2}\int I_1 \frac{d\Omega}{4\pi} = \tfrac{1}{2}\cdot\frac{I_1(0)}{1+\beta_1}\cdot\sigma(\tfrac{1}{2} + \tfrac{1}{4}\beta_1), \tag{9}$$

as follows from (5), $d\Omega$ being the element of the solid angle.

* A. Unsöld, *Physik der Sternatmosphären*, Berlin, 1939, p. 34, Table 3.
† H. Zanstra, *M.N.*, **101**, 250, 1941.

From (7), (8) and (9) follows the *theoretical degree of polarization of radiation emitted towards the observer:*

$$p=\frac{(\epsilon_L+\epsilon'_L)-(\epsilon_R+\epsilon'_R)}{(\epsilon_L+\epsilon'_L)+(\epsilon_R+\epsilon'_R)}=\frac{\frac{\sigma'}{\sigma}\cdot\frac{3}{32}\beta_1}{\frac{\sigma'}{\sigma}\left(1+\frac{15}{32}\beta_1\right)+(1+\frac{1}{2}\beta_1)}. \tag{10}$$

For $H\alpha$ we had $\sigma'/\sigma=0{\cdot}53$ (3*a*) and (6*a*) $\beta_1=0{\cdot}67$, then (10) yields $p=0{\cdot}016$ or 1·6 per cent. This result is entered in the first row of Table IV of the next section.

Now consider the line D_3 of neutral helium. For λ5876, Abbot's observations at $\cos\theta=1$ and 0·312 lead to a coefficient of darkening for the continuous photospheric background $\beta=1{\cdot}51$ and at $\cos\theta=1$ and 0·661 to $\beta=1{\cdot}22$, average 1·36. The Utrecht Photometric Atlas* shows at λ5875·62 only a faint line of depth 7 per cent, and at λ5875·96 no lines at all, and so we take

$$\beta_1=\beta=1{\cdot}36. \tag{6b}$$

Substituting the values (3 *b*) and (6 *b*) into (10), we obtain $p=0{\cdot}026$ or a degree of polarization of 2·6 per cent for the D_3 line of neutral helium. The result is entered in the first row of Table IV of the next section.

4. *The combined effect of limb darkening and elevation. Comparison with observation.*—The foregoing section dealt with prominence material just above the photosphere. The more general case of material at a point P of a prominence at an altitude h above the photospheric surface of radius $R_\odot$ will now be considered. This can be done by replacing the formulae (7) and (8) for oscillator scattering by somewhat more complicated expressions originally derived by Minnaert† for scattering of photospheric light by free electrons, but which apply equally well to oscillator scattering of an emission line. If θ be the angle with the normal of the emerging radiation which is observed and ϕ the angle with the normal for the tangent from P to the solar surface, so that $\sin\phi=1/(1+h/R_\odot)$, the equations are

$$\epsilon'_L-\epsilon'_R=A\sigma'\sin^2\theta\left\{\cos\phi\sin^2\phi+\tfrac{1}{8}\beta_1\left[3\sin^2\phi-1+\frac{\cos^2\phi}{\sin\phi}(1+3\sin^2\phi)\log\frac{1+\sin\phi}{\cos\phi}\right]\right\}, \tag{11}$$

$$\epsilon'_L=A\sigma'\left\{\left(\tfrac{4}{3}-\cos\phi-\frac{\cos^3\phi}{3}\right)+\tfrac{1}{8}\beta_1\left[5+\sin^2\phi-\frac{\cos^2\phi}{\sin\phi}(5-\sin^2\phi)\log\frac{1+\sin\phi}{\cos\phi}\right]\right\}, \tag{12}$$

with the abbreviation

$$A=\frac{I_1(0)}{1+\beta_1}\left(\frac{3}{16}\right). \tag{13}$$

These are Minnaert's formulae (6) and (7) in our notation, except that the scattering coefficient per electron he used has been replaced by the scattering coefficient σ' per cm. for oscillator scattering in the line, so as to make it applicable to our case.

* M. Minnaert, G. F. W. Mulders and J. Houtgast, *Photometric Atlas of the Solar Spectrum*, Schnabel, Amsterdam, 1940.

† M. Minnaert, *Zeit. f. Astrophys.*, **1**, 209, 1930.

Further, for the isotropically scattered radiation the integration over $d\Omega$ takes place for the solid angle within the tangent cone subtended from P by the solar surface, so that (9) for isotropic scattering is to be replaced by

$$\epsilon_L = \epsilon_R = A\sigma\{\tfrac{4}{3}(1-\cos\phi) + \tfrac{2}{3}\beta_1(1-\cos^2\phi)\} \qquad (14)$$

with A given by (13).

For $h=0$, or $\theta=\phi=\pi/2$, these equations reduce to those of Section 3.

Table IV contains the values of the degree of polarization from (10) computed from these general formulae (11) to (14) for the elevations 0, 25,000 km. and 50,000 km., the latter being approximately the height of the average prominence. The quantity $p/100$ representing the percentage of polarization is given for the case $\theta=90°$, where point P is seen as far as possible from the limb and the case $\theta=\phi$, where P is seen at the limb. As might be expected, the polarization increases with increasing height: for *Hα* it rises from 1·6 to 7·5 per cent and for the helium line from 2·6 to 8·4 per cent as the altitude becomes 50,000 km. If the prominence is seen at the limb, in front of or behind the solar disk, the polarization becomes only slightly less.

TABLE IV

Theoretical degree of polarization (per cent) for a prominence of small total optical depth at various heights h: lines Hα and D_3

h km.	$h/R_\odot$	*Hα*: $p/100$ at max. dist.	limb	*He I*(D_3): $p/100$ at max. dist.	limb
0	0·0000	1·6	1·6	2·6	2·6
25,000	0·0359	5·6	5·2	6·5	6·0
50,000	0·0718	7·5	7·0	8·4	7·2
		Obs. (Lyot) 0·8–1·2		Obs. (Lyot) 0·9–1·5	

In his 1934 publication Lyot's conclusions from forty prominences are that prominences near the solar equator show a polarization in *Hα* of about 0·3 per cent with vibration approximately parallel to the Sun's limb, or plane of polarization perpendicular to the limb. For latitudes between 36° and 44° the polarization becomes larger, between 0·5 and 1·2 per cent, but the plane of polarization is no longer perpendicular to the limb, but may deviate towards the north for prominences on the northern hemisphere, the deviations being between 0° and 22°. In three cases, contiguous prominences at high latitudes showed very different planes of polarization. Dense prominences generally showed uniform polarization, but in one case of a diffuse cloud the values varied much from point to point. The observations were made during a period of feeble solar activity and he judges the material to be too limited to allow general conclusions.

In his 1937 note discussing observations of the year 1935 he states that polarization of *Hα* generally is between 0·8 and 1·2 per cent and deviations of the plane of polarization occur up to 30°, in the same sense as above. These values of $p/100$, which occur most frequently, are entered at the bottom of Table IV as "observed".

For the D_3 line of *He I*, Lyot's 1935 observations give polarizations between 0·9 and 1·5 per cent, but deviations of the plane of polarization up to 40°.

Prominences generally are observed at an altitude between 25,000 and 50,000 km. The theoretical degree of polarization is therefore five to six times the maximum of the observed value. The discrepancy might partly be attributed to the fact that the theory has been worked out for the mechanism of resonance, whereas, in addition to this, the lines are excited appreciably by fluorescence and ionization and re-combination, while also electron impact might perhaps play a part. One might also think of other depolarizing agencies like phase-disturbing collisions*, while in the case of $H\alpha$ the assumption of low total optical depths probably is not justified, and the hyperfine structure was not taken into account thus far. However this may be, it is gratifying that the theory is more than sufficient to explain the polarization observed by Lyot, although, in the simple form it is given in the present paper, the increase of polarization towards higher latitudes and the deviation of the plane of polarization that he observes are as yet unexplained.

5. *Remarks.*—Considering the passage of circular into linear polarization represented in Fig. 1B, the following may be remarked. We take the average E^2 as a measure of intensity, E being the value of the vibrating electric field. Let $E_0 = \text{const.}$ be the electric vector for each of the circular vibrations σ_1 (clockwise) and σ_2 (counterclockwise), then the energy of each is $E_0^2 = i_\sigma$. When the auxiliary magnetic field is removed, the angular frequencies ω of these two circular motions become the same, but their phase difference remains arbitrary. Their resultant then is a linear vibration in the xy-plane of arbitrary direction, amplitude $2E_0$ and energy $\frac{1}{2} \cdot 4E_0^2 = 2E_0^2$. Statistically the average energy of vibration along the y-axis is then equal to that along the x-axis, or E_0^2, viz. i_σ. The assumption made in the text is therefore justified. Also, the third component i_π has an arbitrary phase difference with the components i_σ, so that statistically speaking the energies of the three components may be added to $i_\pi + 2i_\sigma$, as was assumed in the text.

The writer is indebted to Professor M. Minnaert of Utrecht and to Mr P. F. A. Klinkenberg of the Zeeman Laboratory in Amsterdam for valuable information.

Astronomical Institute,
University of Amsterdam:
July 1950.

* *Cf.* H. Zanstra, *M.N.*, **101**, 266, 1941; **106**, 225, 1946.

MEAN AREAS AND HELIOGRAPHIC LATITUDES OF SUNSPOTS IN THE YEAR 1945

Royal Observatory, Greenwich

(Communicated by the Astronomer Royal)

(Received 1950 June 13)

The following results are in continuation of those given in *M.N.*, **109,** 481, 1949, and are derived from the measurement at Greenwich of photographs taken at the Royal Observatories of Greenwich and the Cape and at the Kodaikanal Observatory, India. There were six gaps in the series. For these days, copies of original solar negatives were together supplied by the Mount Wilson Observatory, California, and the U.S. Naval Observatory, Washington, D.C.

Table I gives the mean daily areas of umbrae, whole spots and faculae for each synodic rotation of the Sun included in the year 1945; the means for each year as a whole are included in Table II, which summarizes the yearly values from 1933 to 1945.

TABLE I

Mean Daily Areas

No. of Rotation	Rotation Commenced U.T. 1944–45	Days Photographed	Projected*			Corrected for Foreshortening†		
			Umbrae	Whole Spots	Faculae	Umbrae	Whole Spots	Faculae
1221	Dec. 18·74	27	66	358	704	56	309	867
1222	Jan. 15·07	28	36	184	486	29	144	592
1223	Feb. 11·42	27	62	323	516	47	241	639
1224	Mar. 10·75	27	161	928	631	117	674	744
1225	Apr. 7·05	27	123	669	697	93	499	835
1226	May 4·30	28	51	246	729	44	220	895
1227	May 31·52	27	103	541	955	82	423	1135
1228	June 27·72	27	140	753	866	102	554	1088
1229	July 24·92	27	90	480	779	66	349	936
1230	Aug. 21·15	28	29	150	556	24	126	690
1231	Sept. 17·40	27	237	1365	739	179	1012	929
1232	Oct. 14·69	27	163	935	1019	135	779	1233
1233	Nov. 10·99	27	99	554	1139	75	422	1364
1234	Dec. 8·30	28	73	374	979	56	294	1168

* Expressed in millionths of the Sun's disk.

† Expressed in millionths of the Sun's hemisphere.

Table III gives for each rotation in the year 1945 the mean daily area of the whole spots (corrected for foreshortening) and the mean heliographic latitude of the spotted areas for both northern and southern hemispheres.

The mean heliographic latitude of the entire spotted area and the mean distance from the equator of all spots are also tabulated. The mean values for the year 1945 are included in Table IV.

Tables II and IV are in continuation of similar tables given in *Monthly Notices*: for the years 1874 to 1888—**49,** 381–382; 1889 to 1902—**63,** 465–466;

1901 to 1914—**76,** 402–403; 1913 to 1924—**85,** 1007–1008; 1923 to 1933—**94,** 870–871.

The rotations in Tables I and III are numbered in continuation of Carrington's series.

The chief features of the record are as follows:—

(1) The steep rise in sunspot activity that began after the rather shallow and brief minimum at the epoch, 1944.2 (Tables I and II). The vigorous rise is particularly well shown by the mean areas of faculae for each solar rotation given in Table I.

TABLE II

Mean Areas and Heliographic Latitudes

	No. of Days		Mean Daily Areas					
			Projected*			Corrected for Foreshortening†		
Year	Photo-graphed	Without Spots	Umbrae	Whole Spots	Faculae	Umbrae	Whole Spots	Faculae
1933	365	234	24	120	225	18	88	267
1934	365	145	27	142	297	22	119	354
1935	365	21	152	810	910	117	624	1100
1936	366	0	288	1529	2106	217	1141	2545
1937	365	0	509	2795	2856	375	2074	3505
1938	365	0	501	2706	2578	371	2019	3205
1939	365	0	404	2163	1907	295	1579	2349
1940	366	0	279	1434	1224	200	1039	1522
1941	365	8	167	915	1041	120	658	1282
1942	365	16	112	591	666	79	423	809
1943	365	48	73	410	457	51	295	561
1944	366	157	30	160	281	23	126	338
1945	365	14	102	560	773	78	429	939

* Expressed in millionths of the Sun's disk.
† Expressed in millionths of the Sun's hemisphere.

(2) On only 14 days were no sunspots recorded, and even on these occasions faculae near the Sun's limb were present.

(3) From the onset of the new cycle up to the end of 1945, the southern hemisphere was more active in sunspots than the northern (Tables III and IV). In the latter phase of the old cycle, the northern hemisphere predominated in this respect (*M.N.*, **109,** 482, 1949).

(4) The number and distribution of spot groups of duration (*a*) two days or longer: (*b*) one day, are as follows:—

	(*a*)	(*b*)
North spots	56	13
South spots	101	35
Total	157	48

The highest latitudes in which the longer-lived spots appeared were 35° north and 38½° south. Corresponding latitudes for the 1-day spots were 29° north and 43° south respectively.

TABLE III

No. of Rotation	Rotation Commenced U.T.	Spots North of the Equator: Mean Daily Area	Spots North of the Equator: Mean Heliographic Latitude	Spots South of the Equator: Mean Daily Area	Spots South of the Equator: Mean Heliographic Latitude	Mean Latitude of Entire Spotted Area	Mean Distance from Equator of all Spots
	1944–45		°		°	°	°
1221	Dec. 18·74	177	23·74	132	26·75	+ 2·15	25·03
1222	Jan. 15·07	70	22·67	75	10·95	+ 5·26	16·60
1223	Feb. 11·42	46	22·50	195	15·09	− 7·94	16·50
1224	Mar. 10·75	19	30·80	655	24·88	−23·28	25·05
1225	Apr. 7·05	4	27·35	496	12·02	−11·75	12·13
1226	May 4·30	20	28·14	200	19·90	−15·54	20·65
1227	May 31·52	23	28·59	400	24·21	−21·29	24·45
1228	June 27·72	148	22·29	406	20·27	− 8·87	20·81
1229	July 24·92	332	23·32	16	20·27	+21·27	23·18
1230	Aug. 21·15	27	25·24	99	17·15	− 7·96	18·90
1231	Sept. 17·40	388	8·48	625	20·86	− 9·62	16·12
1232	Oct. 14·69	242	24·37	537	23·19	− 8·43	23·56
1233	Nov. 10·99	146	24·69	277	19·55	− 4·30	21·33
1234	Dec. 8·30	125	23·34	156	17·06	+ 0·87	19·85

TABLE IV

Year	Days Photographed	Spots North of the Equator: Mean Daily Area	Spots North of the Equator: Mean Heliographic Latitude	Spots South of the Equator: Mean Daily Area	Spots South of the Equator: Mean Heliographic Latitude	Mean Latitude of Entire Spotted Area	Mean Distance from Equator of all Spots
			°		°	°	°
1933	365	86	10·60	2	8·35	+10·23	10·56
1934	365	44	16·45	74	28·09	−11·49	23·75
1934	365 Old Cycle	19	4·10	1	4·37	+ 3·79	4·11
	365 New Cycle	26	25·44	74	28·31	−14·46	27·57
1935	365	205	22·42	419	23·72	− 8·57	23·30
1936	366	463	19·36	678	21·02	− 4·63	20·35
1937	365	1317	17·63	757	15·96	+ 5·36	17·02
1938	365	899	15·55	1120	14·17	− 0·94	14·79
1939	365	649	14·64	931	12·57	− 1·39	13·42
1940	366	499	11·65	540	10·72	+ 0·03	11·17
1941	365	427	11·31	232	8·67	+ 4·28	10·38
1942	365	252	9·32	171	8·45	+ 2·14	8·99
1943	365	249	9·01	46	15·87	+ 5·11	10·09
1943	365 Old Cycle	249	9·01	27	8·33	+ 7·33	8·95
	365 New Cycle	0	...	20	26·13	−26·13	26·13
1944	366	42	19·00	83	22·81	− 8·70	21·53
1944	366 Old Cycle	7	4·17	6	7·61	− 1·14	5·72
	366 New Cycle	35	22·18	77	24·02	− 9·63	23·45
1945	365	121	20·13	309	20·26	− 8·92	20·22

(5) The mean weighted latitude of all spots was 20°·22 (Table IV). The characteristic overlap in latitude of old and new cycle spots at the minimum epoch practically ceased in 1945. Only eight spots of the old cycle were indicated by the Mount Wilson observations of magnetic polarities. These few low latitude sunspots (mean latitude 7°) do not materially affect the mean latitude for the year.

Other notes on the sunspots of 1945 will be found in *M.N.*, **106,** 76, 1946.

An appended table gives the mean daily areas of whole spots and of faculae (corrected for foreshortening and expressed in millionths of the Sun's hemisphere) for each calendar month of 1945.

Monthly Mean Daily Areas of Sunspots and Faculae

1945

Month	Spots	Faculae	Month	Spots	Faculae
Jan.	182	727	July	506	1068
Feb.	92	622	Aug.	271	816
Mar.	515	628	Sept.	451	826
Apr.	585	807	Oct.	1114	1148
May	283	963	Nov.	399	1365
June	399	1083	Dec.	325	1195

Royal Greenwich Observatory,
Herstmonceux Castle, Sussex:
1950 *June* 9.

CONTENTS

Printed in London by Taylor & Francis, Ltd., 1951 February.